Interkingdom chemical communication mediates intimate bacterial-fungal interactions

By

Joseph E. Spraker

A dissertation submitted in partial fulfillment of

the requirements for the degree of

Doctor of Philosophy

(Plant Pathology)

at the

UNIVERSITY OF WISCONSIN-MADISON

2016

Final Oral Committee:

Nancy Keller, Professor, Medical Microbiology & Immunology and Bacteriology

Caitilyn Allen, Professor, Plant Pathology

Cameron Currie, Professor, Bacteriology

Audrey Gasch, Professor, Genetics

Anne Pringle, Professor, Botany & Bacteriology

ABSTRACT

Fungi and bacteria have been ubiquitous neighbors in nearly every imaginable ecological niche for hundreds of millions of years, yet relatively little is known of how these organisms communicate. Historically our understanding of bacterial-fungal interactions (BFIs) are largely limited to antibiosis, especially against pathogens of animals and plants. Recently the tremendous impact of the polymicrobial milieu (i.e. microbiomes) on animal and plant health has been recognized and research has started to emerge regarding community composition and dynamics resulting from both abiotic and biotic interactions. Understanding what the chemical communication signals are and their outcomes in BFIs is essential to moving beyond antibiosis and finding new modes of modulating polymicrobial systems in agriculture, medicine, and industry.

This thesis explores the language of microbial interkingdom communications and its impacts on microbial development, morphology and symbioses. I examined a variety of interaction conditions including: volatile, diffusible, and direct-contact interactions between the bacterial plant pathogen, *Ralstonia solanacearum*, and plant associated fungi. The outcomes of these interactions impact both *R. solanacearum* and the fungi they interact with, causing shifts in development, secondary metabolism, dispersal, and endosymbiotic interactions. Specifically, volatile interactions resulted in dramatic reductions in bacterial EPS and melanin production with concomitant reductions in fungal sporulation and increased aflatoxin production, potentially modulated by overlapping volatile profiles. Diffusible and physical interactions between *R. solanacearum* and many fungi, such as *Aspergillus flavus* and *Fusarium fujikuroi*, resulted in

fungal chlamydospore development, bacterial endosymbiosis, and dramatic shifts in secondary metabolite regulation; all driven by the bacterial lipopeptide ralsolamycin.

By coupling *in vitro* coculture methodologies with modern metabolomics and genetic manipulations of bacteria and fungi, this thesis provides a deeper understanding of the chemistry and biology of this intermicrobial communication. While many of the findings are novel, I anticipate that they represent a more common yet undescribed phenomenon of other bacterial-fungal interactions in the soil and on plant surfaces. Further research into the developing field of bacterial-fungal chemical communication will undoubtedly contribute significantly to both basic and applied fields of microbial ecology, agriculture, and medicine.

ACKNOWLEDGEMENTS

Throughout my graduate studies I have had the opportunity to interact with a multitude of intellectually vibrant people who have spent the better part of their adult lives passionately engaged in trying to attain a better understanding of the world they inhabit. This includes undergraduates whom I taught, graduate students whom I learned with, and professors and staff whom I learned from.

While I would like to thank everyone, I must specifically acknowledge my mentor Nancy Keller for helping me to grow both personally and professionally. I consider myself very fortunate to have had the opportunity to work with her for the past five years and know I will continue to learn from her well beyond my PhD. She has assembled a group of excellent people who have provided support, advice, and laughter throughout my graduate studies. While every lab member deserves huge thanks, Dr. JinWoo Bok deserves a special thanks as he challenged me intellectually on a daily basis while providing me with constant friendship and support. Dr. Philipp Wiemann also deserves thanks for his help and input working with *Fusarium.* Additionally, my thesis committee past and present (Caitilyn Allen, Audrey Gasch, Cameron Currie, Anne Pringle, and Jean Michel Ane) deserves great thanks for their insights and critical feedback on my work.

Finally, I am eternally grateful to my family and friends who have been nothing but supportive as I've worked to complete my PhD. My partner Cary has supported me in every way throughout my PhD and I cannot thank her enough for her constant love. My children Behren and Huxley Anne kept me from spending all of my time in the lab and helped me realize the value of personal time in being more focused and efficient at work. I also must thank my extended family, both Spraker's and Miao's, for all of their encouragement and support.

TABLE OF CONTENTS

CHAPTER 1: Introduction

This chapter is a part of review article in preparation for submission to *Frontiers in Microbiology*.

1.1. PLANT ASSOCIATED BACTERIAL FUNGAL INTERACTIONS

The rhizosphere and surrounding soil consists of a multitude of microenvironments that are populated by diverse macro- and microbiota that interact in many ways including antagonism, mutualism, parasitism, commensalism, and coexistence (1). These interactions are dynamic and are dependent on environmental factors including (but not limited to) abiotic factors such as, nutrients, water, and space. Bacteria and fungi have been ubiquitous neighbors in this environment for millions of years, yet relatively little is known of how these organisms communicate until recently. The composition and function of microbial communities is dictated by both the local environment as well as the manifold outcomes of interactions by the members of the community (2). These interactions can be mediated by secreted proteins and small-molecules which directly impact the growth and survival of other organisms in the community. Alternatively, molecules can diffuse long distances to impact non-proximal organisms. Traditionally it is thought that the majority of these interactions are antagonistic as microbes are thought to be in constant battle for resources, although an emerging theme in microbial ecology suggests that many of the compounds thought to be involved in antibiosis may in fact serve an alternative purpose of modulating subtle shifts in physiology and behavior, facilitating other symbiotic outcomes (3).

Bacterial-fungal interactions are ubiquitous in nature and may represent one of the oldest interkingdom dialogues on Earth. Interest in microbial communication stems largely from a desire to better control specific members of microbial communities most commonly for purposes of disease control. While in medicine many antimicrobial compounds have been derived from microbial sources (4), often in agriculture people utilize microbial derived compounds as well as

the producing organisms themselves to provide "biocontrol" against target disease causing organisms (1). Because disease control can result from competition for resources, antibiosis, and/or predation; study of potential biocontrol agents forms a good portion of our understanding of the different modes of antagonistic bacterial fungal interactions. Outside of disease control, there are many exciting new discoveries in the arena of bacterial-fungal interactions (BFIs) which suggest that there are many other outcomes which may be of importance for the sustainable production of agricultural and forest products.

1.2. BIOTIC OUTCOMES

There are many outcomes of BFIs that have been described to date ranging from competition for common resources to intimate endosybioses **(Figure 1)**. Here I attempt to highlight a few of these outcomes to describe the ubiquity and complexity of some of these interactions and discuss their potential impact on the participating microorganisms. While many of these interactions are between plant associated bacteria and fungi, I do describe some interactions of saprophytic microbes as their lifestyles are dependent upon degrading plant material so they are common inhabitants of the plant environment.

1.2.1. Antibiosis

One of the best described outcomes of BFIs is that of antibiosis, which is likely due to its ubiquity and ease of screening *in vitro.* Fungal derived antibacterial compounds were the first to spark interest in intermicrobial antibiosis with the discovery of penicillin by Alexander Fleming (5). Subsequently a large number of medically useful fungal produced antibacterial compounds have been discovered *in vitro* including cephalosporin, strobilurin, usnic acid, fumagillin and nigrisporin. Likewise, bacterial derived antifungal compounds such as nikkomycins, polyoxins,

bacillomycins, iturins, fengycins, 2,4-diacetylphloroglucinol, and pyoluteorin have been discovered and show diverse modes of action. Although the intent of this review is not to catalogue all known antibiotic compounds, I provide this short list to highlight the variety and importance of compounds that have been discovered to date. Although antibiosis has long been a focal aspect of bacterial fungal interactions, there are many more-subtle outcomes in BFIs.

1.2.2. Shifts in development and physiology

Developmental and physiological shifts have been highlighted in a number of BFI studies and their potential impacts on ecological processes have been presumed. The arbuscular mycorrhizal fungus *Glomus intraradices* shows hyphal elongation and sporulation in response to trisaccharides produced by *Paenibacillus validus* (6). Additionally, basidiocarp primordia development by *Agaricus bisporus* and *Pleurotus ostreatus* has been linked to specific bacterial community members in the fungal casing layer (7, 8) although the specific mechanisms of these interactions were not elucidated. Some bacterial lipopeptides, such as fengycin and ralsolamycin have been shown to have antifungal properties at higher concentrations, but induce intercalated mitospore development at lower concentrations (9, 10). Finally, *Geosiphon pyriforme* forms specialized compartments for its autotrophic endosymbiont, *Nostoc punctiforme*, only upon uptake of the cyanobacterium (11). Although many of these developmental shifts are clear results of BFIs, there are still many unanswered questions about the signaling required in the initiation and process of these shifts in development.

Physiological shifts are directly linked to development shifts and are thus also commonplace in the BFIs described above. Since microbes are often required to respond to cues from one-another these shifts can result in an exchange of nutrients or an exchange of combative compounds such as antibiotics. Cocultures between the fungus *Lyophyllum* sp. strain Karsten and

three bacterial species showed that *Burkholderia terrae* BS001 was uniquely capable of suppressing mushroom formation and inducing a release of glycerol into the media (12). This specific release of glycerol was utilized by the bacterium and suggests a shift in fungal physiology to the benefit of the bacterium. While this example highlights a physiological shift resulting in trophic exchange, many fungi will also respond to BFIs with greatly altered secondary metabolite production (13). *Fusarium pallidoroseum* produced three novel decalin-type tetramic acid analogues related to the cytotoxic compound equisetin when it was cocultured with the bacterium *Saccharopolyspora erythraea* (14). A common inhabitant of the rhizosphere and frequently deployed biocontrol bacterium, *Bacillus subtilis,* has been shown to increase the production of known metabolites and induce the production of novel SM in the endophytic fungus *F. tricinctum* (15). Interestingly, the authors note that this shift in SM production was time dependent as cultures inoculated at the same time showed little difference in SM production. This implies that developmental progression at the time of encounter can greatly impact the physiological responses of fungi to bacterial signals and these temporal dynamics are undoubtedly important in the natural environment.

1.2.3. Dispersal and endosymbioses

Aside from changes in development, BFIs can affect both bacterial and fungal dispersal. Some interactions result in a shift in fungal sporulation patterns which would negatively impact dispersal in the environment. For example, volatile compounds produced by *Ralstonia solanacearum* significantly reduced the conidial production of *Aspergillus flavus* and *A. nidulans,* but increased the production of conidiation by *A. niger*. (16). Additionally, *B. subtilis* volatiles caused a decrease in conidiation amongst six plant pathogenic fungi and oomycetes (17). Aside from sporulation, it has been shown that bacteria are able to move through substrates

and across air gaps by riding on fungal hyphae (18, 19). This mode of transportation could be important for bacterial dispersal and community establishment as fungal hyphae penetrate free-water limited soil, which would normally limit bacterial dispersal by swimming. A unique study demonstrated that while fungal hyphae can help disperse *Paenibacillus vortex* across air gaps, reciprocally bacterial swarming can contribute to fungal spore dispersal *in vitro* (20). All of these examples highlight the complexity of interactions between bacteria and fungi and underscore the roles that each play in the movement of the other.

Alternatively, dispersal can be mediated by endocellular associations, although the ubiquity of these associations is only recently coming to light. Endobacteria of the arbuscular mycorrhizal fungus, *Gigaspora margarita,* were shown to be vertically transmitted through mitospores, and they were also present in extraradical mycelia (21). Similarly, sporulation of the fungal plant pathogen *Rhizopus microsporus* is only possible when it is infected with its endosymbiotic partner, *Burkholderia rhizoxinica,* which likely helps to ensure the vertical transmission of the endosymbiont (22). Although our understanding of bacterial endosymbionts is still in its infancy, recent work by Hoffman *et al.* suggests that endofungal bacteria may be ubiquitous amongst plant associated fungi, finding that endofungal bacteria are phylogenetically diverse and are ubiquitous amongst foliar endophytic fungi from diverse plant hosts (23). This suggests that movement of bacteria within fungal hyphae and spores may be a more common component of microbial movement than has been described. Recently I found that the plant pathogenic bacterium *R. solanacearum* is able to induce fungal chlamydospores development and invade these structures (10). I speculate that this invasion may help the bacterium persist in the soil in the absence of plant hosts, contributing to temporal dynamics of plant infection.

Continued research into the mechanisms and outcomes of bacterial endosymbioses will likely provide many interesting new insights into this unique type of BFI.

1.3. MODES OF COMMUNICATION

The scale of microbial communities is very important when considering how microbes may be interacting with one another. Since the microbial environment is often considered on the scale of microns and millimeters (24) there can be considerable heterogeneity in environment across a relatively small natural space. When considering the impacts of microbial communication on community composition and outcomes, there are many different modes that may be considered relevant to the defined environment. Each mode has implications across different scales of microbial communities, and under different abiotic conditions. Some compounds can diffuse long distances through airspace (volatile), others will diffuse shorter distances through aqueous environments (diffusible), and others are only impactful when microbes are in physical contact (direct). Because of the many modes of communication that bacteria and fungi may use to interact with one another, it is no surprise that the outcomes of these interactions can be quite diverse (**Figure 1**). Here I highlight some of the best described modes of communication and discuss their potential impacts on soil ecology.

1.3.1. Volatile interactions

Interactions between bacteria and fungi can occur on a relatively large spatial scale via compounds that can travel through airspace. Volatile organic compounds (VOCs) generally have a high vapor pressure and low molecular weight, allowing them to readily evaporate under normal atmospheric pressures and temperatures and diffuse to distant locations from the site of production (25). VOCs are ideal for long distance inter- and intra-microbial communication and

are represented mostly by alcohols, thiols, aldehydes, esters, terpenoids, and fatty acid derivatives (26). Bacteria and fungi from soil, plants, and animals are known to produce VOCs and there has been substantial work done to characterize these compounds and identify their ecological functions. Many small VOCs (<100 D) such as methane, acetate, and butyrate are produced and consumed by a variety of microbes and contribute to carbon flux through communities. Small VOCs and volatile inorganic carbon compounds, such as CO_2, can have significant impacts on microbial communities, but they are commonly linked to primary metabolism so they will not be discussed in detail here. Slightly larger VOCs (100~300 D) are of great interest to researchers looking to understand chemical communication between bacteria and fungi as the increased complexity of larger molecules correlates to a greater variety in responses by target organisms.

Bacterial VOCs have been shown to impact many aspects of fungal growth, development, and physiology both positively and negatively (27, 28). Germination and mycelial growth are two commonly impacted phenotypes from bacterial fungal volatile interactions. For example, Fernando *et al* demonstrated that 7% of bacteria isolated from canola and soybean produced VOCs that were both antagonistic to germination and mycelial growth of *Sclerotinia sclerotiorum* (29). When individual compounds identified from different bacteria, such as: benzathioazole, cyclohexanol, n-decanal, dimethyltrisulfide, 2-ethyl-1 hexanol, and nonanal; were tested, they all showed a complete inhibition of *S. sclerotiorum* growth and germination. These data exemplify that while individual VOCs may effectively function as intermicrobial communication signals, there are likely synergistic impacts of multiple compounds from different community members all shaping the outcomes of microbial interactions.

Not all VOC mediated bacterial-fungal interactions result in inhibition. Mackie *at al.* showed that of 60 randomly selected isolates from soil, all of the bacteria had some impact on at least one of five fungal isolates (including two oomycetes) tested, either positive or negative (27). Of these bacteria some had variable effects depending on the target organism, reducing growth rates of some fungi while enhancing others. This variation in outcome depending on which organism are included in the interaction emphasizes the potential impact that VOCs may have in shaping microbial communities. Additionally, it has been shown that some bacteria and fungi participate in two-way signaling. As mentioned previously, volatile coculture of the plant pathogenic bacterium *R. solanacearum,* and the toxigenic fungus *A. flavus,* resulted in a reduction in conidiation by *A. flavus* and a concomitant increase in aflatoxin production. On the other side of this interaction, *R. solanacearum* showed decreased growth, and decreased melanin and extracellular polysaccharide production (16). Sampling of the airspace of these cocultures and axenic cultures indicated that there is an overlap in VOC profiles between these two microbes which may impact autoinduction systems. Although all of the described studies characterized shift in growth or development, further exploration of microbial volatile signaling will undoubtedly show that VOCs also contribute to subtler shifts in physiology too.

1.3.2. Diffusible interactions

Bacteria and fungi also communicate over shorter distances (µm to mm) using larger (>300 D) non-volatile, specialized signals. These signals can be both proteinaceous or non-proteinaceous and diffuse through aqueous environments where they can interact with local members of the community. Like bacterial quorum sensing signals, interkingdom bacterial-fungal signals can have variable effects depending not only on the target organism, but also on the perceived concentration of the signal. Although it has yet to be described in great detail, it is

fair to assume that these signals also work in tandem with other compounds produced by the interacting partners as well as the local organismal community, acting either synergistically or antagonistically, to temper the responses of target organisms.

Although proteinaceous interaction are likely very important to bacterial-fungal interactions, relatively little work has described their impact on these symbioses. Both bacteria and fungi acquire nutrients via extracellular digestion, such that they secrete digestive enzymes into their local environment in order to degrade large, complex organic molecules into smaller components which can then be taken into the cell via diffusion or active uptake. These enzymes may include cellulases, chitinases, glucanases, proteases and lysozymes (30, 31) and are likely involved not only in direct interactions between microbes but also through their impact on nutrient availability as bacteria may be better able to grow in substrates degraded by fungi, and vice versa. Although little has been documented about the roles of enzymes in BFIs, secreted chitinases have been indicated to contribute to bacterial mycophagy (31).

There is some evidence of fungi feeding on bacteria, a lifestyle termed bacterivory, by fungi such as *Agaricus bisporus*, *Pleurotus ostreatus*, and *Lentinula edodes* (32, 33). Glycosidases, peptidases, and amidases have all been implied to be important bacteriolytic enzymes produced by bacterivorous fungi (34). From these studies it can be deduced that fungal bacteriophagy can be both from lysis as well as digestion of bacterial cell walls. Recent research suggests that *Morchella crassipes* may actually "farm" bacteria for food prior to sclerotia formation (35). In this study ^{13}C-labeled media was used to show initial transfer of carbon resources from *M. crassipes* to *Pseudomonas putida* as well as a subsequent transfer of carbon from bacteria to fungi during the "harvesting" phase of the interaction. Aside from direct consumption of bacteria, fungi also regularly consume bacterial exudates in a more cooperative

fashion. These interactions are exemplified by lichenized fungi who utilize carbon fixed by autotrophic bacterial endosymbionts such as *Geosiphon pyriforme* which harbors the photosynthetic cyanobacterium, *Nostoc punctiforme* (11). Further, this specialized association is capable of fixing atmospheric nitrogen facilitated by other non-photosynthetic endosymbiotic bacteria (36, 37). While fungal bacterivory and farming has only been described in a handful of cases it warrants further study as it may be a common lifestyle for other important fungi.

Aside from enzyme mediated interactions, there are many well documented cases of BFIs mediated by small secreted metabolites. Although termed secondary metabolites (SMs), as they are not necessary for growth under laboratory conditions, the importance of these compounds is likely far greater under natural abiotic and biotic conditions. One of the best known examples of bacterial fungal interactions mediated by secondary metabolites is antibiosis which are thought to contribute to niche securement and persistence. Antibiosis results from the inhibition of key cellular functions in the target organism. One of the most famous bacterial fungal interactions was the discovery of the beta-lactam antibacterial compound penicillin. This compound was discovered from *Penicillium* contamination on a *Staphylococcus* culture plate (5). This incidental finding has since revolutionized treatment of infectious diseases and has lead to an extensive search for novel chemistries from natural sources.

Bacteria are known to produce a variety of antifungal compounds and many of these compounds have been utilized to control fungal plant diseases. 2,4-diacetylphloroglucinol (DAPG) is one of the most commonly described antifungal compounds from biocontrol strains of *Pseudomonas* (38) although it is also produced by other bacterial genera such *Lysobacter gummosus*, an amphibian colonist (39). This compound has broad spectrum antifungal activity thought to stem from a disruption of mitochondrial proton gradients resulting in the cessation of

respiration and ATP synthesis (40). Although this is a potent biocontrol compound, many fungi have developed resistance mechanisms to DAPG such as enzymatic detoxification (41) as well as efflux and laccase-mediated degradation (42). Due to constantly evolving resistance mechanisms it is thought that these SMs are not produced alone, but instead work synergistically with other SMs to help derail or override resistance mechanisms (43–45).

Many fungi also produce SMs with bioactivity toward bacteria. For example, many *Fusarium* spp. are able to produce fusaric acid, which is toxic to both bacteria and fungi (46–50). Aside from direct antibiosis, fusaric acid has also been shown to suppress bacterial production of antifungal compounds by biocontrol *Pseudomonas* spp. such as, phenazine-1-carboxamide and DAPG. Using a *lacZ* reporter assay, *Pseudomonas fluorescens* CHA0 showed a dose dependent reduction in the transcription of the DAPG biosynthetic gene *phlA,* although not impacting bacterial growth (51). These data suggest that while not toxic to the bacterium, fusaric acid can still modulate bacterial physiology in order to suppress the production of antifungal compounds. Alternatively, *P. fluorescens* strain WCS365 shows chemotaxis towards and hyphal colonization of fusaric acid producing strains of *F. oxysporum*, a response dependent on the sensory kinase gene *cheA* (52). Interestingly, fusaric acid also can select against tetracycline resistance genes (53, 54) suggesting that there may be a dynamic evolutionary interplay between resistance mechanisms towards both bacterial and fungal metabolites. This interplay may help shape communities within the context of polymicrobial metabolic communication.

The focus on the antifungal (DAPG) and antibacterial (fusaric acid) described in detail above are meant to highlight the complexities of the types of BFIs that are traditionally deemed as “antibiosis”. Looking beyond death will allow researchers to find alternative functions for compounds initially labelled antibiotics. For example, bacterial lipopeptides from the plant

pathogen *R. solanacearum* as well as the plant protective *B. subtilis* both show broad antifungal activity, although at sublethal concentrations both compounds induce chlamydospore formation (10, 55). Ultimately, there are other potential outcomes than death when microbial SMs are produced and perceived, which highlights the importance of evaluating many ecological functions of microbial SMs, and recognizing that they may serve multiple purposes.

1.3.3. Direct interactions

Bacteria rely on secretion systems to release large biomolecules into the local environment and neighboring cells. These systems can range from simple transporters to large protein complexes with specialized functions. In gram-negative bacteria these multicomponent secretion systems have been catalogued into six types, Type I to Type VI, each exhibiting differences in components and molecular mechanisms. These systems are often associated with virulence in host organisms, but have also been implicated in interactions between bacteria and fungi. Specifically, Type I and Type II systems are known to secrete lipases, proteases, and beta-glucanases, which have been implicated in antifungal phenotypes of different bacterial species (56, 57). Type II systems that secrete chitinases were shown to be essential for bacterial entry into fungal hyphae in the aforementioned *Burkholderia-Rhizopus* endosymbiotic system. Type III and Type IV systems are used to directly inject macromolecules such as proteins and DNA into host cells and they have been implicated mostly in their interactions with higher eukaryotic hosts such as plants and animals, although there is a growing body of literature that suggests that these systems can also impact BFIs. Specifically, Type III secretion systems have been shown to be essential for the maintenance of endosymbiotic bacteria in the *Rhizopus-Burkholderia* interactions, although the mechanisms of this system are yet to be discerned as there is no direct evidence of bacterial effectors mediating these interactions (22). Similarly, it was found that

Type III systems impact the role of mycorrhizal helper bacteria, *Pseudomonas fluorescens* BBc6R8, in *Laccaria* bicolor colonization of *Pinus* roots (58). Although it was not elucidated whether this was an impact directly on the fungus, or instead on modulating plant host responses to the fungus, it is clear that these secretion systems have the potential to greatly impact multipartite symbioses.

Alternatively, *Agrobacterium tumifaciens* utilize Type IV systems to inject transformative plasmids into host plants (59). Although this interaction with fungi has not been explicitly documented from a natural setting, it is fascinating that this transformation system has been adopted for biotechnological purposes and used to transform a number of fungi *in vitro* (60). This suggests that Type IV systems may have a yet undescribed function in rhizosphere BFIs, mediating the transfer of genetic material from bacteria to fungi. Interestingly a growing number of studies have suggested the integration of bacterial genetic material into fungal genomes (61–64). While it is tempting to assume that some of these transfers may have been mediated by bacterial Type IV secretion systems, the mechanisms of these gene transfer events have yet to be explored.

Type V and VI systems have not received any attention in BFIs to my knowledge although they may also play a role due to their implications in pathogenesis and interactions with higher eukaryotes. Briefly, Type V secretions systems secrete virulence factors and adhesins through the outer membrane which can contribute to attachment and biofilm formation (65). These systems may also be important for maintaining extracellular contact with fungi and potentially for fungal mediated translocation, although these mechanisms have yet to be explored. Type VI are a newly classified member of the gram-negative secretion systems, which have been shown to be important for virulence and infectivity of eukaryotic cells and are highly

conserved across pathogenic (i.e. *Vibrio*, *Pseudomonas*), beneficial (i.e. *Rhizobia*), and environmental proteobacteria (66). Because of the ubiquity and diversity of the impacts that Type VI systems may have, it will be interesting to see if they play a role in future BFI studies.

Fungi have not been as extensively investigated for factors mediating physical interactions with bacteria. This bias may be because fungi are larger and therefore they are perceived as only being acted upon by bacteria, and not vice-versa. Nonetheless, they are likely active participants in known physical interactions such as attachment and endosymbioses. Lectins, proteins produced by organisms to react with sugars, are one of the few examples shown to be important on the fungal side of the interaction. A glycosylated arginase acting as a lectin from the lichen *Peltigera canina* was shown to be involved in recruitment and attachment of cyanobacterial cells to the mycobiont thallus (67), a synonymous function to interactions with algal cells. Lectins are widespread in micro- and macro-fungi, although they have been predominantly reported from mushroom forming fungi (68). In soil-borne fungi, some lectins have been shown to contribute to defense against predatory nematodes and insects (69–71), although their interactions with bacteria have not been examined. Lectins have been shown to mediate interactions between bacterial and fungal pathogens and their hosts, both plants and animals (72). Since both fungal and bacterial cell walls are heavily decorated with diverse carbohydrate moieties, it doesn't take a far stretch of the imagination to predict that these proteins may be involved in many BFIs.

1.4. PERSPECTIVES FOR FUTURE RESEARCH

The findings from the studies described above all contribute to a greater understanding of soil and plant associated bacterial fungal interactions, specifically how they are mediated and their potential outcomes. While I focus mainly on the interactions of just bacteria and fungi it

should be noted that these interactions may also impact outcomes of interactions with plant or animal hosts in the soil. The majority of the interactions described in this review are focused solely on discreet paired interactions *in vitro.* While very helpful for meticulously dissecting interactions and identifying communication signals, these findings should be validated in natural environments before evaluating their ecological significance. Further, since many of the described bacterial fungal interactions are context dependent, it will be important to also integrate environmental data into these studies as they may greatly impact the progression of BFIs in nature.

New tools for examining polymicrobial interactions will be vital to better understanding the implications of BFI signals on complex microbial consortia. Traditional coculture techniques both in liquid and solid media have proven very useful for exploring BFIs and have lead to great discoveries toward better understanding these complex interactions. As this field continues to grow there are a number of very useful methodologies that have emerged to help better explore the signals and outcomes of BFIs. I will briefly discuss some of these tools here to help guide the reader toward potentially useful methodologies for future research.

1.4.1. Imaging

Imaging of BFIs is a crucial component of understanding how microbes interact and respond to each other. Electron microscopy (EM) has been utilized by many researchers to determine how bacteria interact with fungal hyphae. Levy *et al.* utilized EM of *Burkholderia* spp. to explore colonization of *Gigaspora decipiens* spores and hyphae and found that previously undescribed fibrillar structures were used to adhere to the hyphal surface (73). Confocal microscopy has greatly improved over the past decade and many researchers have employed these techniques to explore BFIs. Because of the enhanced spatial resolution of confocal

microscopy, this technique has proven to be indispensable for exploring close associations of bacteria and fungi, especially when using fluorescence in situ hybridization to assess endosymbioses from environmental samples (74, 75). Because BFIs are temporally dynamic it is also useful to be able to monitor these interactions as they progress. While traditional time-course studies have set a groundwork for understanding general processes in bacterial fungal interactions (76), modern tools have been developed to allow continuous, non-destructive monitoring of interactions through time. Stanley *et al*. recently used novel microfluidic devices to continuously monitor interactions between *Coprinus cinerea* and *B. subtilis*, showing dynamics in attachment, growth rates, and cell-death resulting from these interactions (77). Although other examples of BFIs explored using microfluidics are limited, these devices provide an exciting new avenue for exploring microbial interactions over time at a microscopic level.

1.4.2. Metabolomics

Many new tools for studying the signaling molecules of BFIs are becoming more available to researchers. Specifically, recent advances in mass spectrometry (MS) acquisition and analysis methods have helped to elucidate novel communication signals of soil borne bacteria and fungi. Solid phase microextraction (SPME) devices are small filaments which can adsorb VOCs from the airspace of. They can then be desorbed directly into the gas chromatography MS (GCMS) for analysis. These devices have been used in cocultures as well as directly from soils to identify compounds mediating intermicrobial interactions (16, 78, 79). Another technique used for VOC profiling is the electronic nose, or e-nose, which doesn't provide specific identities of compounds in sampled air, but instead provides information about the entire profile, allowing researchers to make global comparisons between samples or to detect specific microbial profiles in the environment (80–83). To my knowledge this method hasn't been used to directly examine

paired *in vitro* BFIs, although it has been used to profile the progression of truffle aromas over time (80), which are thought to be attributable to the fungus, *Tuber*, as well as its bacterial associates (84).

For examining diffusible interactions plating colonies in opposition then extracting and assaying metabolites to examine outcomes (i.e. antibiosis, growth stimulation, chemotaxis) has been the gold standard. Many recently developed techniques are extraction free which helps reduce inherent bias of extraction methods and gives a more complete picture of the molecular interplay of microbial interactions. Imaging MS is a very promising platform for examining BFIs as it allows researchers to not only determine what compounds are in a sample, but to also map the location of those compounds to specific locations of a coculture (85). Matrix assisted laser desorption Imaging Mass Spec (MALDI-IMS) is an extraction free method that can be used to assess the mass spectral patterns of interacting microbes on solid media. This method was used to identify the fungal chlamydospore inducing compound, ralsolamycin (10), and to map the metabolic interactions and conversion of bacterial phenazines by the fungus *Aspergillus fumigatus* (86). Nanospray Desorption Electrospray Ionization Mass Spec (nanoDESI-MS) provides the ability to analyze metabolites directly from living environmental samples and provides the researcher with the precision to examine regions in the 10s of μm (87, 88). When these MS techniques are combined with modern computational analytics such as metabolic networking platforms, researchers are able to get a bigger picture of the metabolic exchange of intermicrobial interactions (89).

1.4.3. Genomics and transcriptomics

As the cost of next generation sequencing drops and more genomic data becomes available, there will be increased opportunity to understand the genetic underpinnings of BFIs.

Analyzing genomes of bacteria involved in endosymbioses (90) and mycophagy (91) have allowed a glimpse into the potential genes involved in their interactions with fungal partners. One aspect of this will be a greater opportunity to understand how genetic elements may shuffle around between members of the soil community. It is well established that horizontal gene transfer (HGT) is an important contributor to prokaryotic genome evolution, and can be mediated by transduction, transformation, and conjugation (92). There is also recent evidence that HGT occurs, although seemingly less frequently, in fungi (93). Interestingly, a few genomic studies have indicated that HGT events may occur between bacteria and fungi (61, 62). Although the mechanisms of these transfers have yet to be elucidated, it is possible that Type IV secretion systems similar to that utilized by *Agrobacterium* spp. play a role as they have been used to successfully transform fungi *in vitro* (60).

Transcriptomics tools have become increasingly important for understanding how genes are regulated during biotic interactions. Mela *et al.* used a dual transcriptomics approach to explore the bacterial genes involved in mycophagy by *Collimonas fungivorans* and the fungal response to this attack (94). These data indicated a complex interaction involving antibiosis and nutrient competition in both organisms. On the bacterial side chitinases and SMs played an important role in mycophagy, and the fungal response to attack was dominated by differential expression on genes related to cell wall and lipid degradation, nitrogen deficiency, and cell defense. Similarly, RNA-seq analysis of the plant pathogenic fungus *Rhizoctonia solani* response to challenge by bacterial biocontrol strains of *Serratia* spp. showed that both primary and secondary metabolic genes involved in activation of defense and counterattack mechanisms (toxin production) were up-regulated (95). Although there are commonalities in fungal response to bacterial antagonism in both of these studies, there is also some common ground between

positive and negative BFIs. A dual-transcriptomics microarray study of the interaction between the mycorrhizal fungus *Laccaria bicolor* and three bacterial partners (a helper strain, a commensal strain, and an antagonistic strain) showed that there were negative correlations in transcripts involved in primary metabolism between antagonistic and non-antagonistic interactions, but that the fungus had a unique response to each bacterium. Although each bacterium responded differently to the fungus, all three bacteria showed shifts in genes involved with cell wall modification, suggesting that changes to the cell wall may be an important general response to interactions with *L. bicolor* (96). The relatively small size of microbial genomes and differences in mRNA processing between prokaryotes and eukaryotes makes BFIs an ideal system to explore with dual transcriptomics. As more studies emerge using these methodologies a more cohesive understanding of "fundamental" attributes of BFIs will likely emerge.

1.5. CONCLUSIONS AND THESIS OVERVIEW

This chapter was written to provide a broad overview of the many flavors of BFIs described to date. Although its references aren't exhaustive, I've attempted to use specific examples to provide a general scope of the many modes and outcomes of BFIs as well as tool swhich may enhance future study. Although research over the past half a century has been largely biased towards antagonisms this foundational work has provided excellent insights and tools for exploring other BFIs. More recently researchers have started exploring non-antagonistic BFIs in greater detail such as: the endofungal bacterial systems, the mycorrhizal helper bacteria, and fungal mediated bacterial transport; which have broadened the scope of BFI studies. As these and other model BFI systems are established and new methodologies are integrated, our knowledge of the many interactions that have evolved between bacteria and fungi over the past 1.5 billion years will undoubtedly be awe inspiring. Some researchers suggest that microbial

produced “antibiotics” are more likely communication molecules causing shifts in physiology in target organisms under natural conditions (97, 98). Thus studying BFIs will likely lead to the discovery not only of novel metabolites but also may provide an appreciation for new functions of “old” molecules. Additionally, as more interactions are explored researchers may find novel lifestyles for organisms that have been extensively studied only outside of BFIs.

It is now well established that practically all plant tissues, internal and external, are colonized by a diversity of bacteria and fungi (99). While many of these microbes have been described and their mechanistic interactions with plants have been well documented, relatively little is known about how these microbes interact with each other. The work presented in subsequent chapters of this thesis explores the modes and outcomes of interactions between the potent bacterial wilt pathogen, *R. solanacearum,* and soil fungi. The overarching hypothesis driving this research is: *Ralstonia solanacearum* has evolved into a successful plant pathogen in a polymicrobial environment, therefore it has evolved to also interact with plant associated fungi.

Efforts to address this hypothesis led to an exploration of the volatile (Chapter 2), diffusible, and direct (Chapter 3-4) interactions of *R. solanacearum* with soil fungi. Primarily these interactions are described in the context of interactions with the mycotoxigenic fungi, *Aspergillus flavus* or *Fusarium fujikuroi*, although in all of these studies the outcomes of these interactions with other fungi were examined to determine the relative specificity of the described phenotypes. Chapter 4 specifically highlights metabolic shifts driven by *R. solanacearum* and demonstrates the interplay of abiotic and biotic conditions on BFI outcomes. An appendix listing additional work published during my PhD is included to demonstrate my other research interests beyond of BFIs.

1.6. FIGURES AND LEGENDS

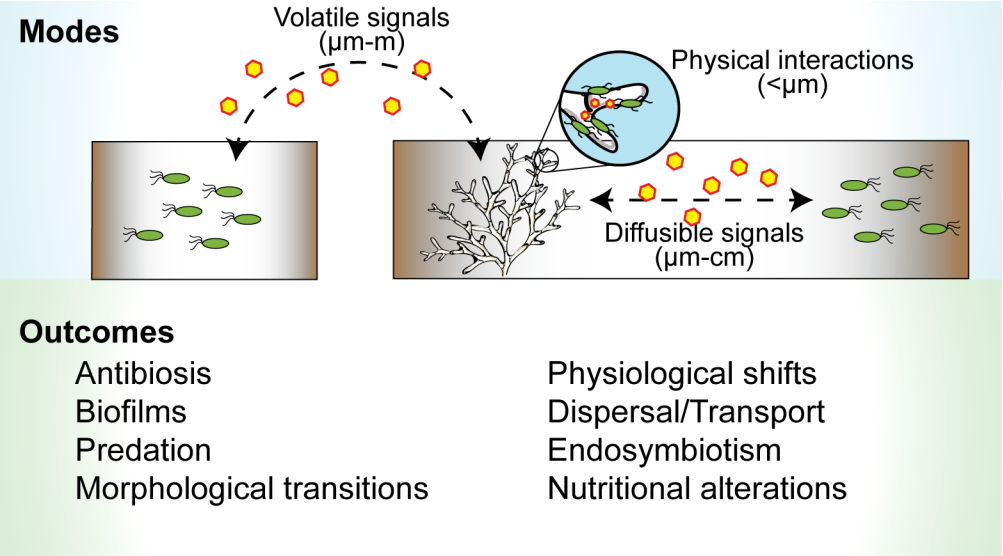

Figure 1. BFIs - Modes and outcomes of interactions

Bacterial-fungal interactions (BFIs) are encompass many modes of interactions and can involve multidirectional signaling across a range of scales (indicated in parentheses). The outcomes of BFIs can be manifold and are dynamic across time and environments. One signal may may not only alter the outcomes of interactions with the interacting partner but may in turn impact other organisms, or interactions with the abiotic environment.

1.7. REFERENCES

1. **Pal KK**, **McSpadden Gardener B**. 2006. Biological control of plant pathogens. Plant Heal Instr.
2. **Konopka A**. 2009. What is microbial community ecology? ISME J **3**:1223–30.
3. **Davies J**, **Ryan KS**. 2012. Introducing the parvome: Bioactive compounds in the

microbial world. ACS Chem Biol **7**:252–259.

4. **Cragg GM**, **Newman DJ**. 2013. Natural products: A continuing source of novel drug leads. Biochim Biophys Acta - Gen Subj **1830**:3670–3695.
5. **Fleming A**. 1929. On the antibacterial action of cultures of a *Penicillium*, with special reference to their use in the isolation of *B. influenzae*. Br J Exp Pathol **10**:226–236.
6. **Hildebrandt U**, **Ouziad F**, **Marner FJ**, **Bothe H**. 2006. The bacterium *Paenibacillus validus* stimulates growth of the arbuscular mycorrhizal fungus *Glomus intraradices* up to the formation of fertile spores. FEMS Microbiol Lett **254**:258–267.
7. **Reddy MS**, **Patrick Z a**. 1990. Effect of bacteria associated with mushroom compost and casing materials on basidiomata formation in *Agaricus bisporus*. Can J Plant Pathol Can Phytopathol.
8. **Cho YS**, **Weon HY**, **Joh JH**, **Lim JH**, **Kim KY**, **Son ES**. 2008. Effect of casing layer on growth promotion of the edible mushroom *Pleurotus* **36**:40–44.
9. **Li L**, **Ma M**, **Huang R**, **Qu Q**, **Li G**, **Zhou J**, **Zhang K**, **Lu K**, **Niu X**, **Luo J**. 2012. Induction of chlamydospore formation in *Fusarium* by cyclic lipopeptide antibiotics from *Bacillus subtilis* C2. J Chem Ecol **38**:966–974.
10. **Spraker JE**, **Sanchez LM**, **Lowe T**, **Dorrestein PC**, **Keller NP**. 2016. *Ralstonia solanacearum* lipopeptide induces chlamydospore development in fungi and facilitates bacterial entry into fungal tissues. ISME J 1–14.
11. **Gehrig H**, **Schüssler A**, **Kluge M**. 1996. *Geosiphon pyriforme*, a fungus forming endocytobiosis with *Nostoc* (cyanobacteria), is an ancestral member of the Glomales: evidence by SSU rRNA analysis. J Mol Evol **43**:71–81.
12. **Nazir R**, **Warmink JA.**, **Voordes DC**, **van de Bovenkamp HH**, **van Elsas JD**. 2013.

Inhibition of mushroom formation and induction of glycerol release-ecological strategies of *Burkholderia terrae* BS001 to create a hospitable niche at the fungus *Lyophyllum* sp. strain Karsten. Microb Ecol **65**:245–254.

13. **Netzker T**, **Fischer J**, **Weber J**, **Mattern DJ**, **König CC**, **Valiante V**, **Schroeckh V**, **Brakhage AA.** 2015. Microbial communication leading to the activation of silent fungal secondary metabolite gene clusters. Front Microbiol **6**:1–13.

14. **Whitt J**, **Shipley SM**, **Newman DJ**, **Zuck KM**. 2014. Tetramic acid analogues produced by coculture of *Saccharopolyspora erythraea* with *Fusarium pallidoroseum*. J Nat Prod **77**:173–177.

15. **Ola ARB**, **Thomy D**, **Lai D**, **Brötz-Oesterhelt H**, **Proksch P**. 2013. Inducing secondary metabolite production by the endophytic fungus *Fusarium tricinctum* through coculture with *Bacillus subtilis*. J Nat Prod **76**:2094–2099.

16. **Spraker JE**, **Jewell K**, **Roze L V.**, **Scherf J**, **Ndagano D**, **Beaudry R**, **Linz JE**, **Allen C**, **Keller NP**. 2014. A volatile relationship: Profiling an interkingdom dialogue between two plant pathogens, *Ralstonia solanacearum* and *Aspergillus flavus*. J Chem Ecol **40**:502–513.

17. **Chaurasia B**, **Pandey A**, **Palni LMS**, **Trivedi P**, **Kumar B**, **Colvin N**. 2005. Diffusible and volatile compounds produced by an antagonistic *Bacillus subtilis* strain cause structural deformations in pathogenic fungi in vitro. Microbiol Res **160**:75–81.

18. **Kohlmeier S**, **Smits THM**, **Ford RM**, **Keel C**, **Harms H**, **Wick LY**. 2005. Taking the fungal highway: Mobilization of pollutant-degrading bacteria by fungi. Environ Sci Technol **39**:4640–4646.

19. **Simon A**, **Bindschedler S**, **Job D**, **Wick LY**, **Filippidou S**, **Kooli WM**, **Verrecchia EP**,

Junier P. 2015. Exploiting the fungal highway: Development of a novel tool for the in situ isolation of bacteria migrating along fungal mycelium. FEMS Microbiol Ecol **91**:1–13.

20. **Ingham CJ**, **Kalisman O**, **Finkelshtein A**, **Ben-Jacob E**. 2011. Mutually facilitated dispersal between the nonmotile fungus *Aspergillus fumigatus* and the swarming bacterium *Paenibacillus vortex*. Proc Natl Acad Sci **108**:19731–19736.
21. **Bianciotto V**, **Genre A**, **Jargeat P**, **Lumini E**, **Bécard G**, **Bonfante P**. 2004. Vertical transmission of endobacteria in the arbuscular mycorrhizal fungus <I>Gigaspora margarita</I> through generation of vegetative spores. Appl Environ Microbiol **70**:3600–3608.
22. **Lackner G**, **Moebius N**, **Hertweck C**. 2011. Endofungal bacterium controls its host by an *hrp* type III secretion system. ISME J **5**:252–261.
23. **Hoffman MT**, **Arnold AE**. 2010. Diverse bacteria inhabit living hyphae of phylogenetically diverse fungal endophytes. Appl Environ Microbiol **76**:4063–4075.
24. **Young IM**, **Crawford JW**, **Nunan N**, **Otten W**, **Spiers A**. 2009. Chapter 4 Microbial Distribution in Soils. Physics and ScalingAdvances in Agronomy, 1st ed. Elsevier Inc.
25. **Schulz S**, **Dickschat JS**. 2007. Bacterial volatiles: the smell of small organisms. Nat Prod Rep **24**:814–842.
26. **Effmert U**, **Kalderás J**, **Warnke R**, **Piechulla B**. 2012. Volatile mediated interactions between bacteria and fungi in the soil. J Chem Ecol **38**:665–703.
27. **Mackie A.**, **Wheatley R.** 1999. Effects and incidence of volatile organic compound interactions between soil bacterial and fungal isolates. Soil Biol Biochem **31**:375–385.
28. **Wheatley RE**. 2002. The consequences of volatile organic compound mediated bacterial

and fungal interactions. Antonie van Leeuwenhoek, Int J Gen Mol Microbiol **81**:357–364.

29. **Fernando WGD**, **Ramarathnam R**, **Krishnamoorthy AS**, **Savchuk SC**. 2005. Identification and use of potential bacterial organic antifungal volatiles in biocontrol. Soil Biol Biochem **37**:955–964.

30. **Salyers AA**, **Reeves A**, **D'Elia J**. 1996. Solving the problem of how to eat something as big as yourself: Diverse bacterial strategies for degrading polysaccharides. J Ind Microbiol Biotechnol **17**:470–476.

31. **De Boer W**, **Klein Gunnewiek PJ a**, **Lafeber P**, **Janse JD**, **Spit BE**, **Woldendorp JW**. 1997. Anti-fungal properties of chitinolytic dune soil bacteria. Soil Biol Biochem **30**:193–203.

32. **Barron GL**. 2003. Predatory fungi, wood decay, and the carbon cycle. Biodiversity **4**:3–9.

33. **Thorn RG**, **Tsuneda A**. 1992. Interactions between various wood-decay fungi and bacteria: antibiosis, attack, lysis, or inhibition. Rep Tottori Mycol Inst **30**:13–20.

34. **Grant WD**, **Rhodes LL**, **Prosser BA**, **Asher RA**. 1986. Production of bacteriolytic enzymes and degradation of bacteria by filamentous fungi. Microbiology **132**:2353–2358.

35. **Pion M**, **Spangenberg JE**, **Simon A**, **Bindschedler S**, **Flury C**, **Chatelain A**, **Bshary R**, **Job D**, **Junier P**. 2013. Bacterial farming by the fungus *Morchella crassipes*. Proc R Soc - Biol Sci **280**:20132242.

36. **Kluge M**, **Mollenhauer D**, **Mollenhauer R**, **Kape R**. 1992. Geosiphon pyriforme, an endosymbiotic consortium of a fungus and a cyanobacterium (*Nostoc*), fixes nitrogen. Bot Acta **105**:343–344.

37. **Schussler A**, **Bonfante P**, **Schnepf E**, **Mollenhauer D**, **Kluge M**. 1996. Characterization of the *Geosiphon pyriforme* symbiosome by affinity techniques confocal laser-scanning

microscopy (CLSM) and electron microscopy. Protoplasma **190**:53–67.

38. **Haas D**, **Défago G**. 2005. Biological control of soil-borne pathogens by fluorescent pseudomonads. Nat Rev Microbiol **3**:307–319.

39. **Brucker RM**, **Harris RN**, **Schwantes CR**, **Gallaher TN**, **Flaherty DC**, **Lam BA**, **Minbiole KPC**. 2008. Amphibian chemical defense: Antifungal metabolites of the microsymbiont *Janthinobacterium lividum* on the salamander *Plethodon cinereus*. J Chem Ecol **34**:1422–1429.

40. **Troppens DM**, **Dmitriev RI**, **Papkovsky DB**, **O'Gara F**, **Morrissey JP**. 2013. Genome-wide investigation of cellular targets and mode of action of the antifungal bacterial metabolite 2,4-diacetylphloroglucinol in *Saccharomyces cerevisiae*. FEMS Yeast Res **13**:322–334.

41. **Schouten A**. 2004. Defense responses of *Fusarium oxysporum* to 2,4-diacetylphloroglucinol, a broad-spectrum antibiotic produced by *Pseudomonas fluorescens*. Mol Plant Microbe Interact **17**:1201–1211.

42. **Schouten A**, **Maksimova O**, **Cuesta-Arenas Y**, **Van Den Berg G**, **Raaijmakers JM**. 2008. Involvement of the ABC transporter BcAtrB and the laccase BcLCC2 in defence of *Botrytis cinerea* against the broad-spectrum antibiotic 2,4- diacetylphloroglucinol. Environ Microbiol **10**:1145–1157.

43. **Challis GL**, **Hopwood D**. 2003. Synergy and contingency as driving forces for the evolution of multiple secondary metabolite production by Streptomyces species. Proc Natl Acad Sci U S A **100** Suppl:14555–14561.

44. **Mavrodi D V.**, **Blankenfeldt W**, **Thomashow LS**. 2006. Phenazine compounds in fluorescent *Pseudomonas* spp. biosynthesis and regulation. Annu Rev Phytopathol

44:417–445.

45. **Haas D**, **Keel C**. 2003. Regulation of antibiotic production in root-colonizing *Pseudomonas* spp. and relevance for biological control of plant disease. Annu Rev Phytopathol **41**:117–53.

46. **Bacon CW**, **Hinton DM**, **Porter JK**, **Glenn AE**, **Kuldau G**. 2004. Fusaric acid, a *Fusarium verticillioides* metabolite, antagonistic to the endophytic biocontrol bacterium *Bacillus mojavensis*. Can J Bot Can Bot **82**:878–885.

47. **Son SW**, **Kim HY**, **Choi GJ**, **Lim HK**, **Jang KS**, **Lee SO**, **Lee S**, **Sung ND**, **Kim JC**. 2008. Bikaverin and fusaric acid from *Fusarium oxysporum* show antioomycete activity against *Phytophthora infestans*. J Appl Microbiol **104**:692–698.

48. **Kwon HR**, **Son SW**, **Han HR**, **Gyung Ja Choi**. 2007. Nematicidal activity of bikaverin and fusaric acid isolated *Fusarium oxysporum* against pine wood nematode, *Bursaphelenchus xylophilus*. Plant Pathol J.

49. **Bacon CW**, **Hinton DM**, **Hinton A**. 2006. Growth-inhibiting effects of concentrations of fusaric acid on the growth of *Bacillus mojavensis* and other biocontrol *Bacillus* species. J Appl Microbiol **100**:185–194.

50. **Brown DW**, **Lee S**, **Kim L**, **Ryu J**, **Lee S**, **Seo Y**, **Kim YH**, **Busman M**, **Yun S**, **Proctor RH**, **Lee T**. 2015. Identification of a 12-gene Fusaric acid biosynthetic gene cluster in *Fusarium* species through comparative and functional genomics. Mol Plant-Microbe Interact **28**:319–332.

51. **Notz R**, **Maurhofer M**, **Dubach H**. 2002. Fusaric acid-producing strains of Fusarium oxysporum alter 2, 4-diacetylphloroglucinol biosynthetic gene expression in Pseudomonas fluorescens CHA0 in vitro and. Appl Environ Microbiol **68**:2229–2235.

52. **de Weert S**, **Kuiper I**, **Lagendijk EL**, **Lamers GEM**, **Lugtenberg BJJ**. 2004. Role of chemotaxis toward fusaric acid in colonization of hyphae of *Fusarium oxysporum* f. sp. *radicis-lycopersici* by *Pseudomonas fluorescens* WCS365. Mol Plant Microbe Interact **17**:1185–1191.

53. **Bochner BR**, **Huang H**, **Schieven GL**, **Ames BN**. 1980. Positive selection for loss of tetracycline resistance. J Bacteriol **143**:926–933.

54. **Chait R**, **Shrestha S**, **Shah AK**, **Michel JB**, **Kishony R**. 2010. A differential drug screen for compounds that select against antibiotic resistance. PLoS One **5**:1–8.

55. **Li L**, **Qu Q**, **Tian B**, **Zhang KQ**. 2005. Induction of chlamydospores in *Trichoderma harzianum* and *Gliocladium roseum* by antifungal compounds produced by *Bacillus subtilis* C2. J Phytopathol **153**:686–693.

56. **Sajben E**, **Manczinger L**, **Nagy A**, **Kredics L**, **Vágvölgyi C**. 2011. Characterization of pseudomonads isolated from decaying sporocarps of oyster mushroom. Microbiol Res **166**:255–267.

57. **Soler-Rivas C**, **Jolivet S**, **Arpin N**, **Olivier JM**, **Wichers HJ**. 1999. Biochemical and physiological aspects of brown blotch disease. FEMS Microbiol Rev **23**:591–614.

58. **Cusano AM**, **Burlinson P**, **Deveau A**, **Vion P**, **Uroz S**, **Preston GM**, **Frey-Klett P**. 2011. Pseudomonas fluorescens BBc6R8 type III secretion mutants no longer promote ectomycorrhizal symbiosis. Environ Microbiol Rep **3**:203–210.

59. **Tzfira T**, **Citovsky V**. 2000. From host recognition to T-DNA integration: the function of bacterial and plant genes in the Agrobacterium-plant cell interaction. Mol Plant Pathol **1**:201–212.

60. **de Groot MJ**, **Bundock P**, **Hooykaas PJ**, **Beijersbergen a G**. 1998. *Agrobacterium*

tumefaciens-mediated transformation of filamentous fungi. Nat Biotechnol **16**:839–842.

61. **Richards TA**, **Leonard G**, **Soanes DM**, **Talbot NJ**. 2011. Gene transfer into the fungi. Fungal Biol Rev **25**:98–110.

62. **Lawrence DP**, **Kroken S**, **Pryor BM**, **Arnold AE**. 2011. Interkingdom gene transfer of a hybrid NPS/PKS from bacteria to filamentous ascomycota. PLoS One **6**.

63. **Moran Y**, **Fredman D**, **Szczesny P**, **Grynberg M**, **Technau U**. 2012. Recurrent horizontal transfer of bacterial toxin genes to eukaryotes. Mol Biol Evol **29**:2223–2230.

64. **Keeling PJ**, **Palmer JD**. 2008. Horizontal gene transfer in eukaryotic evolution. Nat Rev Genet **9**:605–618.

65. **Costa TRD**, **Felisberto-Rodrigues C**, **Meir A**, **Prevost MS**, **Redzej A**, **Trokter M**, **Waksman G**. 2015. Secretion systems in Gram-negative bacteria: structural and mechanistic insights. Nat Rev Microbiol **13**:343–359.

66. **Bingle LE**, **Bailey CM**, **Pallen MJ**. 2008. Type VI secretion: a beginner's guide. Curr Opin Microbiol **11**:3–8.

67. **Díaz EM**, **Vicente-Manzanares M**, **Sacristan M**, **Vicente C**, **Legaz M-E**. 2011. Fungal lectin of *Peltigera canina* induces chemotropism of compatible *Nostoc* cells by constriction-relaxation pulses of cyanobiont cytoskeleton. Plant Signal Behav **6**:1525–36.

68. **Varrot A**, **Basheer SM**, **Imberty A**. 2013. Fungal lectins: Structure, function and potential applications. Curr Opin Struct Biol **23**:678–685.

69. **Pohleven J**, **Renko M**, **Magister Š**, **Smith DF**, **Künzler M**, **Štrukelj B**, **Turk D**, **Kos J**, **Sabotič J**. 2012. Bivalent carbohydrate binding is required for biological activity of *Clitocybe nebularis* lectin (CNL), the N,N′-diacetyllactosediamine (GalNAcβ1-4GlcNAc,LacdiNAc)-specific lectin from basidiomycete *C. nebularis*. J Biol Chem

287:10602–10612.

70. **Trigueros V**, **Lougarre A**, **Ali-Ahmed D**, **Rahbé Y**, **Guillot J**, **Chavant L**, **Fournier D**, **Paquereau L**. 2003. *Xerocomus chrysenteron* lectin: Identification of a new pesticidal protein. Biochim Biophys Acta - Gen Subj **1621**:292–298.

71. **Hamshou M**, **Smagghe G**, **Shahidi-Noghabi S**, **De Geyter E**, **Lannoo N**, **Van Damme EJM**. 2010. Insecticidal properties of *Sclerotinia sclerotiorum* agglutinin and its interaction with insect tissues and cells. Insect Biochem Mol Biol **40**:883–890.

72. **Pistole T**. 1981. Interaction of bacteria and fungi with lectins and lectin-like substances. Annu Rev Microbiol **35**:85–111.

73. **Levy A**, **Levy A**, **Chang BJ**, **Chang BJ**, **Abbott LK**, **Abbott LK**, **Kuo J**, **Kuo J**, **Harnett G**, **Harnett G**, **Inglis TJJ**, **Inglis TJJ**. 2003. Invasion of spores of the arbuscular mycorrhizal fungus *Gigaspora decipiens* by *Burkholderia* spp. Appl Environ Microbiol **69**:6250–6256.

74. **Grube M**, **Berg G**. 2009. Microbial consortia of bacteria and fungi with focus on the lichen symbiosis. Fungal Biol Rev **23**:72–85.

75. **Hoffman MT**, **Gunatilaka MK**, **Wijeratne K**, **Gunatilaka L**, **Arnold AE**. 2013. Endohyphal bacterium enhances production of indole-3-acetic acid by a foliar fungal endophyte. PLoS One **8**:31–33.

76. **Benoit I**, **van den Esker MH**, **Patyshakuliyeva A**, **Mattern DJ**, **Blei F**, **Zhou M**, **Dijksterhuis J**, **Brakhage A a.**, **Kuipers OP**, **de Vries RP**, **Kovács ÁT**. 2014. *Bacillus subtilis* attachment to *Aspergillus niger* hyphae results in mutually altered metabolism. Environ Microbiol.

77. **Stanley CE**, **Stöckli M**, **van Swaay D**, **Sabotič J**, **Kallio PT**, **Künzler M**, **deMello AJ**,

Aebi M. 2014. Probing bacterial–fungal interactions at the single cell level. Integr Biol **6**:935–945.

78. **Chuankun X**, **Minghe M**, **Leming Z**, **Keqin Z**. 2004. Soil volatile fungistasis and volatile fungistatic compounds. Soil Biol Biochem **36**:1997–2004.

79. **Stoppacher N**, **Kluger B**, **Zeilinger S**, **Krska R**, **Schuhmacher R**. 2010. Identification and profiling of volatile metabolites of the biocontrol fungus *Trichoderma atroviride* by HS-SPME-GC-MS. J Microbiol Methods **81**:187–193.

80. **Pennazza G**, **Fanali C**, **Santonico M**, **Dugo L**, **Cucchiarini L**, **Dach?? M**, **D'Amico A**, **Costa R**, **Dugo P**, **Mondello L**. 2013. Electronic nose and GC-MS analysis of volatile compounds in *Tuber magnatum* Pico: Evaluation of different storage conditions. Food Chem **136**:668–674.

81. **Tognon G**, **Campagnoli A**, **Pinotti L**, **Dell'Orto V**, **Cheli F**. 2005. Implementation of the electronic nose for the identification of mycotoxins in durum wheat (*Triticum durum*). Vet Res Commun **29**:391–393.

82. **Pallottino F**, **Costa C**, **Antonucci F**, **Strano MC**, **Calandra M**, **Solaini S**, **Menesatti P**. 2012. Electronic nose application for determination of *Penicillium digitatum* in Valencia oranges. J Sci Food Agric **92**:2008–2012.

83. **Campagnoli A**, **Cheli F**, **Savoini G**, **Crotti a.**, **Pastori a. GM**, **Dell'Orto V**. 2009. Application of an electronic nose to detection of aflatoxins in corn. Vet Res Commun **33**:273–275.

84. **Splivallo R**, **Ottonello S**, **Mello A**, **Karlovsky P**. 2011. Truffle volatiles: From chemical ecology to aroma biosynthesis. New Phytol **189**:688–699.

85. **Watrous JD**, **Dorrestein PC**. 2011. Imaging mass spectrometry in microbiology. Nat

Rev Microbiol **9**:683–694.

86. **Moree WJ**, **Phelan V V.**, **Wu C-H**, **Bandeira N**, **Cornett DS**, **Duggan BM**, **Dorrestein PC**. 2012. Interkingdom metabolic transformations captured by microbial imaging mass spectrometry. Proc Natl Acad Sci **109**:13811–13816.

87. **Laskin J**, **Heath BS**, **Roach PJ**, **Cazares L**, **Semmes OJ**. 2012. Tissue imaging using nanospray desorption electrospray ionization mass spectrometry. Anal Chem **84**:141–8.

88. **Traxler MF**, **Kolter R**. 2012. A massively spectacular view of the chemical lives of microbes. Proc Natl Acad Sci **109**:10128–10129.

89. **Watrous J**, **Roach P**, **Alexandrov T**, **Heath BS**, **Yang JY**. 2012. Mass spectral molecular networking of living microbial colonies **109**:1743–1752.

90. **Lackner G**, **Moebius N**, **Partida-Martinez LP**, **Boland S**, **Hertweck C**. 2011. Evolution of an endofungal lifestyle: deductions from the *Burkholderia rhizoxinica* genome. BMC Genomics **12**:210.

91. **Song C**, **Schmidt R**, **de Jager V**, **Krzyzanowska, Dorota; Jongedijk E**, **Cankar K**, **Beekwilder J**, **van Veen A**, **de Boer W**, **van Veen JA**, **Garbeva P**. 2015. Exploring the genomic traits of fungus-feeding bacterial genus *Collimonas*. BMC Genomics **in press**:1–17.

92. **Ochman H**, **Lawrence JG**, **Groisman E a**. 2000. Lateral gene transfer and the nature of bacterial innovation. Nature **405**:299–304.

93. **Fitzpatrick DA**. 2012. Horizontal gene transfer in fungi. FEMS Microbiol Lett **329**:1–8.

94. **Mela F**, **Fritsche K**, **de Boer W**, **van Veen J a**, **de Graaff LH**, **van den Berg M**, **Leveau JHJ**. 2011. Dual transcriptional profiling of a bacterial/fungal confrontation: *Collimonas fungivorans* versus *Aspergillus niger*. ISME J **5**:1494–1504.

95. **Gkarmiri K**, **Finlay RD**, **Alström S**, **Thomas E**, **Cubeta M a**, **Högberg N**. 2015. Transcriptomic changes in the plant pathogenic fungus *Rhizoctonia solani* AG-3 in response to the antagonistic bacteria *Serratia proteamaculans* and *Serratia plymuthica*. BMC Genomics **16**:630.

96. **Deveau A**, **Barret M**, **Diedhiou AG**, **Leveau J**, **de Boer W**, **Martin F**, **Sarniguet A**, **Frey-Klett P**. 2014. Pairwise transcriptomic analysis of the interactions between the ectomycorrhizal fungus *Laccaria bicolor* S238N and three beneficial, neutral and antagonistic soil bacteria. Microb Ecol **69**:146–159.

97. **Davies J**. 2006. Are antibiotics naturally antibiotics? J Ind Microbiol Biotechnol **33**:496–499.

98. **Davies J**. 2013. Specialized microbial metabolites: functions and origins. J Antibiot (Tokyo) **66**:361–4.

99. **Partida-Martínez LP**, **Heil M**. 2011. The Microbe-Free Plant: Fact or Artifact? Front Plant Sci **2**:1–16.

CHAPTER 2: Profiling an interkingdom dialogue between two plant pathogens, *Ralstonia solanacearum* and *Aspergillus flavus*

This work has been published as:

Spraker J, Roze L, Jewell K, Scherf J, Linz J, Beaudry R, Allen C, Keller NP. (2014) A Volatile Relationship: Profiling an interkingdom dialogue between two plant pathogens, *Ralstonia solanacearum* and *Aspergillus flavus*. *Journal of Chemical Ecology.* **40** (5): 502-513

Dr. Ludmila Roze performed the GC-MS experiments and Mr. Jacob Scherf performed the melanin quantification.

2.1. ABSTRACT

Microbes in the rhizosphere have a suite of extracellular compounds, both primary and secondary, that communicate with other organisms in their immediate environment. Here, I describe a two-way volatile interaction between two widespread and economically important soil-borne pathogens of peanut, *Aspergillus flavus* and *Ralstonia solanacearum*, a fungus and bacterium, respectively. In response to *A. flavus* volatiles, *R. solanacearum* reduced expression of the major virulence factor extracellular polysaccharide (EPS) production. In parallel, *A. flavus* responded to *R. solanacearum* volatiles by reducing conidia production, both on plates and on peanut seeds and by increasing aflatoxin production on peanut. Volatile profiling of these organisms using solid-phase micro-extraction gas chromatography mass spectroscopy (SPME-GCMS) provided a first glimpse at the compounds that may drive these interactions.

2.2. INTRODUCTION

Soil contains a spatially and temporally complex milieu of microbes that are in constant competition for space and resources. Specifically, the microbial consortia that inhabit the environment surrounding the roots (rhizosphere) is dynamic and is composed of many cohabitating bacterial and fungal species. Rhizosphere-associated microbes rely on diverse interacting physical and chemical signals to communicate with plants, animal, and other microbes (1, 2). Many plant-associated microbes can protect plants via antibiosis or through regulation of innate plant defenses (3). Inversely, many plant pathogens can mitigate plant defense responses by disrupting the plant's ability to perceive or respond to the pathogen (4). Because plant health and productivity has motivated most studies, little research has focused on how pathogens interact in the absence of the host.

Aspergillus flavus is a ubiquitous soil-dwelling fungus and an economically important pathogen of many agricultural crops. This fungus contributes significantly to crop loss and mycotoxin contamination in many staple agricultural products world-wide, including corn and peanut (5). Notably, *A. flavus* is the most common producer of aflatoxins, the most potent natural carcinogens known (6). This fungus also was recently identified as an emerging causal agent of invasive aspergillosis in immunocompromised humans, contributing especially to disease in developing countries in the Mideast and India (7). This organism produces abundant asexual conidia, which are wind dispersed and can function as a source of secondary inoculum in grain storage conditions. A developing body of research demonstrates that *A. flavus* responds to small diffusible molecules that coordinate both growth and development and detect and respond to host compounds (8–11). Specifically, oxygenated fatty acids, known as oxylipins, regulate sexual and asexual development as well as secondary metabolite production in the Aspergilli; they also contribute to plant-host interactions (8, 12–14).

Ralstonia solanacearum is a species complex of related pathogenic bacteria with a collective host range of more than 200 plant species from over 50 plant families, causing bacterial wilt disease of many economically important agricultural crops such as potato, tomato, and peanut (15). After invading the xylem elements of plant vascular tissue, these bacteria produce substantial amounts of extracellular polysaccharides (EPS), which contributes to vascular occlusion, resulting in rapid wilt and death of the host (16). *Ralstonia solanacearum* is capable of persisting in the soil in the absence of host plants for relatively long periods of time. The mechanisms of this long-term persistence are still unclear although the bacterium has been shown to survive in proximal weed hosts (17) and in surface water (18). It also can enter a viable but nonculturable state (19). *Ralstonia solanacearum* produces a suite of quorum sensing

molecules (QSMs) such as acyl-homoserine lactones. In addition, an oxylipin quorum sensing compound, 3-hydroxy palmitic acid methyl ester (3-OH PAME) plays a major role in the global regulation of *R. solanacearum* virulence factors including EPS, cell wall-degrading enzymes, and motility (20).

While interactions between these two pathogens have not been studied previously, knowledge about their growth habits and pathogenicity on plants suggests that they interact in agricultural and possibly natural ecosystems. Both organisms are well described pathogens of peanut (5, 21). Their global distribution in soils and broad host range made them good candidates for studies of inter-microbial communication. Further, there is precedent for such interactions. *Pseudomonas* spp. can inhibit growth of soil dwelling fungi (22–24), and a recent study suggests that some *Pseudomonas* and associated species could be used as biocontrol agents to inhibit aflatoxin production by *Aspergillus* spp. in peanuts (25) Bacteria-fungal encounters are common in the rhizosphere, where volatile compounds may function as communication signals between Kingdoms (26).

Volatile organic compounds (VOCs) generally are small molecules that have a high vapor pressure under normal environmental conditions. This trait allows them to evaporate or sublime readily and freely diffuse through the air. Many microbes produce abundant VOCs, which are useful for both inter- and intra-specific communication (27). Diverse bacterial volatiles can affect fungal growth, development, and metabolism, both positively and negatively (28, 29). In contrast, few fungal volatiles have been shown to affect the growth and development of bacteria (30). Interestingly, these microbially produced VOCs can not only have significant impacts on the microbial scale, but they can also affect the fitness of plants and animals (31). Here, I demonstrate that an active volatile-mediated signaling occurs between *R. solanacearum*

and *A. flavus* when the two organisms are grown in enclosed conditions with common airspace but no physical contact. This is the first report, to my knowledge, of a two-way volatile interaction where each organism significantly affects the other's physiology and development in a volatile co-culture environment.

2.3. MATERIALS AND METHODS

2.3.1. Strains and culture conditions

All strains used in these experiments are listed in Table 1. All bacterial cultures were streaked on Casamino Acid Peptone Glucose (CPG) agar (32) and grown at 30ºC. Liquid bacterial cultures were grown from single colonies overnight in CPG broth at 30°C and 180 rpm. For all experiments these cultures then were pelleted by centrifugation at 11,000 rpm, washed twice in equal volumes of sterilized, double-distilled water, and quantified spectroscopically using OD_{600} values. Cell suspensions were adjusted to a final concentration of 2×10^9 cells/ml, and 5µl were spotted at three points on each plate; with 1×10^7 cells/spot.

Fungal cultures routinely were grown at 30°C on glucose minimal medium (GMM) (33), and conidial suspensions were made by applying a 0.01% Tween 80 solution to the plate followed by agitation with a plastic cell spreader. After collection, these conidial suspensions were quantified using a hemocytometer and appropriate dilutions were made for experiments.

2.3.2. Volatile interaction assays

All organisms were grown in sterile, open-faced 60 × 15 mm Petri plates (Fisher Scientific), in the plate bottoms (bacteria) or lids (fungi). These small plates were contained within a 150 × 15 mm Falcon Petri plate (BD Biosciences) that served as a common airspace

chamber. Conidial stocks were added to molten GMM top agar (7 g/L agar) to a final concentration of 1×10^6 spores/ml and 10 ml were added to the plate lids. Liquid cultures of bacteria were spotted onto CPG agar as described above. Plates were incubated at 30º C for 5 d before data were collected.

2.3.3. Conidial quantification on solid media

Three 1 cm diameter cores were punched from the centers of the five-day fungal cultures and transferred to a sterile round-bottom Falcon tube (BD Biosciences) containing 3ml of sterile water. The fungal mass and agar were then homogenized, and 1ml was removed from each sample for conidial quantification. Conidia were quantified by using a hemocytometer. Two technical replicates, one from each plate in the chamber, were quantified from four separate plates and pooled. Treatments were compared with students T-test using GraphPad Prism ver. 5.0 (GraphPad Software, CA - 2007).

2.3.4. Peanut assay culture conditions

Following a modified standard peanut surface sterilization and infection technique (8), peanuts were placed in the volatile co-culture chambers for 5 d. Peanut cotyledons (cv. NemaTAM, provided by James Starr of Texas A&M University) with testa and embryos removed were first separated and one half of each peanut went into either an axenic *A. flavus* group or co-cultured *A. flavus* group to maintain relative uniformity of the quality of the two test groups. An additional group of control cotyledons were maintained to assure the quality of surface sterilization methods. All cotelydons were surface sterilized in 0.05% sodium hypochlorite for 3 min, washed with sterile distilled water 3 min, washed 5 sec with 70% ethanol, and then washed with sterile distilled water for 3 min. The cotyledons were split into

two groups and immersed in 100 ml of either a 1×10^6 conidia suspension of *A. flavus* WT NRRL3357 or sterile water for 30 min with shaking every five min, and subsequently incubated in groups of 5 cotyledons at 30°C in sterile Petri dishes. Humidity was maintained by lining each dish with moistened filter paper and one central water reservoir. For *R. solanacearum* exposure, two plates inoculated in the same way as for the volatile chambers experiments described above were placed in each chamber for the length of the experiment. The axenic *A. flavus* cultures were exposed to uninoculated CPG media as a negative control. Each treatment was replicated four times. Treatments were: cotyledons inoculated with water and incubated with sterile CPG; cotyledons inoculated with water and incubated in chamber with *R. solanacearum* GMI1000; cotyledons inoculated with *A. flavus* WT NRRL3357 and sterile CPG present; cotyledons inoculated with *A. flavus* WT NRRL 3357 and with *R. solanacearum* WT growing on CPG present. This resulted in a total of 80 seeds (160 cotyledons, where 10 cotyledons were placed per volatile chamber). Two technical replicates from each plate in the chamber were pooled, and four replicates of each treatment were analyzed. Treatments were compared with students T-test using GraphPad Prism ver. 5.0.

2.3.5. Conidiation and aflatoxin analysis on peanut

Conidial quantification and aflatoxin extraction from peanut seed were carried out as previously described (34) with minor modifications. Briefly, 5 cotyledons from each test plate were harvested and ground up in 5 ml 0.01% Tween water. A 100 µl aliquot was removed from each sample, diluted and counted on a hemocytometer, and the remaining sample was used for aflatoxin extraction. Next, 2.5 ml of acetone were added and shaken on a rotary shaker for 1 h at room temperature. Samples were filtered through a Whatman paper into separate vials and 5 ml of methylene chloride (MeCl) were added, and the vials were inverted 5 times then centrifuged at

4000 rpm for 10 min to separate liquid phases. The organic phase was removed and transferred to a clean glass vial and allowed to evaporate overnight. Dried extracts were resuspended in 100 µl acetone and 10 µl were spotted onto a thin layer chromatography (TLC) plate besides an aflatoxin B1 standard. The plates were developed in 9:1 chloroform:acetone in a TLC chamber for approximately 20 min. Plates were visualized at 366 nm and spot intensities were measured using Adobe Photoshop (version 12.0.4; Adobe Systems Incorporated: San Jose, CA, USA - 2010). The absolute intensity of each spot was determined by multiplying the mean pixel intensity by the number of pixels in the selected area of the aflatoxin spot. The relative intensity of each spot was calculated by dividing the absolute intensity of each sample by the average absolute intensity of the AF standards. Two technical replicates were pooled from each of four chambers for each treatment for statistical analyses. Treatments were compared with students T-test using GraphPad Prism ver. 5.0.

2.3.6. Quantification of *R. solanacearum* EPS in vitro Using ELISA

Direct ELISA with anti-EPS antibodies was used to measure *R. solanacearum* EPS levels produced by cells of strain GMI1000 grown for 5 d in volatile co-culture experiments on solid CPG media. As a control, a known EPS-deficient *phcA* mutant was cultured axenically and assayed side-by-side with these experiments. Sterile media was handled the same way as a negative control, and all data were normalized to the readings of these wells. Cells were washed from the culture plates with 2ml sterile 1X phosphate buffered saline with Tween-20 (PBST) solution, pelleted by centrifugation at 11,0000rpm, washed twice in equal volumes of PBST and quantified spectrophotometrically using OD_{600} values. Cell suspensions were adjusted to a final concentration of $1x10^7$ cells/ml, and 100µl were loaded into each well of a polystyrene microtiter plate, centrifuged at 4000 rpm, and incubated overnight at 37ºC to evaporate liquid and adhere

cells/EPS to the ELISA plate. Once dry, the wells were washed three times with 100µl 1X PBST and inverted for 5 min to dry. The wells then were coated with the anti-*Rs* EPS antibody mAb 3.H7 by loading 100ul of cell-free supernatant from 3.H7 cell lines, and incubated overnight at 4ºC (as described previously by Peckham 2011). Again, wells were washed x 3 with 100µl volumes of PBST and inverted for 5 min to dry. A 100µl volume of a 1:2500 dilution of the secondary goat anti-mouse alkaline phosphatase conjugated antibody (Gibco, #13864-012) diluted in 1X ECM (1×PBST containing 0.4% non-fat dried milk), pH 7.4, was added and incubated for 2 h at room temperature. Wells again were washed x 3 with PBST and air dried for five min before addition of 100µl of 1mg/ml (p-nitrophenyl phosphate) PNP substrate solution (Agdia 00404/0100**)**. Wells were developed in the dark for 60 min and color intensity was quantified on a plate reader at 405 nm. Two technical replicates from each plate in the chamber were pooled, and four replicates of each treatment were analyzed. Treatments were compared with one-way ANOVA followed by Tukey's *post-hoc* test using GraphPad Prism ver. 5.0.

2.3.7. *Ralstonia solanacearum* melanin quantification

Using the same volatile chamber culture conditions as described above, 2.65 cm^3 cores from the *R. solanacearum* colonies were removed from the primary inoculation site on the plate after 5 d of growth. Each core was incubated in a covered glass test tube at room temperature overnight in 3 ml of a 1:1 acetone:water solution. The extracted melanin was measured at 335 nm (peak absorbance) to determine relative pigment concentration/sample. Two technical replicates, one from each plate in the chamber were measured from 10 separate chambers. Treatments were compared with students T-test using GraphPad Prism ver. 5.0.

2.3.8. Volatile sampling and SPME-GC/MS analysis

Volatile analysis was performed essentially as described previously (36, 37). In brief, *A. flavus* cultures, alone or in the presence of *R. solanacearum* cultures, were grown in 150 × 15 mm Falcon Petri dish (BD Labware) lid-to-lid containers sealed with 3 layers of Parafilm, for 72 h. A 65 μm polydimethylsiloxane-divinylbenzene solid phase microextraction (PDMS/DVB SPME) fiber (Supelco) was conditioned at 220°C for 1 h. Volatiles for GC/MS analysis were sampled at room temperature by placing the fiber between lids through the parafilm into the headspace. Sorption was carried out for 20 min. To explore the compounds that may be initiating responses in both organisms, I characterized the headspace volatiles produced by both organisms growing individually and in co-culture. Samples were withdrawn from each of the environments after 5 d and analyzed. Compounds in a control injection that was withdrawn from SPME fiber, glass vials, and uninoculated media were also analyzed so that these they could be excluded from the headspace analyses of both the axenic and co-culture experiments.

2.3.9. GC/MS parameters

Volatiles were cryofocused during desorption (3 min) from the fiber in an Agilent 6890 gas chromatograph (Hewlett-Packard Co., Wilmington, DE, USA) injection port. Volatiles were separated on a SPG-5 capillary column (Supelco/Sigma-Aldrich, St. Louis, MO, USA) 30 m in length with 200 μm i.d. having a film thickness 0.2 μm. Inlet: a split/splitless type, temperature 220 °C. A carrier gas was ultrapure helium at a flow rate of 2 ml/min. After removal of liquid nitrogen, the initial temperature of the column (40°C) was increased at 25°C/min to obtain 125 °C then at 50 °C/min to reach a maximum temperature of 250°C, which was maintained for 1 min. Following electron ionization of compounds, masses were detected by time-of-flight mass spectrometry (FCD-650, LECO Corp., St. Joseph, MI, USA). Detector voltage was at 1750 V, acquisition rate was 10 spectra/min, and ion source temperature was 200 °C. Preliminary

identification of metabolites was performed by comparison of their mass spectra with those of authenticated chemical standards using a mass spectrum library (National Institute for Standard Technology, Search Version 1.5, Gaithersburg, MD). Further, chromatographic retention order of volatiles, identified with MS only in both replicates, was determined by comparing their Kovats retention index (RI) with GC retention time (RT) as described before (37). The compounds which did not follow the retention order, or whose RI are unknown, were tentatively identified solely from mass spectral data.

2.4. RESULTS

2.4.1. *Aspergillus flavus* and *R. solanacearum* each affected the other's growth and development via volatile signaling

Initial volatile interaction assays revealed striking phenotypes in both organisms when cocultured, suggesting that a bipartite interaction occurred in these chambers. *Ralstonia solanacearum* cultures exposed to *A. flavus* volatiles exhibited significant physiological aberrations. These colonies were significantly less mucoid and seemed to be reduced in radial dispersal relative to the axenic control plates (**Figure 1**). On CPG agar, *R. solanacearum* produces copious EPS, which contributes to their mucoid appearance in culture. EPS is required for bacterial wilt virulence (38). Additionally, the amount of melanin secreted into the surrounding media in the co-culture chamber was visibly reduced (**Figure 1**).

Similarly, there were noticeable phenotypic differences between the axenic *A. flavus* cultures and the co-culture colonies. The most obvious difference was the drastic reduction of conidia and the production of a fluffy mycelial mat across the co-culture plates. Abundant aerial

hyphae were observed in these plates with only minimal conidiation, primarily at the edge of the plate. In contrast, the axenic *A. flavus* cultures produced abundant conidia.

2.4.2. *Ralstonia solanacearum* volatiles significantly reduced *A. flavus* conidiation and increased aflatoxin production

The fluffy, aconidial phenotype in co-culture assays suggested that *R. solanacearum* volatiles inhibited the normal asexual development of *A. flavus.* These observations were confirmed by microscopic examination of colony morphology as well as by quantification of conidia production from plate cultures (**Figure 2a**). I observed a 35-fold reduction in conidia production in the co-culture environment ($P<0.001$, $N=4$). Interestingly, these colonies showed no obvious reduction in vegetative growth.

Because the aconidial phenotype was so striking on media, I tested the hypothesis that *R. solanacearum* volatiles have a similar effect on conidiation on host seed. *I* developed a volatile co-culture assay using peanuts as the sole source of nutrients for *A. flavus* growth. A visual reduction in conidiation was observed on infected peanuts (**Figure 2b**). This was confirmed by conidial counts from infected peanuts in co-culture experiments after five days of growth. There was a significant decrease in conidial production ($P=0.008$, $N=4$) relative to *A. flavus* infected peanuts in axenic chambers (**Figure 2c**). In contrast to the reduction in conidial production, extraction and chemical analysis of the infected peanuts revealed a slight but significant ($P=0.006$, $N=4$) increase in aflatoxin production on peanuts exposed to *R. solanacearum* volatiles (**Figure 2d-e**).

2.4.3. *Ralstonia solanacearum* volatiles have variable effects on fungal conidiation

Because the decrease in conidiation in response to *R. solanacearum* volatiles was significantly decreased in co-culture, I sought to determine if these volatiles had a conserved effect on other related fungi. Using *A. flavus* as a control, I assayed *R. solanacearum* against an assortment of soil-borne Aspergilli including another plant pathogen, *A. niger*; the opportunistic human pathogens *A. fumigatus* and *A. terreus*; and the model organism, *A. nidulans*; and found that there was a variable response among the different fungi. These assays revealed that *A. flavus*, *A. nidulans* ($P<0.001$, $N=4$), and *A. niger* ($P=0.010$, $N=4$) conidiation levels were significantly affected by *R. solanacearum* volatiles (**Figure 3**). While *A. flavus* and *A. nidulans* had decreased conidiation, *A. niger* showed increased conidiation in the co-culture environment. Neither of the opportunistic human pathogens were significantly altered in their conidial production in co-culture ($P>0.4$, $N=4$).

2.4.4. *Aspergillus flavus* volatiles significantly reduced *R. solanacearum* growth, EPS, and melanin production

Ralstonia solanacearum colony morphology in co-culture chambers was very different from that of bacteria growing in axenic chambers. Notably, these colonies appeared far less mucoid and produced significantly less brown pigment in the media surrounding the colonies. Cell density of the *R. solanacearum* colonies was measured spectrophotometrically to compare growth in axenic vs. co-culture environments. In the co-culture environment, *R. solanacearum* cell numbers were decreased four-fold, suggesting that the *A. flavus* VOCs were retarding bacterial growth (**Figure 4a**).

The mucoid appearance of *R. solanacearum* colonies is the result of extracellular polysaccharide (EPS). This complex mixture of branched N-acetylated galactosamines is a well-characterized bacterial wilt virulence factor; EPS-deficient strains colonize plants poorly and

cause little or no disease (39). Using a monoclonal antibody specific to *R. solanacearum* EPS (3.H7), I measured cell-associated EPS from *R. solanacearum* cultures grown in co-culture environments by ELISA. The data indicate a significant reduction in EPS production per cell in the co-culture environment ($P = 0.003$), showing a nearly five-fold reduction in EPS production. This level of EPS production is comparable to that produced by an axenic culture of a *phcA* mutant (**Figure 4b**). PhcA (Phenotype conversion) is a known global regulator of many virulence-associated genes, including those responsible for EPS production (40). The level of EPS production was not significantly different from those produced by the *phcA* mutant in axenic culture under the same conditions ($P = 0.369$).

I also quantified *R. solanacearum* melanin production by extracting pigments from media of bacterial cultures and measuring the optical absorbance at 335 nm. Melanin production was significantly reduced in the co-culture chambers ($P < 0.001$), showing a 2.5-fold decrease relative to the axenic cultures (**Figure 4c**). These data support initial visual assessments, and quantify the global impacts of *A. flavus* volatiles on *R. solanacearum* cultures.

2.4.5. Profiling of the *R. solanacearum*, *A. flavus*, and co-culture headspace volatile compounds

The apparent interkingdom volatile interactions between *A. flavus* and *R. solanacearum* lead me to hypothesize that they may have overlapping volatile profiles. A variety of chemical families were identified via SPME-GCMS analyses, indicating the complexity of the potential perceived signals of either organism. Those that were present in both replicates for each culture condition, but not present in media are presented in Table 2. The majority of the compounds from either organism were short-chain aliphatics with a large diversity of functional groups. In

total thirty *R. solanacearum*, fourteen *A. flavus*, and sixteen co-culture volatiles were extracted from this dataset based on repeatable measurement and tentative NIST identification.

Comparisons of the predicted volatile components of the axenic cultures showed that eight compounds were produced by both organisms, but twenty-two compounds were unique to *R. solanacearum* while only six were unique to *A. flavus* (**Figure 5a**). Of the eight common to both microbes, only four were detected in co-culture, while the others were at levels below detection using the methods described here. Similarly, five *A. flavus* and fifteen *R. solanacearum* volatiles were detected in axenic cultures but were below the level of detection in the co-culture environment (**Table 2**). While nine of the co-culture volatiles showed less than a 5-fold change in production between the axenic and co-culture experiments, three compounds actually showed a >10-fold change in production, including: propiolic acid; butanoic acid 3-methyl-methyl ester; and (5s)-benzyloxymethyl-4-methyl-2(5H)-furanone (**Figure 5b**). Interestingly, 1-methoxy-1-buten-3-yne, 2-methyl-butane, 2,4,4-trimethyl-1-pentene, and 4,4-dimethyl-1-pentene were unique to the co-culture experiments, suggesting that they may either play a role in the interkingdom communication or may be biomarkers for the physiological changes that are resultant of this interkingdom communication.

2.5. DISCUSSION

Microbial volatiles have been the focus of many studies over the past 20 years as they have many potential applications, including detection and diagnosis of disease and control of food and feed contaminating microbes. Both bacterial and fungal diseases, and even aflatoxin contamination by *Aspergillus* strains, can be detected and sometimes diagnosed based on their VOC profile using electronic noses (41–44). Microbial VOCs can vary significantly from organism to organism, and have even been used to differentiate the human pathogen

Mycobacterium tuberculosis from closely related *Mycobacteria* species (45). Volatile compounds also have been explored for their potential application in food safety as researchers have sought to identify compounds that will reduce microbial growth in pre- or post-harvest agricultural products (46, 47). To this end, many researchers have examined solely the effects of the volatiles of one organism on the other, but to my knowledge, none have explored whether both organisms can participate in a two-way interkingdom volatile dialogue. This question was addressed in the present study.

When *R. solanacearum* and *A. flavus* were first cultured together in common air-space chambers, the phenotypic response was striking, as shown in **Figure 1**. The reduction in conidiation by *A. flavus* on media in co-culture was significant (**Figures 2 and 3a**). This may be a relatively common response for some fungi as suggested by my experiments with other bacteria (**Figure S1**) as well as previous findings that exposure to *Bacillus subtilis* VOCs caused significant aberrations in conidiation, including arrest, in a variety of fungal species (48). Similarly, VOCs produced by *Streptomyces alboflavus* have been shown to reduce conidiation in *Fusarium monoliforme* (49). Interestingly, data from other Aspergilli suggests that even closely related fungi can have variable responses to the same bacterial volatiles (**Figure 3, Figure S2**), and further work is necessary to determine if a common volatile signal is responsible for this range of phenotypes. The reduction in conidiation on host seed was also significant (**Figure 4 b-c**) in co-culture, although less-so than on media, likely indicative of the additional complexity of introduction of a living host to the co-culture. Interestingly, when aflatoxin levels were analyzed from infected seed, there was an increased amount of AFB1 in the co-culture environment. While an increased production of aflatoxins in response to microbial volatiles has not been described before, the purified volatile 2-ethyl-1-hexanol has been shown to increase aflatoxin

production in *A. parasiticus* (50). Sporulation has been both positively and negatively correlated with mycotoxin production in *Aspergillus* spp. Two studies have demonstrated an inverse relationship between conidiation and aflatoxin production in *A. flavus* that is regulated in a density dependent manner (8, 10). More commonly, VOCs are associated with simultaneous reductions in conidiation and/or fungal growth with aflatoxin (50–52).

When *R. solanacearum* was exposed to *A. flavus* volatiles the reduction in melanin and EPS production was significant (**Figures 1 and 4**) suggesting a significant physiological shift in bacterial metabolism. A reduction in cell density also was observed in these cultures, which may suggest some antibacterial or bacteriostatic properties of the *A. flavus* volatiles. While no published data demonstrate a response of this bacterial pathogen to volatiles from other organisms, *R. solanacearum* produces a unique volatile quorum sensing compound, 3-OH PAME, which regulates a variety of virulence factors in a density dependent manner (53, 54). The synthesis of 3-OH PAME is dependent on a methyltransferase, PhcB, and mutation of the *phcBSR* operon results in a reduction in EPS I production, decreased production of cell wall degrading enzymes, and increased motility (55). While melanin production has not yet been shown to be a significant virulence factor in *R. solanacearum,* it should be noted that polyphenol oxidase-produced melanins such as those produced by *R. solanacearum,* (56) are known to function in a protective capacity in other microbes (57).

Using SPME-GCMS, preliminary volatile profiling of the co-culture airspace provided a glimpse at what type of compounds may be involved in this interkingdom communication. Interestingly, four compounds were not detected in either axenic culture but were present in the co-culture environment. Two of these were related pentenes (**Table 2**) that are structurally similar to a VOC identified both in media and *A. flavus* airspace as 2,4,4-trimethyl-2-pentene

(**Table S1**). Another of the co-culture VOCs was isopentane (or 2-methyl-butane) and likely is produced by *R. solanacearum* since this organism seems to be responsible for most of the related alkanes identified in this study such as butane and butanoic acid. The fourth unique co-culture VOC, 1-methoxy-1-buten-3-yne, has been recorded to be produced by a single aflatoxigenic strain (13A) in a survey of volatiles produced on non-sterile cracked corn by seven aflatoxigenic strains (including NRRL 3357) and one atoxigenic strain of *A. flavus.* (58). Because these compounds unique to the co-culture environment have not been characterized for their biological effect on other organisms, it is difficult to ascertain whether they are responsible for the phenotypes observed. Alternatively, they may be produced in response to the interaction itself. Notably these methods only provide tentative identification for many of these volatile compounds, but future experimentation with purified volatiles will be carried out to determine if one or many of them are directly responsible for all of the phenotypes that we've observed for both organisms.

There were eight volatiles produced both by *A. flavus* and *R. solanacearum* in axenic culture, which provide some insight into shared signaling compounds that may be playing a role in the interkingdom crosstalk (**Figure 5a**). Four of these were not detectable in the co-culture experiment, which may indicate that pathways responsible for producing these compounds are turned off, or that the volatiles are being consumed or otherwise squelched. Of the detectable four volatiles, most were changed only a few-fold in co-culture (**Figure 5b**), but propiolic acid was significantly decreased in the co-culture environment. Propiolic acid does not have a well characterized biological function in fungi, but it is a potent inhibitor of methanogenesis in ruminal bacterial culture and also reduces the total volatile fatty-acid production of these cultures, while selectively increasing *Ruminococcus* spp. population sizes relative to other rumen

inhabiting bacteria *in vitro* (59). Since both organisms produce propiolic acid, it is possible that the greater than 15-fold decrease in concentration is responsible for some of the observed phenotypes in co-culture. This subset of volatiles common to both microbes are the primary focus of ongoing research in our lab as we aim to determine if these compounds are signals in both interkingdom interactions and autoregulation.

Interkingdom crosstalk between human pathogenic bacteria and fungi has been described before, resulting in alterations in development and secondary metabolite production. The *Pseudomonas aeruginosa* quorum sensing compound, N-3-oxo-C12 homoserine lactone (3OC12HSL), represses *Candida albicans* filamentation without affecting its growth rate (60). Alternatively, the *C. albicans* produced quorum sensing compound farnesol has been shown to reduce the production of pyocyanin via reduced production of a *Pseudomonas* quinolone signal (61). As described earlier, both *A. flavus* and *R. solanacearum* use similar oxygenated aliphatic compounds to regulate density-dependent physiology and development. While it is possible that the respective QSMs of these organisms may be affecting the development of the other, none of the known QSMs from either organism were detected with the methodologies used here. The phenotypes that I observed are likely not the result of just one volatile compound, but instead a complex blend of compounds each having some less-than-total effect on the recipient microbe. The major aim of this experimentation was to observe and document a two-way interkingdom interaction mediated by VOCs. It is well known that nearly all plant tissues are colonized by microbes, both harmful and beneficial, and often these interactions are dependent on the current biotic and abiotic conditions (62). The data presented here suggest that the VOCs in this interkingdom interaction may mediate the virulence traits of these pathogens in association with host peanuts. Further research into the specific chemical species that influence these traits may

further elucidate how multiple pathogens may interact to determine the outcome of plant-pathogen interactions.

Importantly, the interactions described here occurred in an artificial culture environment, and their biological relevance remains to be determined during survival in soil or co-infection of whole peanut plants. However, the parallel decrease in co-cultured *A. flavus* conidiation observed in culture and on peanut seeds suggests that at least this response is comparable in culture and *in planta*. This study highlights the potential impact of microbial volatiles in an ecological arena. Many of the compounds are likely aiding in niche securement and colony establishment through tempering of normal physiological behavior of other microorganisms. The spatial and temporal range of these compounds greatly increases the potential interaction radius of the producing microbe, thus contributing to the dynamic nature of the soil microbiome. While the complexities of microbial volatile communication between two microbes can be difficult to grapple with, continued research in this field will surely expose that the interplay of volatiles from a variety of soil microbes plays an important role shaping soil microbial ecology.

2.6. ACKNOWLEDGEMENTS

This material is based upon work supported by the National Science Foundation under grant no. EFRI-1136903 to N.P.K. and an NSF Graduate Research Fellowship under grant no. DGE-1256259 to J.E.S. I thank Dr. Gabriel Peckham at Black Ivory Biotech for the 3.H7 cell lines, and James Starr of Texas A&M University for peanuts used in these experiments.

2.7. FIGURES AND LEGENDS

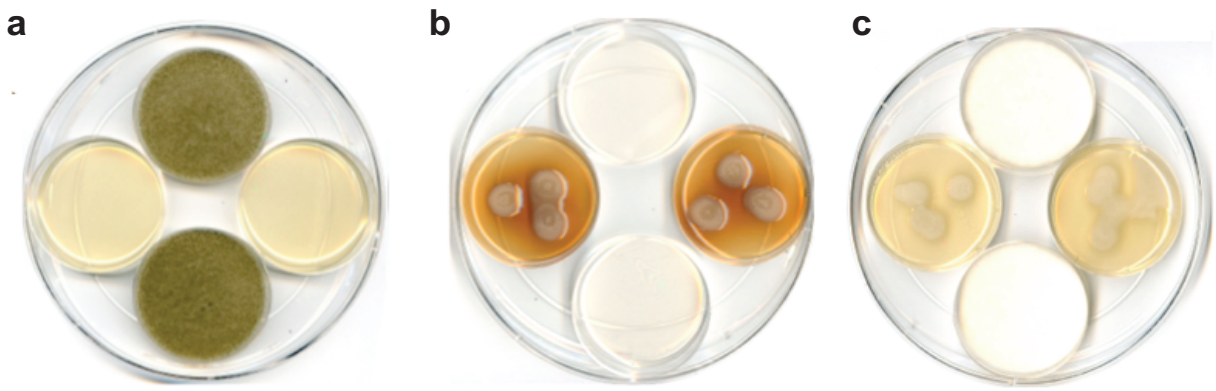

Figure 1. Volatile interaction of *Aspergillus flavus* and *Ralstonia solanacearum* alters growth and development of both organisms

a) *A. flavus* grown axenically in volatile chamber showing normal conidiation pattern, **b)** *R. solanacearum* grown axenically showing normal extracellular polysaccharide (EPS) production and pigment production, **c)** Co-culture of *A. flavus* and *R. solanacearum* in volatile chamber showing reduced *A. flavus* conidiation and reduced *R. solanacearum* EPS and melanin production.

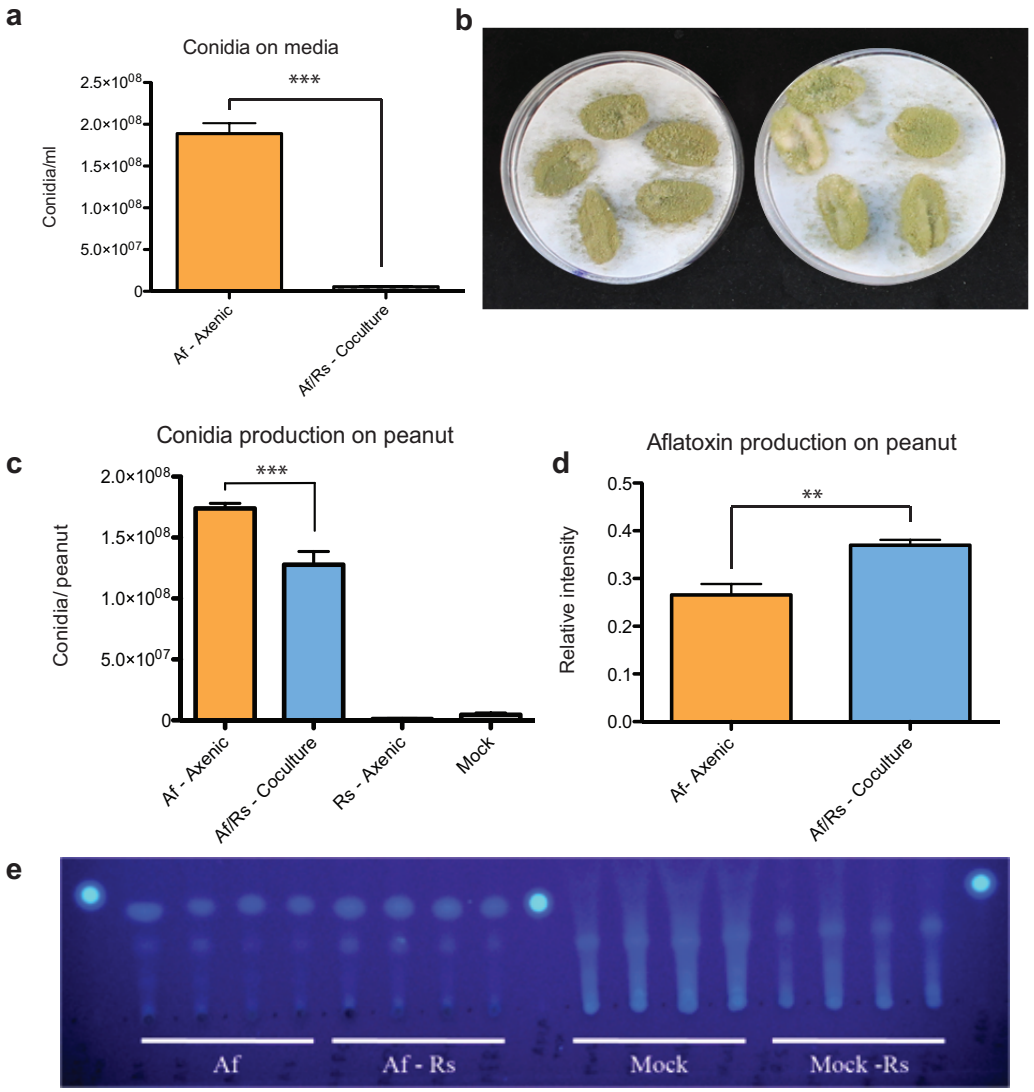

Figure 2. *Aspergillus flavus* conidia production is significantly reduced by *Ralstonia* volatiles but aflatoxin production is not affected.

a) Mean ± SEM of conidia counts from media. *T*-test indicates significant difference between axenic and co-culture conidiation ($P<0.001$, $N = 4$). **b)** Representative plates showing conidiation habit of *A. flavus* on peanut cotyledons in both axenic (left) and co-culture (right) chambers. **c)** Mean ± SEM of conidia counts on peanut. T-test indicates a significant difference between axenic and co-culture conidiation ($P=0.008$, $N=4$). **d)** Relative quantification of aflatoxin B1

from axenic and co-culture conditions. **e)** TLC analysis indicates that there is no significant difference in aflatoxin production on peanut between *A. flavus* axenic (Af) and co-culture (Af-Rs).

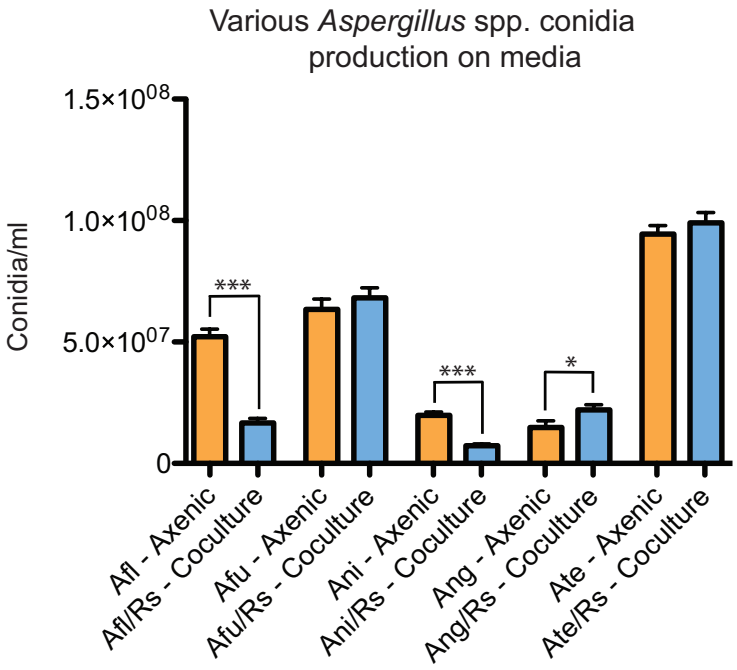

Figure 3. *Ralstonia solanacearum* volatiles have variable effects on fungal conidiation.

Mean ± SEM of conidia counts from media of different Aspergilli. T-test indicates a very significant difference ($P<0.001$, $N=4$) between axenic and co-cultures for *A. flavus* and *A. nidulans*; and a significant difference ($P=0.0104$, $N=4$) for *A. niger*. Abbreviations are as follows: Afl – *A. flavus*, Afu – *A. fumigatus*, Ani – *A. nidulans*, Ang – *A. niger*, Ate – *A. terreus*, Rs – *R. solanacearum*.

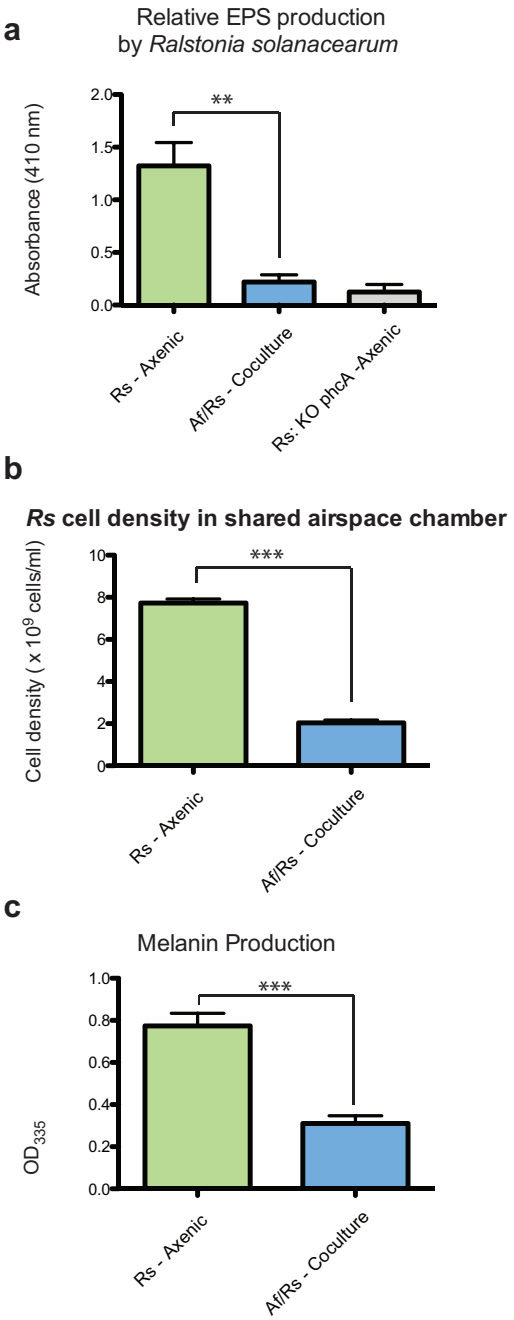

Figure 4. *Aspergillus flavus* volatiles significantly reduce *Ralstonia solanacearum* growth, extracellular polysaccharide (EPS), and melanin production

a) *A. flavus* (Af) volatiles significantly reduce *R. solanacearum* (Rs) growth in coculture (N=4, P<0.001) EPS production when *R.* solanacearum (Rs) is grown in co-culture. Results shown are

expressed as the mean + SEM of EPS ELISA measurements at 405 nm. **b)** Rs cell density was reduced significantly in coculture with Af (N=4, $P<0.0001$). Results shown are expressed as the mean + SEM of cell density as calculated based on measurement of OD600 from washed cultures. **c)** Rs melanin production was significantly reduced in response to coculture (N=10, $P<0.0001$). Results shown are expressed as the mean + SEM of extracted melanin as measured by OD 335.

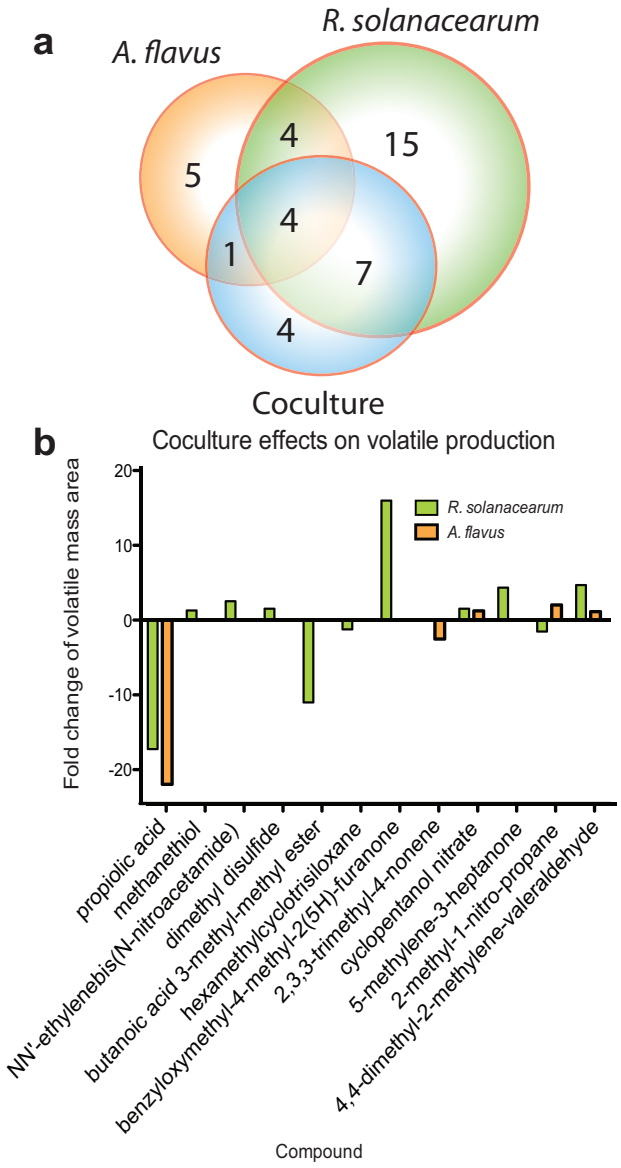

Figure 5. Comparisons of volatile organic compound (VOC) profiles indicate some similarities

a) Venn diagram showing the similarities and differences between volatile profiles detected for each organism, both in axenic and co-culture conditions. **b)** Comparisons of mean values show differences in detection of each of the identified microbial compounds between axenic and co-culture environments (data provided in Table S2).

2.8. TABLES

Table 1. Bacterial and fungal cultures utilized for these experiments.

Strains	Relevant characteristics/genotype	Reference
Fungal strains		
Aspergillus flavus - NRRL 3357	Wild type, isolated from peanut	He et al. 2007
Aspergillus fumigatus - Af293	Wild type, isolated from aspergillosis patient	Nierman et al. 2005
Aspergillus nidulans - FGSCA4	Wild type	McCluskey et al. 2010
Aspergillus niger - CBS513.88	Wild type	Pel et al. 2007
Aspergillus terreus - NIH 2624	Wild type (synonymous - FGSCA1156)	McCluskey et al. 2010
Bacterial strains/ mutants		
Ralstonia solanacearum - GMI1000	Wild type, isolated from tomato (French Guyana)	Boucher et al. 1987
R. solanacearum - Δ*phcA*	*phcA::GmR* in GMI1000	Schneider et al. 2009
Pseudomonas aeruginosa - PA14	Wild type, clinical isolate UCBPP-PA14	Rahme et al. 1995
Escherichia coli - DH5 α	Derived from *E. coli* strain DH5	Hanahan 1985

Table 2. Tentative volatiles detected from SPME-GCMS experiments, grouped by chemical family.

Compounds produced by *A. flavus* are indicated by *Af* while compounds produced by *R. solanacearum* are indicated by *Rs.* Those marked with a question mark (?) are only detected in the co-culture chamber so no producing organism could be identified. All volatiles that were detected in the co-culture chambers are marked with an asterisk (*). [a] Indicates compounds whose retention order further support their identities.

Chemical Family	Volatile Organic Compounds	Producing Organism
alcohol	2,2,4-trimethyl-3-penten-1-ol[a]	*Rs*
	1-butanol[a]	*Rs,Af*
	cyclopentanol, nitrate[a]	*Rs,Af**
aldehyde	4,4-dimethyl-2-methylene-valeraldehyde[a]	*Rs,Af**
alkane	2,2,4-trimethylpentane[a]	*Af*
	2-heptyl-1,3-dioxolane[a]	*Af*
	2-chloro-2-nitro-propane[a]	*Rs*
	propane	*Rs*
	butanoic acid, methyl ester[a]	*Rs*
	butane	*Rs*
	1-(2,2-dichloro-1-methylcyclopropyl)-2,2-dimethylpropane	*Rs*
	3-chloro-1,1,2,2-tetramethylcyclopropane	*Rs*
	chloroform[a]	*Rs,Af*
	2-methyl-1-nitropropane[a]	*Rs,Af**
	2-methylbutane[a]	?*
alkene	3,3,4,4-tetrafluoro-1,5-hexadiene	*Af*
	2,3,3-trimethyl-4-nonene	*Af**
	spiro[2.4]hepta-4,6-diene[a]	*Rs*
	2,4,4-trimethyl-1-pentene[a]	?*
	4,4-dimethyl-1-pentene	?*
alkyl	1-methylpentylhydroperoxide	*Rs*
alkyne	1-methoxy-1-buten-3-yne[a]	?*
amide	N,N'-ethylenebis(N-nitroacetamide)	*Rs**
amine	3-fluoro-á,5-dihydroxy-N-methyl-benzeneethanamine	*Af*
	2,5-dimethoxy-4-(methylsulfone)amphetamine	*Rs,Af*
	O-(2-methylpropyl)-hydroxylamine	*Rs,Af*
benzene	ethylbenzene[a]	*Rs*
carboxylic acid	propiolic acid	*Rs,Af**
ester	ethanethioic acid S-methyl ester[a]	*Rs*
	butanoic acid 3-methyl-, methyl ester[a]	*Rs**
ketone	acetone[a]	*Rs*
	benzyloxymethyl-4-methyl-2(5H)-furanone	*Rs**
	5-methylene-3-heptanone[a]	*Rs**
	5-methyl-5-hepten-3-one[a]	*Rs*
	4-methyl-6-hepten-3-one	*Af*
nucleotide	2-amino-5-chloropyrimidine	*Rs*
siloxane	hexamethylcyclotrisiloxane	*Rs**
thioether	dimethyl sulfide[a]	*Rs*
thiol	methanethiol[a]	*Rs**
	dimethyl disulfide[a]	*Rs**

2.9. SUPPLEMENTARY FIGURES AND LEGENDS

2.9.1. Supplementary figures

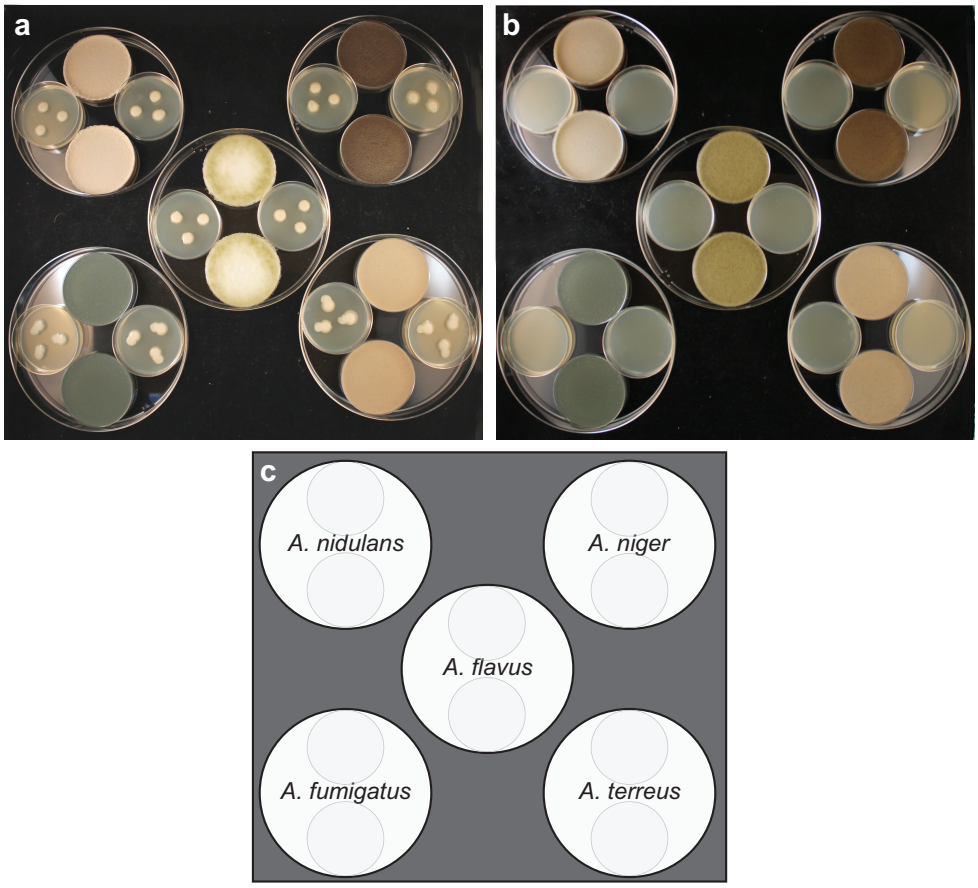

Fig S1. *R. solanacearum volatiles have variable effects on fungal conidiation*

a) Photos of representative conidiation of different Aspergilli in axenic culture **b)** Photos of representative conidiation of different Aspergilli in co-culture **c)** Key to layout of photo for panels **a** and **b.**

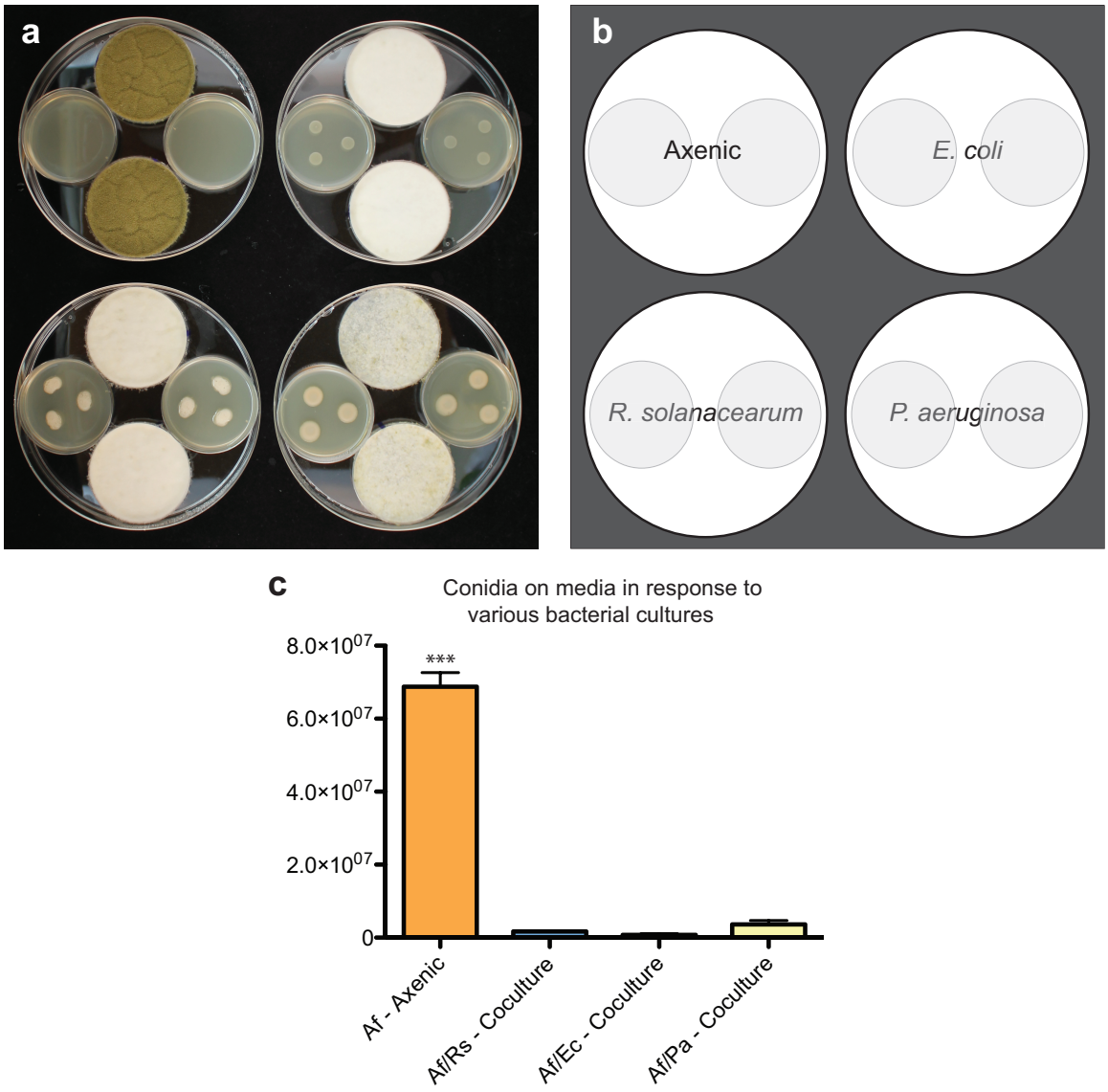

Fig S2. *A. flavus produces less conidia in response to various bacteria*

a) Photos of representative differential conidiation of *A. flavus* in response to co-culture with various bacteria **b)** Key to layout of photo for panel **a**. **c)** Mean + SEM of conidial counts in response to co-culture with different bacteria. *Asterisks* indicate statistical significance according to one-way ANOVA followed by Tukey's *post-hoc* test ($p<0.0001$, N=4).

2.9.2. Supplementary tables

Table S1. *Total compiled data from SPME-GCMS experiments.* Detectable quantities for each run shown, as well as their difference and average value.

Culture Condition	Compound name	Quant - Run1	Quant - Run2	Difference	Average
Media only	1-Propene, 2-methyl-, tetramer	5746	3944	1802	4845
Media only	1-Propene, 2-methyl-, trimer	73301	58682	14619	65991.5
Media only	1,3-Dioxolane, 2-heptyl-	4671	4224	447	4447.5
Media only	2-Hexene, 5,5-dimethyl-, (Z)-	679	483	196	581
Media only	2-Nonen-1-ol	2248	1633	615	1940.5
Media only	2-Pentene, 2,4,4-trimethyl-	81140	64289	16851	72714.5
Media only	2,3,4-Trimethyl-hex-3-enal	500	349	151	424.5
Media only	3-Cyclopropylcarbonyloxytridecane	28	410	382	219
Media only	3-Hexadecyloxycarbonyl-5-(2-hydroxyethyl)-4-methylimidazolium ion	3016	306	2710	1661
Media only	3,6-Octadecadiynoic acid, methyl ester	412	87	325	249.5
Media only	5-Methyl-1-hexyn-3-ol	407	1519	1112	963
Media only	Acetic acid, hydroxy-	11899	12808	909	12353.5
Media only	Benzaldehyde	17970	18525	555	18247.5
Media only	Bicyclo[4.2.0]octa-1,3,5-triene	995	75410	74415	38202.5
Media only	Diazene, bis(1,1-dimethylethyl)-	8605	7127	1478	7866
Media only	Heptane, 2-bromo-	692	14675	13983	7683.5
Media only	Heptane, 3-bromo-	495	7647	7152	4071
Media only	Methanesulfonyl azide	1391	495	896	943
Media only	Oxygen	31756	22811	8945	27283.5
Media only	Pentanal	3643	5549	1906	4596
Media only	Propane, 2,2-dimethyl-	195603	161506	34097	178554.5
Media only	Unknown 1	716030	703297	12733	709663.5
Af- Axenic	1-Butanol	329	7208	6879	3768.5
Af- Axenic	1-Propene, 2-methyl-, trimer	6481	60078	53597	33279.5
Af- Axenic	1,3-Dioxolane, 2-heptyl-	2549	2280	269	2414.5
Af- Axenic	1,5-Hexadiene, 3,3,4,4-tetrafluoro-	40	3538	3498	1789

Af- Axenic	2-Pentene, 2,4,4-trimethyl-	170187	69474	100713	119830.5
Af- Axenic	2,5-Dimethoxy-4-(methylsulfone)amphetamine	317	205	112	261
Af- Axenic	4-Nonene, 2,3,3-trimethyl-, (E)-	3293	804	2489	2048.5
Af- Axenic	6-Hepten-3-one, 4-methyl-	9549	2890	6659	6219.5
Af- Axenic	Benzeneethanamine, 3-fluoro-á,5-dihydroxy-N-methyl-	359	1403	1044	881
Af- Axenic	Bicyclo[4.2.0]octa-1,3,5-triene	25703	44373	18670	35038
Af- Axenic	Chloroform	14472	11424	3048	12948
Af- Axenic	Cyclopentanol, nitrate	4748	1186	3562	2967
Af- Axenic	Hydroxylamine, O-(2-methylpropyl)-	690	1634	944	1162
Af- Axenic	Pentane, 2,2,4-trimethyl-	1937	310	1627	1123.5
Af- Axenic	Propane, 2-methyl-1-nitro-	322	137	185	229.5
Af- Axenic	Propane, 2,2-dimethyl-	510166	312598	197568	411382
Af- Axenic	Propiolic acid	246976	4704	242272	125840
Af- Axenic	Valeraldehyde, 4,4-dimethyl-2-methylene-	20583	9702	10881	15142.5
Rs- Axenic	(-)-(5s)-Benzyloxymethyl-4-methyl-2(5H)-furanone	1669	680	989	1174.5
Rs- Axenic	1-Butanol	208	90641	90433	45424.5
Rs- Axenic	1-Propene, 2-methyl-, trimer	97433	59665	37768	78549
Rs- Axenic	2-Amino-5-chloropyrimidine	125	836	711	480.5
Rs- Axenic	2,5-Dimethoxy-4-(methylsulfone)amphetamine	32516	90	32426	16303
Rs- Axenic	3-Heptanone, 5-methylene-	1944	1369	575	1656.5
Rs- Axenic	3-Penten-1-ol, 2,2,4-trimethyl-	2058	980	1078	1519
Rs- Axenic	5-Hepten-3-one, 5-methyl-	569	944	375	756.5
Rs- Axenic	Acetone	683524	29055	654469	356289.5
Rs- Axenic	Bicyclo[4.2.0]octa-1,3,5-triene	65979	147797	81818	106888
Rs- Axenic	Butane	6606	4612	1994	5609
Rs- Axenic	Butanoic acid, 3-methyl-, methyl ester	241535	170100	71435	205817.5
Rs- Axenic	Butanoic acid, methyl ester	19905	775	19130	10340
Rs- Axenic	Chloroform	19948	10836	9112	15392
Rs- Axenic	Cyclopentanol, nitrate	2996	1773	1223	2384.5
Rs- Axenic	Cyclopropane, 3-chloro-1,1,2,2-tetramethyl-	2819	28576	25757	15697.5
Rs- Axenic	Cyclotrisiloxane, hexamethyl-	19102	19067	35	19084.5
Rs- Axenic	Dimethyl sulfide	405	652	247	528.5
Rs- Axenic	Disulfide, dimethyl	76432	38823	37609	57627.5
Rs- Axenic	Ethanethioic acid, S-methyl ester	54680	41115	13565	47897.5

Rs- Axenic	Ethylbenzene	108958	70297	38661	89627.5
Rs- Axenic	Hydroperoxide, 1-methylpentyl	150	1514	1364	832
Rs- Axenic	Hydroxylamine, O-(2-methylpropyl)-	1436	389	1047	912.5
Rs- Axenic	Methanethiol	8300	975	7325	4637.5
Rs- Axenic	N,N'-Ethylenebis(N-nitroacetamide)	23348	423	22925	11885.5
Rs- Axenic	Propane	392	464	72	428
Rs- Axenic	Propane, 1-(2,2-dichloro-1-methylcyclopropyl)-2,2-dimethyl-	618	310	308	464
Rs- Axenic	Propane, 2-chloro-2-nitro-	298	58349	58051	29323.5
Rs- Axenic	Propane, 2-methyl-1-nitro-	384	1034	650	709
Rs- Axenic	Propane, 2,2-dimethyl-	127472	79950	47522	103711
Rs- Axenic	Propiolic acid	153916	43532	110384	98724
Rs- Axenic	Spiro[2.4]hepta-4,6-diene	44161	27628	16533	35894.5
Rs- Axenic	Valeraldehyde, 4,4-dimethyl-2-methylene-	6285	1031	5254	3658
Co-culture	(-)-(5s)-Benzyloxymethyl-4-methyl-2(5H)-furanone	21626	15934	5692	18780
Co-culture	1-Methoxy-1-buten-3-yne	774	708	66	741
Co-culture	1-Pentene, 2,4,4-trimethyl-	7881	4071	3810	5976
Co-culture	1-Pentene, 4,4-dimethyl-	2116	35457	33341	18786.5
Co-culture	1-Propene, 2-methyl-, trimer	213886	83823	130063	148854.5
Co-culture	2-Pentene, 2,4,4-trimethyl-	113053	78977	34076	96015
Co-culture	3-Heptanone, 5-methylene-	9249	5121	4128	7185
Co-culture	4-Nonene, 2,3,3-trimethyl-, (E)-	537	1089	552	813
Co-culture	Bicyclo[4.2.0]octa-1,3,5-triene	127580	148749	21169	138164.5
Co-culture	Butane, 2-methyl-	1919	1842	77	1880.5
Co-culture	Butanoic acid, 3-methyl-, methyl ester	20448	16961	3487	18704.5
Co-culture	Cyclopentanol, nitrate	4952	2380	2572	3666
Co-culture	Cyclotrisiloxane, hexamethyl-	17546	13164	4382	15355
Co-culture	Disulfide, dimethyl	98263	78886	19377	88574.5
Co-culture	Methanethiol	7120	4818	2302	5969
Co-culture	N,N'-Ethylenebis(N-nitroacetamide)	59848	542	59306	30195
Co-culture	Propane, 2-methyl-1-nitro-	663	265	398	464
Co-culture	Propane, 2,2-dimethyl-	559799	221330	338469	390564.5
Co-culture	Propiolic acid	6051	5406	645	5728.5
Co-culture	Valeraldehyde, 4,4-dimethyl-2-methylene-	21296	13091	8205	17193.5

Table S2. *Co-culture VOC analysis.* Mass area data collected from two independent biological samples were averaged. Microbe specific fold changes for each volatile were calculated based on comparisons of averages with that of the co-culture reading.

	Coculture area			**Rs area**				**Af area**			
Coculture Compounds	**Rep 1**	**Rep 2**	**Average**	**Rep 1**	**Rep 2**	**Average**	**Fold Change**	**Rep 1**	**Rep 2**	**Average**	**Fold Change**
Propiolic acid	6051	5406	5728.5	153916	43532	98724	17.23383085	246976	4704	125840	21.9673562
Methanethiol	7120	4818	5969	8300	975	4637.5	-1.287115903	-	-	-	-
Butane, 2-methyl-	1919	1842	1880.5	-	-	-	-	-	-	-	-
1-Methoxy-1-buten-3-yne	774	708	741	-	-	-	-	-	-	-	-
N,N'-Ethylenebis(N-nitroacetamide)	59848	542	30195	23348	423	11885.5	-2.540490514	-	-	-	-
Disulfide, dimethyl	98263	78886	88574.5	76432	38823	57627.5	-1.537017917	-	-	-	-
Butanoic acid, 3-methyl-, methyl ester	20448	16961	18704.5	241535	170100	205817.5	11.00363549	-	-	-	-
Cyclotrisiloxane, hexamethyl-	17546	13164	15355	19102	19067	19084.5	1.242885054	-	-	-	-
(-)-(5s)-Benzyloxymethyl-4-methyl-2(5H)-furanone	21626	15934	18780	1669	680	1174.5	-15.98978289	-	-	-	-
1-Pentene, 2,4,4-trimethyl-	7881	4071	5976	-	-	-	-	-	-	-	-
4-Nonene, 2,3,3-trimethyl-, (E)-	537	1089	813	-	-	-	-	3293	804	2048.5	2.519680197
Cyclopentanol, nitrate	4952	2380	3666	2996	1773	2384.5	-1.53742923	4748	1186	2967	-1.235591507
3-Heptanone, 5-methylene-	9249	5121	7185	1944	1369	1656.5	-4.337458497	-	-	-	-
Propane, 2-methyl-1-nitro-	663	265	464	384	1034	709	1.528017241	322	137	229.5	-2.021786492
1-Pentene, 4,4-dimethyl-	2116	35457	18786.5	-	-	-	-	-	-	-	-
Valeraldehyde, 4,4-dimethyl-2-methylene-	21296	13091	17193.5	6285	1031	3658	-4.700246036	20583	9702	15142.5	-1.135446591

2.10 REFERENCES

1. **Badri D V.**, **Weir TL**, **van der Lelie D**, **Vivanco JM**. 2009. Rhizosphere chemical

dialogues: plant-microbe interactions. Curr Opin Biotechnol **20**:642–650.

2. **Philippot L**, **Raaijmakers JM**, **Lemanceau P**, **van der Putten WH**. 2013. Going back to the roots: the microbial ecology of the rhizosphere. Nat Rev Microbiol **11**:789–99.

3. **Berendsen RL**, **Pieterse CMJ**, **Bakker PAHM**. 2012. The rhizosphere microbiome and plant health. Trends Plant Sci **17**:478–486.

4. **Jones JDG**, **Dangl JL**. 2006. The plant immune system. Nature **444**:323–329.

5. **Klich MA.** 2007. *Aspergillus flavus*: The major producer of aflatoxin. Mol Plant Pathol **8**:713–722.

6. **Amaike S**, **Keller NP**. 2011. *Aspergillus flavus*. Annu Rev Phytopathol **49**:107–133.

7. **Chakrabarti A**, **Singh R**. 2011. The emerging epidemiology of mould infections in developing countries. Curr Opin Infect Dis **24**:521–526.

8. **Brown SH**, **Scott JB**, **Bhaheetharan J**, **Sharpee WC**, **Milde L**, **Wilson R**, **Keller NP**. 2009. Oxygenase coordination is required for morphological transition and the host-fungus interaction of *Aspergillus flavus*. Mol Plant Microbe Interact **22**:882–894.

9. **Forseth RR**, **Amaike S**, **Schwenk D**, **Affeldt KJ**, **Hoffmeister D**, **Schroeder FC**, **Keller NP**. 2013. Homologous NRPS-like gene clusters mediate redundant small-molecule biosynthesis in *Aspergillus flavus*. Angew Chemie - Int Ed **52**:1590–1594.

10. **Horowitz Brown S**, **Zarnowski R**, **Sharpee WC**, **Keller NP**. 2008. Morphological transitions governed by density dependence and lipoxygenase activity in *Aspergillus flavus*. Appl Environ Microbiol **74**:5674–5685.

11. **Gao X**, **Brodhagen M**, **Isakeit T**, **Brown SH**, **Göbel C**, **Betran J**, **Feussner I**, **Keller NP**, **Kolomiets M V**. 2009. Inactivation of the lipoxygenase ZmLOX3 increases

susceptibility of maize to *Aspergillus* spp. Mol Plant Microbe Interact **22**:222–231.

12. **Brodhagen M**, **Keller NP**. 2006. Signalling pathways connecting mycotoxin production and sporulation. Mol Plant Pathol **7**:285–301.

13. **Brodhagen M**, **Tsitsigiannis DI**, **Hornung E**, **Goebel C**, **Feussner I**, **Keller NP**. 2008. Reciprocal oxylipin-mediated cross-talk in the *Aspergillus*-seed pathosystem. Mol Microbiol **67**:378–391.

14. **Affeldt KJ**, **Brodhagen M**, **Keller NP**. 2012. *Aspergillus* oxylipin signaling and quorum sensing pathways depend on G protein-coupled receptors. Toxins (Basel) **4**:695–717.

15. **Denny TP**. 2006. Plant pathogenic *Ralstonia* species, p. 573–644. *In* S. S. Gnanamanickam (1st ed.), Plant-Associated Bacteria. Springer Publishing, Dordrecht.

16. **Huang J**, **Carney BF**, **Denny TP**, **Weissinger AK**, **Schell MA**. 1995. A complex network regulates expression of eps and other virulence genes of *Pseudomonas solanacearum* J. Bateriol. **177:** 1259-1267.

17. **Hayward A.** 1991. Biology and epidemiology of bacterial wilt caused by *Pseudomonas solanacearum*. Annu Rev Phytopathol **29:** 65–87.

18. **van Elsas JD**, **Kastelein P**, **Vries PM De**, **van Overbeek LS**. 2001. Effects of ecological factors on the survival and physiology of *Ralstonia solanacearum* bv. 2 in irrigation water. Can. J. Microbiol. **854**:842–854.

19. **van Overbeek LS**, **Bergervoet JHW**, **Jacobs FHH**, **van Elsas JD**. 2004. The Low-Temperature-induced viable-but-nonculturable state affects the virulence of *Ralstonia solanacearum* biovar 2. Phytopathology **94**:463–469.

20. **Genin S**, **Denny TP**. 2012. Pathogenomics of the *Ralstonia solanacearum* species

complex. Annu Rev Phytopathol **50**:67–89.

21. **Middleton KJ**, **Hayward AC**. 1990. Bacterial wilt of groundnuts. collaborative res. plan. meet., Genting Highlands, Malaysia, 18-19 March. Proc ACIAR/ICRISAT **31**:1–58.

22. **Le CN**, **Kruijt M**, **Raaijmakers JM**. 2012. Involvement of phenazines and lipopeptides in interactions between *Pseudomonas* species and *Sclerotium rolfsii*, causal agent of stem rot disease on groundnut. J Appl Microbiol **112**:390–403.

23. **Khare E**, **Arora NK**. 2011. Dual activity of pyocyanin from *Pseudomonas aeruginosa* — antibiotic against phytopathogen and signal molecule for biofilm development by rhizobia. Can. J. Microbiol. **713**:708–713.

24. **Haas D**, **Défago G**. 2005. Biological control of soil-borne pathogens by fluorescent pseudomonads. Nat Rev Microbiol **3**:307–319.

25. **Wang K**, **Yan PS**, **Ding QL**, **Wu QX**, **Wang ZB**, **Peng J**. 2013. Diversity of culturable root-associated/endophytic bacteria and their chitinolytic and aflatoxin inhibition activity of peanut plant in China. World J Microbiol Biotechnol **29**:1–10.

26. **Wenke K**, **Kai M**, **Piechulla B**. 2010. Belowground volatiles facilitate interactions between plant roots and soil organisms. Planta **231**:499–506.

27. **Bitas V**, **Kim H-S**, **Bennett JW**, **Kang S**. 2013. Sniffing on microbes: diverse roles of microbial volatile organic compounds in plant health. Mol Plant Microbe Interact **26**:835–43.

28. **Wheatley RE**. 2002. The consequences of volatile organic compound mediated bacterial and fungal interactions. Antonie van Leeuwenhoek, Int J Gen Mol Microbiol **81**:357–364.

29. **Mackie A**, **Wheatley R.** 1999. Effects and incidence of volatile organic compound

interactions between soil bacterial and fungal isolates. Soil Biol Biochem **31**:375–385.

30. **Effmert U**, **Kalderás J**, **Warnke R**, **Piechulla B**. 2012. Volatile mediated interactions between bacteria and fungi in the soil. J Chem Ecol **38**:665–703.

31. **Theis KR**, **Venkataraman A**, **Dycus JA**, **Koonter KD**, **Schmitt-Matzen EN**, **Wagner AP**, **Holekamp KE**, **Schmidt TM**. 2013. Symbiotic bacteria appear to mediate hyena social odors. Proc Natl Acad Sci U S A **110**:19832–7.

32. **Hendrick CA**, **Sequeira L**. 1984. Lipopolysaccharide-defective mutants of the lipopolysaccharide-defective mutants of the wilt pathogen *Pseudomonas solanacearum.* Appl Environ Microbiol. **48**: 94-101.

33. **Shimizu K**, **Keller NP**. 2001. Genetic Involvement of a cAMP-dependent protein kinase in a G protein signaling pathway regulating morphological and chemical transitions in *Aspergillus nidulans*. Genetics. **157:** 591-600.

34. **Duran RM**, **Cary JW**, **Calvo A. M**. 2009. The Role of veA in *Aspergillus flavus* infection of peanut, corn and cotton. Open Mycol J **3**:27–36.

35. **Peckham GD**. 2011. Mouse MAb 3.H7 Recognizes *Ralstonia solanacearum* Race 3 Biovar 2 Strains. Hybridoma. **30:** 571–573.

36. **Song J**, **Fan L**, **Beaudry RM**. 1998. Application of Solid Phase Microextraction and Gas Chromatography / Time-of-Flight Mass Spectrometry for rapid analysis of flavor volatiles in tomato and strawberry fruits. J. Ag. Food Chem. **8561**:3721–3726.

37. **Roze L V**, **Chanda A**, **Laivenieks M**, **Beaudry RM**, **Artymovich K a**, **Koptina A V**, **Awad DW**, **Valeeva D**, **Jones AD**, **Linz JE**. 2010. Volatile profiling reveals intracellular metabolic changes in *Aspergillus parasiticus*: veA regulates branched chain amino acid

and ethanol metabolism. BMC Biochem **11**:33.

38. **Saile E**, **McGarvey JA**, **Schell MA**, **Denny TP**. 1997. Role of Extracellular Polysaccharide and endoglucanase in root invasion and colonization of tomato plants by *Ralstonia solanacearum*. Phytopathology **87**:1264–1271.

39. **Huang J**, **Schell M**. 1995. Molecular characterization of the eps gene cluster of *Pseudomonas solanacearum* and its transcriptional regulation at a single promoter. Mol Microbiol **16**:977–989.

40. **Brumbley SM**, **Carney BF**, **Denny TP**. 1993. Phenotype conversion in Pseudomonas solanacearum due to spontaneous inactivation of PhcA, a putative LysR transcriptional regulator. J Bacteriol **175**:5477–5487.

41. **Tognon G**, **Campagnoli A**, **Pinotti L**, **Dell'Orto V**, **Cheli F**. 2005. Implementation of the electronic nose for the identification of mycotoxins in durum wheat (*Triticum durum*). Vet Res Commun **29**:391–393.

42. **Campagnoli A**, **Cheli F**, **Savoini G**, **Crotti a.**, **Pastori a. GM**, **Dell'Orto V**. 2009. Application of an electronic nose to detection of aflatoxins in corn. Vet Res Commun **33**:273–275.

43. **Bruins M**, **Rahim Z**, **Bos A**, **Van De Sande WWJ**, **Endtz HP**, **Van Belkum A**. 2013. Diagnosis of active tuberculosis by e-nose analysis of exhaled air. Tuberculosis **93**:232–238.

44. **Chambers ST**, **Scott-Thomas A**, **Epton M**. 2012. Developments in novel breath tests for bacterial and fungal pulmonary infection. Curr Opin Pulm Med **18**:228–232.

45. **Nawrath T**, **Mgode GF**, **Weetjens B**, **Kaufmann SHE**, **Schulz S**. 2012. The volatiles of

pathogenic and nonpathogenic mycobacteria and related bacteria. Beilstein J Org Chem **8**:290–299.

46. **Roze L V.**, **Koptina A V.**, **Laivenieks M**, **Beaudry RM**, **Jones DA**, **Kanarsky A V.**, **Linz JE**. 2011. Willow volatiles influence growth, development, and secondary metabolism in *Aspergillus parasiticus*. Appl Microbiol Biotechnol **92**:359–370.

47. **Fernando WGD**, **Ramarathnam R**, **Krishnamoorthy AS**, **Savchuk SC**. 2005. Identification and use of potential bacterial organic antifungal volatiles in biocontrol. Soil Biol Biochem **37**:955–964.

48. **Chaurasia B**, **Pandey A**, **Palni LMS**, **Trivedi P**, **Kumar B**, **Colvin N**. 2005. Diffusible and volatile compounds produced by an antagonistic *Bacillus subtilis* strain cause structural deformations in pathogenic fungi in vitro. Microbiol Res **160**:75–81.

49. **Wang C**, **Wang Z**, **Qiao X**, **Li Z**, **Li F**, **Chen M**, **Wang Y**, **Huang Y**, **Cui H**. 2013. Antifungal activity of volatile organic compounds from *Streptomyces alboflavus* TD-1. FEMS Microbiol Lett **341**:45–51.

50. **Roze L V.**, **Beaudry RM**, **Arthur AE**, **Calvo AM**, **Linz JE**. 2007. *Aspergillus* volatiles regulate aflatoxin synthesis and asexual sporulation in *Aspergillus parasiticus*. Appl Environ Microbiol **73**:7268–7276.

51. **De Lucca AJ**, **Carter-Wientjes CH**, **Boué S**, **Bhatnagar D**. 2011. Volatile trans-2-hexenal, a soybean aldehyde, inhibits *Aspergillus flavus* growth and aflatoxin production in corn. J Food Sci **76**:M381–6.

52. **Gandomi H**, **Misaghi A**, **Basti AA**, **Bokaei S**, **Khosravi A**, **Abbasifar A**, **Javan AJ**. 2009. Effect of *Zataria multiflora* Boiss. essential oil on growth and aflatoxin formation

by *Aspergillus flavus* in culture media and cheese. Food Chem Toxicol **47**:2397–2400.

53. **Flavier AB**, **Clough SJ**, **Schell MA**, **Denny TP**. 1997. Identification of 3-hydroxypalmitic acid methyl ester as a novel autoregulator controlling virulence in *Ralstonia solanacearum*. Mol Microbiol **26**:251–259.

54. **Clough SJ**, **Flavier AB**, **Schell MA**, **Denny TP**. 1997. Differential expression of virulence genes and motility in *Ralstonia* (*Pseudomonas*) *solanacearum* during exponential growth. Appl Environ Microbiol **63**:844–850.

55. **Schell MA**. 2000. Control of virulence and pathogenicity genes of *Ralstonia solanacearum* by an elaborate sensory network. Annu Rev Phytopathol 263–292.

56. **Hernández-romero D**, **Solano F**, **Herna D**, **Sanchez-amat A**. 2005. Polyphenol oxidase activity expression in *Ralstonia solanacearum* **71**: 6808-6815.

57. **Nosanchuk JD**, **Casadevall A**. 2003. Microreview: The contribution of melanin to microbial pathogenesis **5**:203–223.

58. **de Lucca AJ**, **Boué SM**, **Carter-Wientjes C**, **Bhatnagar D**. 2012. Volatile profiles and aflatoxin production by toxigenic and non-toxigenic isolates of *Aspergillus flavus* grown on sterile and non-sterile cracked corn. Ann Agric Environ Med **19**:91–98.

59. **Zhou Z**, **Meng Q**, **Yu Z**. 2011. Effects of methanogenic inhibitors on methane production and abundances of methanogens and cellulolytic bacteria in in vitro ruminal cultures. Appl Environ Microbiol **77**:2634–2639.

60. **Hogan DA**, **Vik Å**, **Kolter R**. 2004. A *Pseudomonas aeruginosa* quorum-sensing molecule influences *Candida albicans* morphology. Mol Microbiol **54**:1212–1223.

61. **Cugini C**, **Calfee MW**, **Farrow JM**, **Morales DK**, **Pesci EC**, **Hogan DA.** 2007.

Farnesol, a common sesquiterpene, inhibits PQS production in *Pseudomonas aeruginosa*. Mol Microbiol **65**:896–906.

62. **Partida-Martínez LP**, **Heil M**. 2011. The Microbe-free plant: Fact or artifact? Front Plant Sci **2**:1–16.

CHAPTER 3: *Ralstonia solanacearum* lipopeptide induces chlamydospore development in fungi and facilitates bacterial entry into fungal tissues

This work has been published as:

Spraker J, Sanchez LM, Lowe TM, Dorrestein PA, Keller NP. (2016) *Ralstonia solanacearum* lipopeptide induces chlamydospore development in fungi and facilitates bacterial entry into fungal tissues. *ISMEJ.* doi: 10.1038/ismej.2016.32

Dr. Laura Sanchez performed the IMS and MS/MS experiments and analyses.

3.1. ABSTRACT

Ralstonia solanacearum is a globally distributed soil-borne plant pathogenic bacterium, which shares a broad ecological range with many plant and soil associated fungi. I sought to determine if *R. solanacearum* chemical communication directs symbiotic development of polymicrobial consortia. *Ralstonia solanacearum* produced a diffusible metabolite that induced conserved morphological differentiation in 34 species of fungi across three diverse taxa (Ascomycetes, Basidiomycetes and Zygomycetes). Fungi exposed to this metabolite formed chlamydospores, survival structures with thickened cell walls. Some chlamydospores internally harbored *R. solanacearum*, indicating a newly described endofungal lifestyle for this important plant pathogen. Using imaging mass spectrometry (IMS) and peptidogenomics, I identified an undescribed lipopeptide, ralsolamycin, produced by an *R. solanacearum* non-ribosomal peptide synthetase-polyketide synthase (NRPS-PKS) hybrid. Inactivation of the hybrid NRPS-PKS gene, *rmyA*, abolished ralsolamycin synthesis. *Ralstonia solanacearum* mutants lacking ralsolamycin no longer induced chlamydospore development in fungal coculture and invaded fungal hyphae less well than wild-type. I propose that ralsolamycin contributes to the invasion of fungal hyphae and that the formation of chlamydospores may provide not only a specific niche for bacterial colonization but also enhanced survival for the partnering fungus.

3.2. INTRODUCTION

Ralstonia solanacearum is the causative agent of lethal bacterial wilt and is a globally distributed soil-borne plant pathogen known to infect well over 200 different plant hosts (1). The broad distribution of this bacterium in a wide variety of soil environments suggests that *R. solanacearum* likely encounters a diversity of other soil microbes, including fungi. Although the

molecular interactions between *R. solanacearum* and host plants have been well studied (2), there has been little exploration of *R. solanacearum*'s interactions with soil cohabitants.

Soil is a heterogeneous, complex microcosm replete with inter-organismal interactions, which restructure the physical and chemical composition of the shared environment. Small molecule signals are increasingly recognized as important communication signals in microbial interactions (3). Historically, many of these specialized metabolites (4) have been harnessed for pharmaceutical purposes, and there has been a resurgence of interest in natural products based on microbial crosstalk (5). Genome mining of *R. solanacearum* strain GMI1000 shows that it has the potential to produce a variety of secondary metabolites. A few of these metabolites have been characterized including ralfuranone (6) and the yersinabactin-like siderophore, micacocidin (7). Micacocidin has moderate antimycoplasma and antifungal effects *in vitro* due to its metal chelating properties (8). These and other compounds produced by *R. solanacearum* likely impact how it interacts with microbes in the soil.

Small molecule-mediated antibiosis has been documented in both bacterial and fungal systems (9, 10), but antagonistic interactions are only one potential interaction outcome. Recent advances in the understanding of bacterial/fungal interactions indicate that bacterial natural products can stimulate morphological transitions in many fungi. In particular, bacterial metabolites commonly induce fungal sporulation. For example, *Paenibacillus validus* produces trisaccharides that induce hyphal elongation and sporulation in the arbuscular mycorrhizal fungus *Glomus intraradices* (11). Similarly, the fungal plant pathogen *Rhizopus microsporus* sporulates only when it is infected with its endosymbiotic bacterial partner, *Burkholderia rhizoxinica* (12).

Other research has shown that bacterial volatile organic compounds and diffusible small molecules can induce developmental shifts in fungi aside from sporulation. For example, reciprocal volatile signaling between *R. solanacearum* and the soil fungus *Aspergillus flavus* represses *A. flavus* sporulation and inhibits production of *R. solanacearum* virulence factors (13). Fengycin A, a lipopeptide produced by *Bacillus subtilis*, causes diverse fungal taxa to form chlamydospores, thick walled spores associated with fungal survival in harsh environmental conditions (14). Additionally, phenazine redox metabolites produced by *Pseudomonas aeruginosa* trigger *Aspergillus* spp. to sporulate along a diffusion gradient (15). These developmental shifts may contribute to microbial niche securement in the soil by triggering hard-wired defense or survival mechanisms, however, these ecological mechanisms are largely unexplored.

Here I characterize a small molecule-mediated interaction between the common soil-borne bacterial pathogen *R. solanacearum* and a taxonomic variety of plant- and soil-associated fungi that results in fungal chlamydospore development. Using MALDI imaging mass spectrometry (MALDI-IMS) and tandem mass spectrometry (MS/MS) technologies, I identified a novel diffusible *R. solanacearum* lipopeptide, here named ralsolamycin. I observed a developmental shift in all fungi ranging from chlamydospore formation to growth inhibition along an increasing gradient of ralsolamycin. Inactivating *rmyA*, a gene that encodes a hybrid non-ribosomal peptide synthetase-polyketide synthase (NRPS-PKS) abolished ralsolamycin production. Further, the *rmyA* mutant did not induce chlamydospore formation. Remarkably, I also demonstrate that *R. solanacearum* invades the chlamydospores, a previously undescribed niche that may contribute to the noted environmental persistence of this devastating plant pathogen.

3.3. MATERIALS AND METHODS

3.3.1. Media and growth conditions and coculture experiments

All strains used in this study are listed in Table S1. *Ralstonia solanacearum* strains were routinely grown at 30°C on CPG agar (16), and mucoid colonies were selected for subsequent experiments. Liquid bacterial cultures were grown overnight in CPG at 30°C and 180 rpm. When appropriate, the antibiotic gentamycin (15 mg/L) was added to the media. Overnight liquid cultures of *R. solanacearum* were pelleted by centrifugation, washed twice in equal volumes of sterilized, double-distilled water, quantified using OD_{600} values, and adjusted to ~$2x10^8$ cells/ml. Then 5 µL ($1x10^6$ cells) of bacterial suspension was spotted at each point.

Aspergillus spp. were routinely grown at 30°C on glucose minimal medium (GMM) (17), and conidia were harvested by applying a 0.01% Tween 80 solution to the plate followed by agitation with a plastic cell spreader. Conidial suspensions were quantified using a hemocytometer and diluted in sterile water to $2x10^5$ spores/ml. Then 5 µl containing $1x10^3$ spores was applied to a spot 2 cm away from the *R. solanacearum* spot on CPG plates. The droplets were allowed to dry in a NUAIRE biological safety cabinet (NU425-400), then plates were wrapped with Parafilm once and incubated at room temperature. Due to variable sporulation habits, all other fungi were routinely grown on PDA and allowed to grow at room temperature. For assays, mycelial plugs were remove from actively growing cultures using the wide end of a 1 ml pipette tip and transferred to the assay plate.

For coculture experiments *R. solanacearum* and fungi were plated as described above and incubated for 14 days at room temperature. Chlamydospore formation for all fungi was assessed as the fungal colonies made contact with the *R. solanacearum* cultures. As the colonies expanded and grew into one another, sections of the interaction zone were excised for microscopic

evaluation. For IMS experimentation colonies were grown for 3 days at room temperature before being excised and processed. For assessment of endofungal bacteria, GFP strains of *R. solanacearum* were similarly cocultured with *A. flavus*, but the colonies were inoculated in direct contact to allow for physical interactions.

3.3.2. Microscopy of chlamydospores

Fungal mycelia were harvested from coculture plates by cutting 5 mm x 5 mm sections from the interaction zone between the two cultures and examined for chlamydospore formation. Cell walls were stained with calcofluor white at a final concentration of 1 mg/ml for 1 min prior to microscopy. DAPI staining of nuclei was carried out by submerging these sections in 1 mg/ml DAPI solution for 30 min followed by a wash in 0.1 M phosphate buffered saline pH 7.0 (PBS). Lipid bodies were stained by submerging sections in 10 μg/ml Nile Red, followed by a wash with 0.1 M PBS. Stained samples were wet mounted and imaged on a Zeiss Axio Imager A10 microscope (Carl Zeiss, Oberkochen Germany) equipped with a Zeiss EC Plan- NEOFLUAR 40×/1.3 Oil DIC/∞/0.17 and Zeiss EC Plan- NEOFLUAR 100×/1.3 Oil DIC/∞/0.17 objective and a series 120 X-Cite® light source (EXFO). When different filters could be used, samples were stained with multiple stains to provide comparable images for the different features. Images were collected with AxioVision Release 4.7 software (Carl Zeiss, Oberkochen, Germany).

For counts of chlamydospores of all fungi, interaction zones from coculture with GMI1000 and the *rmyA* mutant were collected and stained with calcofluor as described above. Three separate images of hyphae collected from these interaction zone were captured and chlamydospores per high-powered field were enumerated manually using the cell-counter plug-in of the Fiji software package (18).

Time-lapse microscopy experiments were carried out on a Nikon Eclipse Ti inverted fluorescent microscope (Nikon Instruments, Melville, NY) with a PlanFluor 10× objective attached to a Nikon DS-Qi1Mc CCD camera (Nikon Instruments, Melville, NY). Four filters for four different excitation/emission wavelengths were available: ex-350 nm/em-400 nm; ex-492 nm/em-517 nm; ex-572 nm/em-600 nm; ex-647 nm/em-700 nm. Images were collected with NIS-Elements AR version 4.30.01 software (Nikon Instruments, Melville, NY).

Confocal laser scanning microscopy experiments were prepared as above but performed on a Zeiss 510 Meta microscope (Carl Zeiss, Oberkochen Germany). To verify endohyphal localization of bacteria, 0.5 μm Z-sections were taken across multiple planes of view. An argon ion laser was used to excite GFP labeled cells and linear unmixing calculations were carried out in the Zeiss LSM software to reduce fungal autofluorescence. A helium laser was used to excite the FM4-64 labeled membranes. All confocal images were processed in the open source Fiji software package and all overlays of multiple fluorescence channels are of single confocal Z-planes.

3.3.3. Plasmid construction and genetic manipulation

The primers and plasmids used in this work are listed in Table S2. PCR amplification was carried out on a C1000^{TM} Thermal Cycler from Bio-Rad (Hercules, CA). For creation of the *rmyA* targeted disruption cassette, flanking regions of the targeted promoter and fatty acyl-AMP ligase domain were amplified from GMI1000 genomic DNA using primers RSp0641_5'F and RSp0641_5'R for the upstream sequence and RSp0641_3'F and RSp0641_3'R for the downstream sequence, each amplifying ~1 kb fragments. Both RSp0641_5'R and RSp0641_3'F were designed with overlapping sequences to the 0.8 kb gentamycin resistance cassette, *Gmr*, which was amplified from the plasmid pUCgm using the primer set, GentR_F and GentR_R.

These PCR products were purified with a QIAquick gel extraction kit (Qiagen, Valencia, CA) and quantified before being fused using standard double joint PCR protocols (19). The fusion product was blunt-end ligated into the Zero Blunt PCR cloning kit (Invitrogen, Carlsbad, CA) to create pJES12.3. *R. solanacearum* strain GMI1000 was transformed with pJES12.3 by electroporation and plated on gentamycin media to select for appropriate transformants. Colony PCR using RSp0641_5'F and RSp0641_3'R were used to screen for loss of the targeted *rmyA* promoter and fatty acyl-AMP ligase domain. All PCR steps were carried out with Pfu Ultra II DNA Polymerases (Agilent, Santa Clara, CA).

The GMI1000 strain constitutively expressing GFP was made by using natural transformation to move the Tn5::gfp (20) insertion from genomic DNA of strain K60GFP (21) into the GMI1000 chromosome and transformants were selected on tetracycline plates at a concentration of 15 mg/ml and confirmed with fluorescence microscopy. Subsequently, the Δ*rmyA* strain constitutively expressing GFP was made by using natural transformation to move the Tn5::gfp insertion from the GMI1000-GFP strain. These strains were selected for tetracycline and gentamycin resistance, confirmed with fluorescence microscopy, and verified phenotypically to not induce chlamydospores.

3.3.4. Imaging mass spectrometry

Liquid bacterial cultures were grown overnight in CPG at 30°C and 180 rpm. Overnight liquid cultures of *R. solanacearum* were pelleted by centrifugation, washed 2× in equal volumes of sterilized, double-distilled water, quantified using OD_{600} values, and adjusted to $2x10^8$ cells/ml. Then 5 µL (~$1x10^6$ cells) of this cell suspension was spotted at each point. GMI1000 or K60 (5 µL) were spotted next to *A. flavus* (1 µL) on yeast extract/malt extract ISP2 agar (10 ml) in 100x25 mm Petri dishes (22). All organisms were inoculated on separate Petri dishes as

controls. Samples were incubated at room temperature for 72 hrs. The region of interest and controls were excised from the agar and transferred to the same MALDI MSP 96 anchor plate (Bruker Daltonics, Millerica, MA, USA). A photograph was taken and the aerial hyphae of *A. flavus* were removed gently with a cotton swab dampened with acetonitrile (23). Following the removal of the aerial hyphae another photograph as taken and Universal MALDI matrix (Sigma-Aldrich) was applied using a 53 µm stainless steel sieve (Hogentogler & Co., INC., Columbia, MD, USA). The plate was then transferred to an oven and desiccated at 37 °C overnight.

Following adherence to the MALDI plate, another photographic image was taken and the sample was subjected to MALDI-TOF mass spectrometry (Microflex from Bruker Daltonics, Billerica, MA, USA) for IMS acquisition. Data was acquired in positive reflectron mode, with a 500 µm laser interval in the XY and a mass range of 250-2500 Da. The resulting data was analyzed using FlexImaging software v. 3.0.

3.3.5. Extraction and semi-purification

Ralstonia solanacearum 24 h liquid cultures were filter sterilized using a 0.2 µm pore-size filter and applied to actively growing hyphae of *A. flavus* to determine if direct bacterial contact was necessary for the formation of the chlamydospore-like structures. Within less than 12 h, a large number of mature hyphal cells differentiated into chlamydospores, indicating that direct physical contact between the microbes was unnecessary for chlamydospore development suggesting diffusible metabolite was responsible for chlamydospore development. *Ralstonia solanacearum* GMI1000, K60, and *A. flavus* and their interaction zones were excised from thin agar (1 x 1 cm) and transferred to separate glass scintillation vials. Acetonitrile (1 ml) was added to the samples and sonicated for 10 min. These samples were partitioned against both 50:50 ACN:H_2O and butanol and the resulting mixture was centrifuged at 10,000 rpm for 1 min.

The soluble organic fraction was removed and dried *in vacuo*. Samples were then re-suspended in 100 μL of MeOH for further analysis.

Bulk extraction of the metabolite was done from liquid culture by growing GMI1000 for four days in 1 L of CPG with 100g Amberlite XAD-16 resin (Sigma-Aldrich). The resin was separated from the culture broth via vacuum filtration and rinsed with 500mL double distilled H_2O to remove excess salts and cellular debris. The adsorbed compounds were eluted in 1:1 MeOH/DCM and organic fractions were dried *in vacuo*. Subsequently, these fractions were subjected to solid phase extraction (SPE) using a Waters Sep-Pak C_{18} cartridge (5g) eluting with a 20% step gradient of MeOH/H_2O, ranging from 20-100% MeOH.

3.3.6. MS/MS Data Acquisition

Samples were directly infused into the mass spectrometer using a Triversa nanomate-electrospray ionization source (Advion Biosystems) coupled to a 6.42 T Thermo LTQ-FT-ICR mass spectrometer. For nanomate, samples were diluted in 50:50 MeOH:H_2O with 0.1% formic acid and then directly infused using a back pressure of 0.35-0.5 psi and a spray voltage of 1.3-1.45 kV. FT-MS and ion trap MS/MS spectra were acquired using Tune Plus software version 1.0 and Xcalibur software version 1.4 SR1. The instrument was tuned on *m/z* 816, the 15+ charge state of cytochrome C.

The instrument scan cycle consisted of one 10 min segment, during which a profile FT scan with a resolution of 25,000 was cycled with four data-dependent scans in the ion trap. MS/MS data were collected in a data dependent manner, during which profile mode FT-MS scans (150-1,600 m/z) cycled with four MS/MS scans in the ion trap. The four most abundant peaks were fragmented (2 *m/z* isolation width, a normalized collision energy of 35%, and an activation time of 30 ms) and then added to an exclusion list for 600 s.

3.3.7. Network Analyses

The resulting spectra were converted to mzXML format using msconvert in the ProteoWizard software package (http://proteowizard.sourceforge.net/tools.shtml). The data was then subjected to molecular networking (24). The data was then clustered with MS-Cluster with a parent mass tolerance of 1.0 Da and a MS/MS fragment ion tolerance of 0.3 Da to create consensus spectra. Further, consensus spectra that contained less than 1 spectrum were discarded. A network was then created where edges were filtered to have a cosine score above 0.65 and more than 6 matched peaks. Further edges between two nodes were kept in the network if and only if each of the nodes appeared in each other's respective top 10 most similar nodes.

3.3.8. Phylogenetic analysis of bacteria

Bacterial 16S DNA sequences were obtained from GenBank and aligned using Muscle in the MEGA6 software package (25) using default parameters. The evolutionary history was inferred using the Maximum Parsimony (MP) method. Tree 1 out of 2 most parsimonious trees (length = 1648) is shown. The consistency index is (0.480386), the retention index is (0.730577), and the composite index is 0.372381 (0.350959) for all sites and parsimony-informative sites (in parentheses). The percentage of replicate trees in which the associated taxa clustered together in the bootstrap test (1000 replicates) are shown next to the branches (26). The MP tree was obtained using the Subtree-Pruning-Regrafting (SPR) algorithm (27) with search level 1 in which the initial trees were obtained by the random addition of sequences (10 replicates). The analysis involved 29 nucleotide sequences. All positions containing gaps and missing data were eliminated. There were a total of 1,211 positions in the final dataset.

3.4. RESULTS

3.4.1. A diffusible compound produced by *R. solanacearum* induces chlamydospore development across diverse fungal taxa

Ralstonia solanacearum inhabits a variety of soils and infects over 200 plant hosts. Soils and plants are both associated with many different fungal species so I hypothesized that *R. solanacearum* utilizes chemical signals to mediate interactions with a diversity of fungi. Using the characterized and sequenced *R. solanacearum* strain GMI1000*,* I examined the interaction of cocultures of the bacterium and 34 species of fungi: Thirty Ascomycota species, one Basidiomycota species (*Rhizoctonia solani*), and three Zygomycota species (*Phycomyces blakesleeanus, Mucor bacilliformis* and *M. hiemalis*). I found that a distinct zone of fungal inhibition formed between 2-14 days of co-culture. Additionally, all fungi formed distinct hyphal swellings near (~1.5 cm) the *R. solanacearum* colony, referred to hereafter as the 'interaction zone' (**Figure 1a**).

The hyphal swellings resembled chlamydospores, thick walled spores associated with certain fungal genera and thought to aid in fungal survival under harsh environments (14, 28). The rates of chlamydospore formation varied considerably between species, but all of the fungi tested formed chlamydospores within 14 days of coculture with *R. solanacearum*. Several fungi only formed chlamydospores after being in direct contact with the *R. solanacearum* colony for multiple days: the necrotrophic plant pathogens *Botrytis cinerea* and *Sclerotinia sclerotiorum*, the coprophilous fungus *Sordaria fimicola*, one *Fusarium* sp. *(verticillioides*) and the Basidiomycete *Rhizoctonia solani*.

To study the hypertrophic structures in detail, the interaction zones of *A. flavus* were excised and characterized. I chose *A. flavus* because volatile mediated interactions between *A. flavus* and *R. solanacearum* do not result in chlamydospore formation (13) and also because the

genus is generally not known to produce chlamydospores. Micromanipulation and fluorescent-histological microscopy confirmed that the hyphal swellings were thick walled, chlamydospores**.** Hoescht staining showed that most chlamydopsores harbored multiple nuclei (**Figure 1b**) although some lacked nuclei. A fungal cell wall specific stain, calcofluor-white, demonstrated that chlamydospore cell walls were thicker than normal hyphae cell walls (**Figure 1b**), and Nile Red staining showed chlamydospores accumulated lipid bodies (**Figure 1c**). Together, the histological evidence suggested that *A. flavus* chlamydospores could be viable structures. To test this hypothesis, chlamydospores were isolated via micromanipulation, washed and placed in fresh media and monitored for germination. After 5 h the chlamydospores germinated with multiple germ-tubes (**Figure 1d, Video S1**).

3.4.2. Endofungal life-style of *R. solanacearum*

Many bacteria live as endofungal symbionts in a variety of fungal hosts. *Ralstonia* spp. are nested within a larger clade of identified endofungal bacteria (**Figure 2a, Table S3**). In order test the hypothesis that *R. solanacearum* was capable of invading fungal hyphae, a constitutive GFP producing *R. solanacearum* strain was cocultured with *A. flavus* for 72 h. After harvesting the resulting mycelial mat and thoroughly washing the hyphae to remove extracellular bacteria, samples were imaged with a fluorescent microscope. Many bacterial cells remained associated with the fungal hyphae, and bacterial aggregates were often associated with chlamydospores, many appearing to be within the chlamydospores. Confocal laser-scanning microscopy confirmed that a substantial number of bacteria were localized to the intracellular space of some chlamydospores (**Figure 2b, Video S2**). Bacteria were rarely found within the non-differentiated hyphae. These data supported our hypothesis that *R. solanacearum* can invade fungal hyphae with specificity to the chlamydospores.

3.4.3. Identification of the chlamydospore inducing compound

To identify *Ralstonia*-specific metabolites that induced chlamydospore formation, I cocultured *A. flavus* with a phylogenetically diverse set of *R. solanacearum* strains to identify a non-chlamydospore producing isolate. Under these conditions strain GMI1000 was the only isolate to induce substantial chlamydospore formation in *A. flavus* (**Figure S1**). I selected the non-chlamydospore inducing *R. solanacearum* strain, K60 for comparative metabolite studies because like GMI1000, the K60 genome was sequenced and publicly available. GMI1000 and K60 interaction zones were excised at 72 h. At this time point, chlamydospores were plentiful but the cultures were not in physical contact. The zones were coated with universal MALDI matrix and subjected to MALDI-TOF IMS (22) to explore the spatial distribution of secreted metabolites and to identify differential signals between these isolates. In total, 22 ions were detected in the bacterial fungal interactions. I attributed production of most metabolites to the bacterium or the fungus based on their spatial distributions with respect to the optical image and their presence in individual cultures.

Isolate GMI1000 produced high amounts of four ions that K60 did not produce. Three of these ions clearly diffused beyond the margins of the bacterial colony and reached the margins of the fungal colony. These ions were different ionized forms (protonated, sodiated, and potassiated species) of one compound with the exact mass of 1291.7142 (**Figure 3a, Figure S2**). The diffusible nature of this compound suggested it was the chlamydospore inducing metabolite. This compound was further characterized by tandem mass spectrometry (MS/MS) coupled with molecular networking analysis. The molecular network analyses showed that the fragmentation pattern of this compound was unique to GMI1000 (**Figure 3b, Figure S3**).

3.4.4. Mapping compound to gene cluster and assessing bacterial colonization

Using tandem mass spectrometry, an automated peptidogenomics analysis (30), and the program Pep2Path (31), a characteristic partial peptide fragmentation pattern associated with the signal of interest was identified with one fragment exhibiting the following residue sequence tag: Gly-Thr-Ser-Ser-Gly-Phe-Ala (**Figure 3b**). Although this sequence tag does not explain the entire mass of the metabolite it does strongly indicate that a non-ribosomal peptide synthase (NRPS) was involved in the synthesis of this compound. Using the *in silico* analysis capabilities of Pep2Path, in combination with AntiSMASH (32), I examined the *R. solanacearum* GMI1000 and K60 genomes to identify putative secondary metabolic gene clusters where a major criterion was to find NRPS clusters unique to the GMI1000 genome that matched the partial sequence tag described above.

One such gene cluster contained two large genes encoding a NRPS-PKS hybrid (RSp0641) and a NRPS (RSp0642). Several lines of evidence suggested this gene cluster produced the chlamydospore inducing metabolite: these genes were absent from the K60 genome, and the domain architecture of both RSp0641 and RSp0642 predicted a product best matched to the 1291.7 *m/z* of the signal identified in the IMS studies. Additionally, the NRPS adenylation domains were predictive of the amino acid residues detected in the MS/MS studies (**Table S4**). I termed this new compound ralsolamycin and named RSp0641 and RSp0642 **r**alsola**my**cin synthase genes *rmyA* and *rmyB*, respectively (**Figure 4a**). The protein products of *rmyA-rmyB* appear to a large secondary metabolite megasynthase containing both PKS and NRPS domains (**Figure 4b**).

In silico analysis using a PKS-NRPS predictor (33) and domain specific BLAST searches, suggested that RmyA contains an initiating fatty acyl-AMP ligase (FAAL) domain at its N-terminus followed by a keto-synthase domain, and two acetyl ornithine aminotransferase

domains coupled to luciferase-like monooxygenases. The remainder of the *rmyA* gene product contains four canonical NRPS modules containing adenylation (A), peptide carrier protein (PCP), and condensation (C) domains. The predicted peptide product of *rmyA* terminates with a PCP domain. Conventional knowledge of PCP domains suggests that the product would remain tethered to RmyA. Similar analysis of RmyB showed that it initiates with a C domain, suggesting that RmyB functionally associates with the C-terminal PCP domain of RmyA. Further, *rmyB* encodes five NRPS modules, ending with a predicted thioesterase (TE) domain. I predict the TE domain cyclizes and releases the final product. The FAAL and PKS domains of RmyAB suggest the product is a lipopeptide (a fatty acid-like moiety attached to an amino acid chain). Table S4 lists all predicted domain substrates and their closest identified homologues.

I disrupted the putative promoter and fatty acyl-AMP ligase (FAAL) domain of *rmyA* (34). The *rmyA* mutant had significantly reduced chlamydospore-inducing activity ($p < 0.05$) in 28 of the 34 assayed fungal cocultures (**Table 1**), including *A. flavus* (**Figure 4c**), and lost all ralsolamycin IMS signals (**Figure 4d**). Furthermore, addition of semi-purified ralsolamycin to *A. flavus* triggers chlamydospore formation (**Figure S4**). This data shows that *rmyA* contributes to ralsolamycin biosynthesis and that ralsolamycin induces fungal chlamydospore formation.

3.4.5. Ralsolamycin contributes to bacterial invasion of fungal cells

Because I saw an abundance of *R. solanacearum* cells internalized in the chlamydospores but not in undifferentiated hyphae, I hypothesized that ralsolamycin is necessary for invasion of fungal tissues. To test this hypothesis, GFP-producing GMI1000 wild type and *rmyA* mutant were cocultured with *A. flavus*. Samples were examined with confocal microscopy using amphiphilic styryl dye FM4-64 as a membrane counterstain. The Δ*rmyA* bacteria rarely invaded the hyphae. In contrast, the wild-type cells were abundant in the chlamydospores (**Figure 5a**).

These findings suggest that ralsolamycin enhances *R. solanacearum*'s invasion of fungal tissues with specificity to chlamydospores.

3.5. DISCUSSION

Fungal chlamydospore development in response to ralsolamycin

Many fungi produce chlamydospores under adverse conditions. However, because not all fungi are known to produce chlamydospores, traditional taxonomic studies use these structures as a trait to delineate evolutionary relationships. The histological data suggest that chlamydospores formed in response to ralsolamycin are similar to those described in the literature (35). I provide the first evidence of chlamydospores formation in many of these fungi including all of the *Aspergillus* species tested. My results also indicate that these structures may be more common across the kingdom Fungi than is currently recognized.

The finding that all tested *Aspergillus* species can produce chlamydospores was unexpected as only *A. parasiticus* chlamydospores have been putatively described (36). These data suggest a novel mode of persistence for this well studied genus. Although most of the assayed fungi formed abundant chlamydospores in response to ralsolamycin, a subset formed relatively few chlamydospores (**Table 1**). I have not ruled out that these taxa may form chlamydospores more abundantly under other conditions. Perhaps differences in plasma membrane composition or signaling cascades amongst these fungi temper the conserved chlamydospore formation response to ralsolamycin. Alternatively, these fungi may respond to specific cues shown to affect chlamydospore formation in other fungi including nutrients (37, 38), light (39), osmolality (40), pH (41), air (37), temperature (38), and other interkingdom signals (14, 42, 43). Regardless of quantity, the finding that all of the fungi developed chlamydospores when exposed to

ralsolamycin supports a conserved differentiation process in the kingdom Fungi in response to this lipopeptide.

Endofungal life-style of *R. solanacearum*

The present data support the hypothesis that *R. solanacearum* colonizes fungal cells, and that formation of the chlamydospores facilitates bacterial entry. Recently diverse fungal lineages have been shown to harbor endofungal bacteria, most of which are gram-negative taxa (29). Of these related genera, *Burkholderia rhizoxinica* and other closely related species have been particularly well studied for their endofungal lifestyle and their role in the production of bioactive secondary metabolites (12, 44–46). My data analyzing Δ*rmyA* and GMI1000 suggest that although ralsolamycin production is not essential for bacterial invasion of fungal hyphae it does contribute significantly to this process and/or that chlamydospores may provide a more suitable site for bacterial growth upon invasion.

Many bacterial lipopeptides such as iturin (47), fengycin (48), lichenysin (49), and syringomycin (50) form pores and permeabilize membranes. I presume that ralsolamycin mediated membrane restructuring contributes to the initiation of chlamydospore formation and may facilitate the passage of *R. solanacearum* into fungal cells. *Ralstonia solanacearum* possesses other factors that could contribute to fungal endosymbioses such as chitinolytic enzymes, known to be important in fungal cell wall reorganization (51), and genes for all of the major Gram-negative protein secretion systems (52). The *R. solanacearum* type III secretion machinery shows significant conservation of gene order and primary sequence to that of *B. rhizoxinica*, a system which has been shown to be important for maintaining a stable endofungal symbiosis of *B. rhizoxinica* with the fungus *R. microsporus* (12) and possibly a similar mechanism contributes to *R. solanacearum* invasion of fungal cells.

Ralstonia solanacearum is known to persist in soils for remarkably long periods of time relative to other bacterial plant pathogens (53). The traits underlying environmental persistence are poorly studied, but external factors such as non-host reservoir plants, permissive soil temperatures, and high soil moisture content may contribute to persistence. My findings suggest that *R. solanacearum* colonization within chlamydospores is a novel persistence mechanism for bacterial survival in the absence of host-plants. The large numbers of bacteria within colonized chlamydospores indicates that they multiply within chlamydospores which may contribute to increasing inoculum load once plants are introduced. The chlamydospores contain substantial amounts of lipid droplets, which could contribute to bacterial replication in these specialized structures. Currently little is known regarding nutritional interactions between bacterial/fungal symbioses (10) and efforts towards elucidating the nutritional interactions and survival outcomes of the *R. solanacearum/*chlamydospore complex are currently underway in our lab.

Because homologs of the ralsolamycin biosynthetic cluster are present in a subset of the *R. solanacearum* strains sequenced to date, it is intriguing to consider that the invasion of chlamydospores may be important to these strains. I did not find any phylogenetic or geographic trends that suggest that ralsolamycin biosynthesis is restricted to a single phylotype, geographic locale, or host plant (**Table S5**); however, as more isolates are sequenced a pattern of occurrence may be uncovered. Additionally, CMR15 homologues of RmyA and RmyB showed 94% and 93% identity although this strain did not induce chlamydospore formation. These data suggest that either this cluster makes a different metabolite, that the genes do not produce functional proteins or that the cluster may be differentially regulated under the conditions tested here. Continued research into these strain differences as well as increasing genomic information will help elucidate the impact of ralsolamycin biosynthesis on *R. solanacearum* biology.

Ralsolamycin identification, characterization and biosynthetic genes

The combination of spatial data from the IMS experiments and the MS/MS network analysis indicates a single compound, ralsolamycin, is largely responsible for the bacterial induction of fungal chlamydospore formation. Multiple *in silico* analyses tools indicate that ralsolamycin is produced by the megasynthase enzyme encoded by the genes *rmyA-rmyB*. These two backbone genes, *rmyA* (a PKS-NRPS hybrid) and *rmyB* (a NRPS) are the two largest ORFs in the GMI1000 genome, approximately 20.7 kb and 17.9 kb, respectively. The bipartite genomes of strains GMI1000 and K60 were analyzed via AntiSMASH (32) to look for canonical backbone secondary metabolite genes. This analysis identified 19 putative secondary metabolic clusters in GMI1000. Of these, only three were predicted to contain putative NRPSs: the micacocidin-producing RSc1806-1811 (7), the ralfuranone-producing RSp1419-1434 (6) and the ralsolamycin-producing RSp0638-0642 cluster characterized here. Identification of the 1290 Da metabolite by IMS as the key metabolite was supported by the Pep2Path program, which can link NRPS-products to their biosynthetic genes based on predictions of adenylation substrate recognition domains (31). This program mapped the partial amino acid sequence-tag G-T-S-S-G back to the hybrid NRPS-PKS backbone gene RSp0641-0642 which encodes 10 predicted adenylation domains in total.

The domain architecture of RmyA is very similar to that responsible for the production of the antifungal lipopeptide mycosubtilin, MycA, produced by *Bacillus subtilis* (54). The presence of the N-terminal FAAL domain followed by a keto-synthase and aminotransferase domain is a known motif in bacterial lipopeptide biosynthesis (55). These domains cooperate to convert carboxylic acid moieties into activated amino acids, which are utilized by subsequent NRPS modules. The remaining modules in RmyA-B appear to have a canonical NRPS adenylation,

peptide carrier, condensation domain structure suggesting normal non-ribosomal peptide biosynthesis beyond the initial FAAL domain. Complete characterization of this compound to verify its amino acid composition is underway.

Although it appears that RmyA and RmyB constitute a single operon, examination of this region suggests that there may be up to five genes involved in its biosynthesis and transport including *rmyA*, *rmyB* and three additional genes: RSp0638, RSp0639, and RSp0640 (**Figure 4a**) encoding a transmembrane cyclic peptide transporter, a metallo-beta-lactamase and an MbtH-like protein, respectively (**Figure. 5b, Table S6**). Comparative analysis of the available *R. solanacearum* strain genomes showed that these five genes are located within a copper resistance cluster common to most *R. solanacearum* strains. Although I have not verified the functions of RSp0638-40, I predict that they participate in the production and transport of ralsolamycin as they are all common components of secondary metabolic clusters.

Conclusions

I have demonstrated that the bacterial plant pathogen *R. solanacearum* strain GMI1000 induces chlamydospore formation in a wide range of fungal taxa, many of which were not known to produce chlamydospores. I used IMS to rapidly identify potential mediators of this diffusible interaction phenotype. Tandem mass spectrometry coupled with *in silico* peptidogenomics tools and molecular genetics identified a putative *R. solanacearum* lipopeptide, ralsolamycin and the PKS-NRPS responsible for its production.

I provide the first evidence that *R. solanacearum* can induce and invade specialized fungal cells, chlamydospores, which may have significant implications for environmental persistence of *R. solanacearum*. Chlamydospores enhance persistence of soil-borne fungi and related organisms (56, 57) and endosymbiotic mutualisms provide survival benefits (58, 59). *Ralstonia*

solanacearum has an unusually long survival time in soil, even when host plants are removed (53). The data suggest ralsolamycin-induced chlamydospores contributes to bacterial invasion of fungal cells, but ralsolamycin is not the sole factor contributing to this process. I speculate that endofungal colonization benefits *R. solanacearum* survival in soil in the absence of plant-host tissue, and *R. solanacearum* co-opts the accumulated lipids in chlamydospores. Further research in our lab aims to determine if this symbiotic phenotype impacts the survival of *R. solanacearum* and if there is any impact on the fungi it interacts with.

3.6. ACKNOWLEDGEMENTS

This research was funded by an NSF Graduate Research Fellowship under grant no. DGE-1256259 to J.E.S. and in part by National Science Foundation Grant Emerging Frontiers in Research and Innovation 1136903 to N.P.K. This work was supported in part by GM097509 (P.C.D.). P.C.D. further acknowledges Bruker and NIH Grant GMS10RR029121 for the support of the shared instrumentation infrastructure that enabled this work. L.M.S. is supported by National Institutes of Health IRACDA K12 GM068524 grant award. T.M.L. is funded by NIH National Research Service Award T32 GM07215 and by Agriculture and Food Research Initiative Competitive Grant # 2015-67011-22799 from the USDA National Institute of Food and Agriculture. I appreciate GFP labeled GMI1000 from Tuan Tran and critical feedback from Dr. Caitilyn Allen, both of the UW-Madison Department of Plant Pathology. The content is solely the responsibility of the authors and does not necessarily represent the official views of the National Science Foundation. Confocal laser scanning microscopy work was done at the UW-Madison Plant Imaging Center with the help of Sara Swanson.

3.7. FIGURES AND LEGENDS

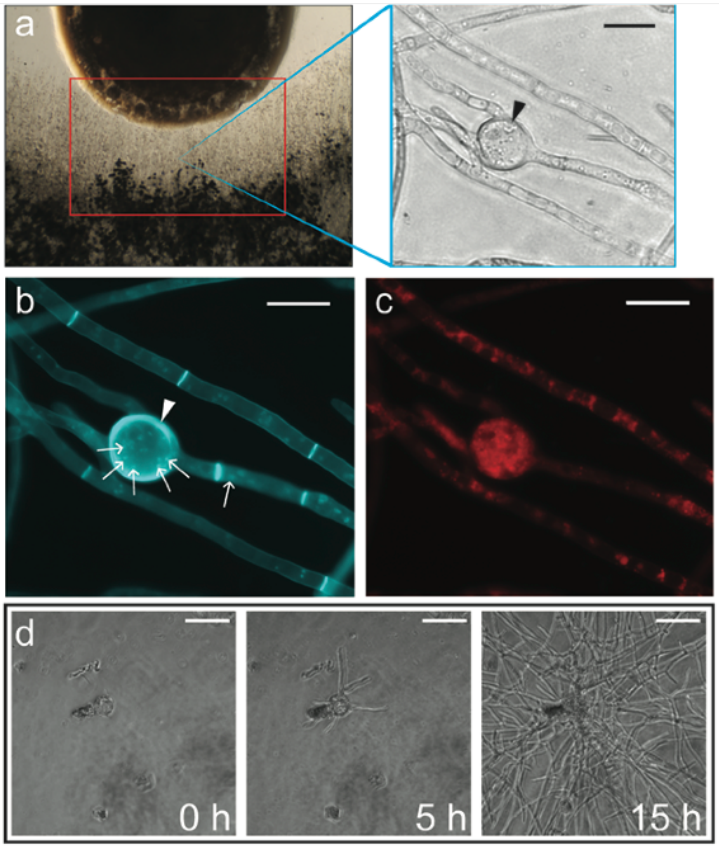

Figure 1. Examination of the interaction zone of the *R. solanacearum*/fungal coculture revealed fungal hypertrophy resembling chlamydospores produced by other fungi

a) *left* – Coculture set-up of bacteria (top) and fungi (bottom). Red box indicates the "interaction zone" where many intercalated chlamydospore-like structures (*right* -black arrows) developed in response to coculture with *R. solanacearum* strain GMI1000. Control images of non-chlamydospore inducing bacterial cocultures can bee seen in Fig S1. Histological analysis of chlamydospores shows that they are **b)** polynucleate (small white arrows), have thickened cell walls (white arrowheads), and **c)** accumulate lipid bodies. **d)** Time-lapse microscopy of isolated chlamydospores placed in fresh media shows these structures are independently viable, and they

can germinate to form a new fungal colony. Complete time-lapse video can be viewed in Video S1.

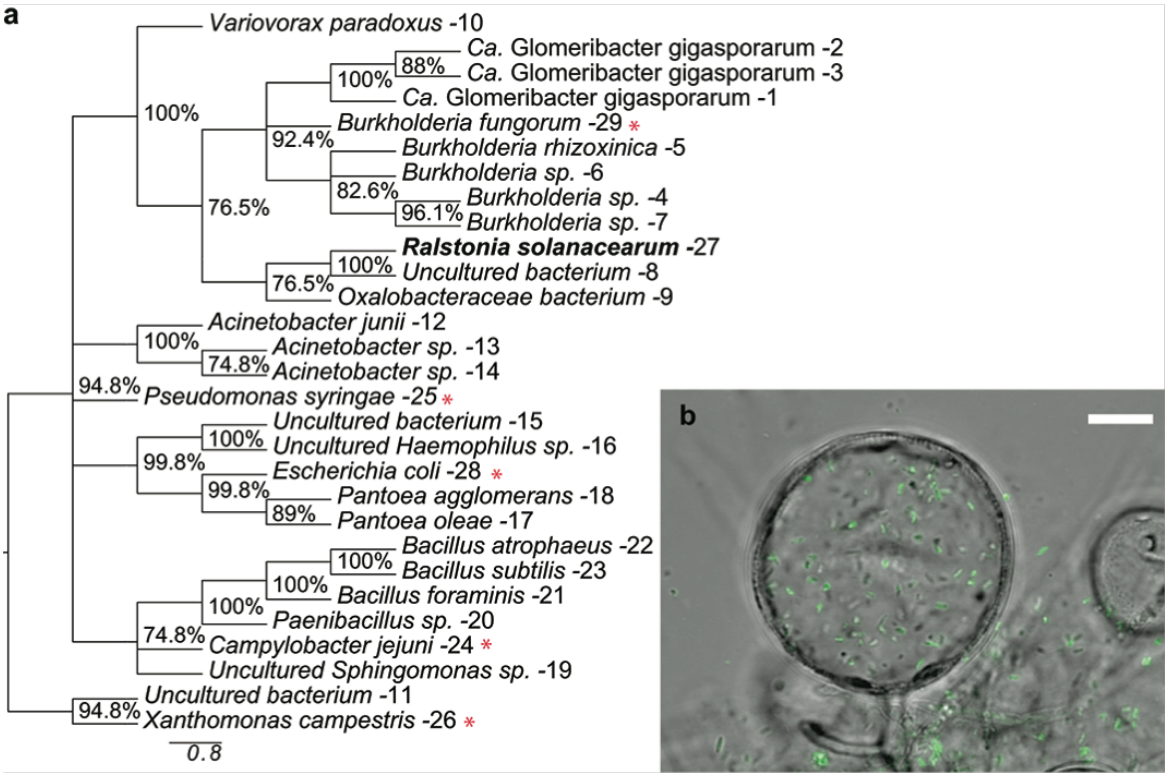

Figure 2. *R. solanacearum* is nested amongst other known endofungal bacteria and can be found within fungal cells.

a) Phylogenetic analysis of endofungal bacteria based on maximum parsimony analysis of 16S ribosomal RNA gene sequences. The percentage of replicate trees in which the associated taxa clustered together in the bootstrap test (1000 replicates) is shown next to the branches. Branches with less than 70% support values were collapsed. GenBank accession numbers are listed in Table S3. Well-known bacterial species not characterized as endofungal symbionts were inserted for reference and are marked with a red asterisk (*). **b)** Confocal Laser Scanning Microscopy

image of GFP-labeled GMI1000 colonizing *A. flavus* chlamydospore. Scale bar (white) represents 10 um. Z-stack scan can be viewed in Video S2.

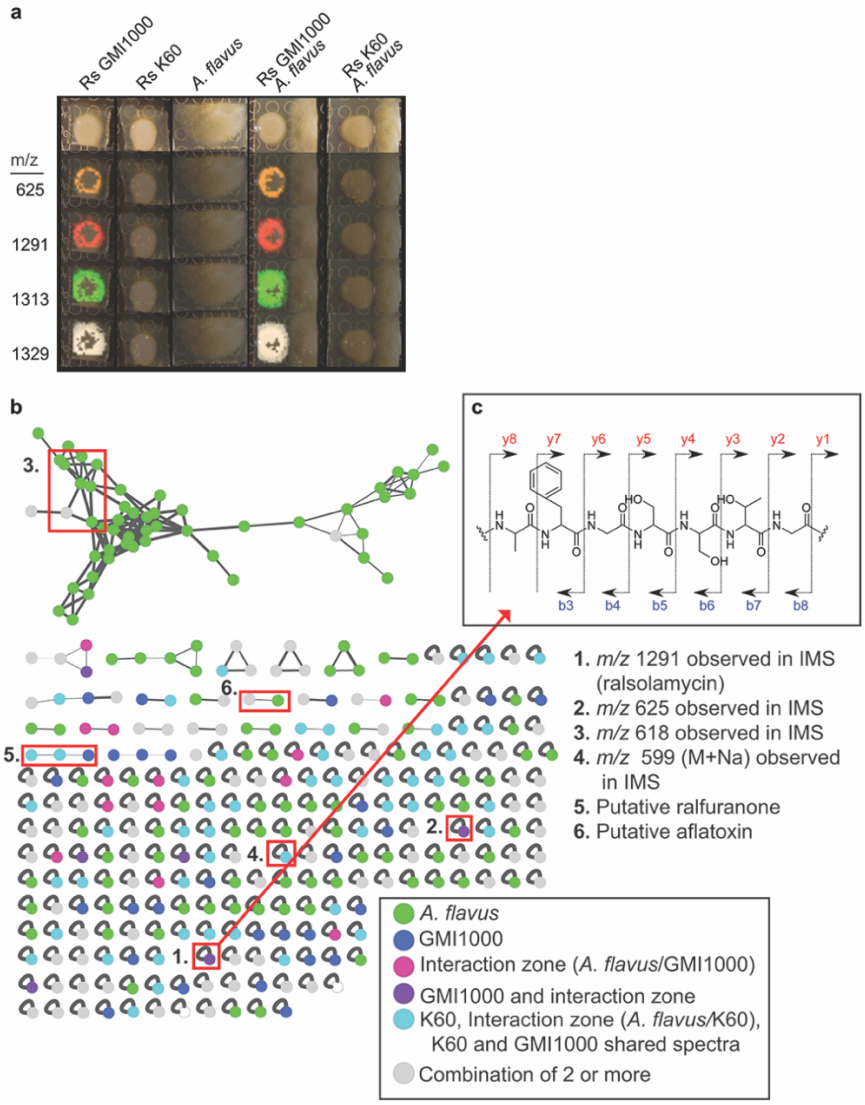

Figure 3. Analysis of differential IMS datasets, MS-MS networks indicate a single lipopeptide produced by *R. solanacearum* strain GMI1000 is responsible for initiating chlamydospore formation.

a) Imaging mass-spectrometry analysis of strains GMI1000 and K60 showing only differential signals from this dataset. Complete dataset is in Fig S4. **b)** Network analyses of microbial

metabolites detected in the MS-MS studies. The network is composed of nodes representing ions associated with the microbial colonies. Nodes are connected by edges, which represent the relatedness of the fragmentation patterns of each spectrum. Nodes only associated with *A. flavus* colonies are green. Nodes only associated with only GMI1000 are dark blue. Nodes associated with the "interaction zone" are labeled in pink, Nodes found in the GMI1000 cultures and "interaction zone" (*A. flavus*/GMI1000) are labeled purple. Nodes associated with any of the K60 culture conditions or that are shared between k60 and GMI1000 are colored in light blue. Nodes common to 2 or more of the previous node classes are labeled in grey. Nodes of interest from the IMS study (1-4) and those that are known products of the microbes (5-6) are highlighted with red boxes and listed on the right of the figure. **c)** MS/MS spectra of extracted metabolites shows a unique fragmentation pattern of G-T-S-S-G-F-A for the compound with a *m/z* of 1291(top right).

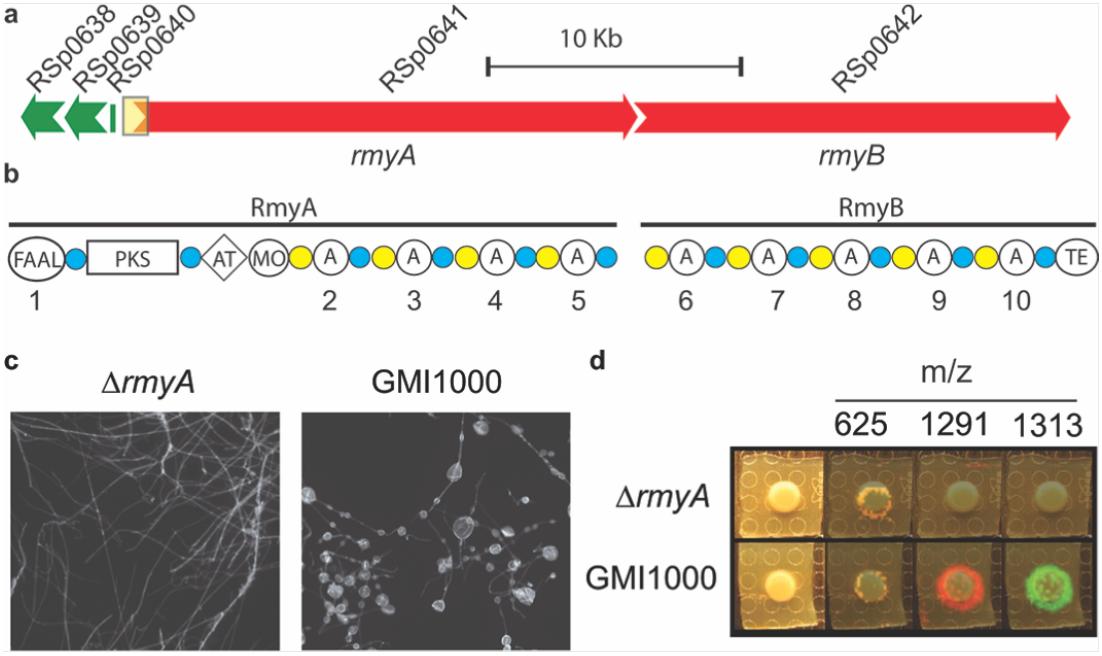

Figure 4. A large PKS-NRPS megasynthase is responsible for ralsolamycin production

a) Graphical representation of the predicted biosynthetic gene cluster as predicted by comparative genomics. Yellow box indicates the region (putative promoter sequence and FAAL encoding sequence) targeted for creation of the *rmyA* mutant using a gentamycin resistance cassette. Genes and their closest protein homologs are listed in Table S6. **b)** Predicted domain architecture of the hybrid PKS megasynthases RmyA and RmyB. FAAL, fatty acid acyl ligase domain; PKS, polyketides synthase domain; AT, aminotransferase domain; MO, monooxygenase domain; A, adenylation domain; TE, thioesterase domain; blue circles, phosphopantetheine attachment site; yellow circles, condensation domains. Adenylation domains are numbered for reference to their predicted substrates listed in Table S4. **c)** *rmyA* mutant does not induce fungal chlamydospores. **d)** *rmyA* mutant does not produce the ralsolamycin signals (*m/z* of 1291 and 1313) but does produce the other GMI1000 specific compound (*m/z* 625).

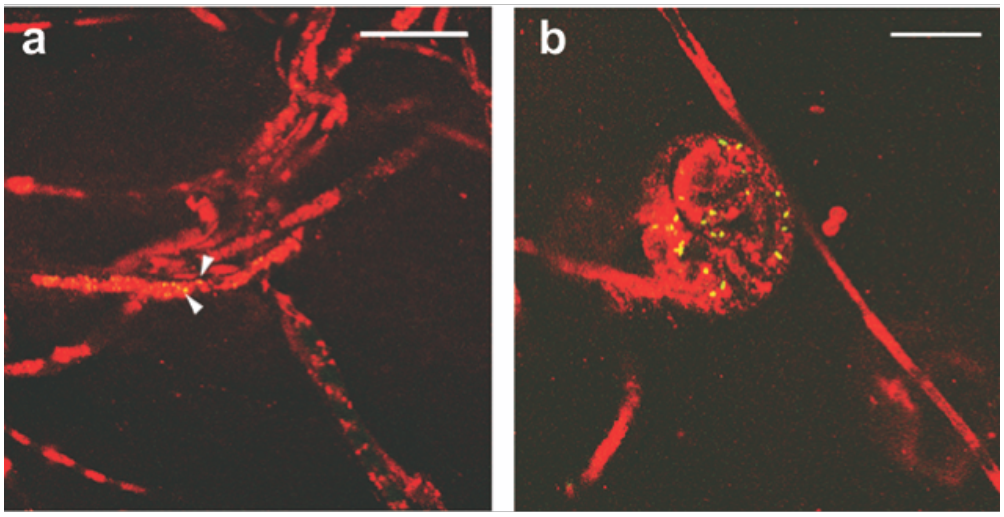

Figure 5. Confocal laser scanning microscopy shows that ralsolamycin impacts bacterial invasion of the fungal thallus.

a) the *rmyA* disruption does not completely inhibit bacterial invasion of fungal hyphae (arrow heads indicate GFP-expressing bacteria) but **b)** much larger populations of wild type bacteria can be found in chlamydospores. White bar indicates 10 μm.

3.8. TABLES

Table 1. Chlamydospore counts per high-power field

Data from microscopic analysis (magnification: 200x) of fungal interactions with *R. solanacearum* strains GMI1000 and Δ*rmyA*. Asterisk (*) indicates strains with significantly greater (p <0.05) chlamydospore counts in coculture with GMI1000 relative to strain Δ*rmyA*. Mean, standard deviations (std-dev) and p-values are listed to show variations between strains.

	GMI1000		Δ*rmyA*		
Fungal species	**mean**	**std-dev**	**mean**	**std-dev**	***p*-value**
*Alternaria alternata**	28.00	8.49	0.33	0.47	1.00E-02
Alternaria solani	88.00	47.77	12.67	5.25	9.09E-02
*Aspergillus aculeatus**	80.00	17.57	6.33	2.87	4.25E-03
*Aspergillus brasiliensis**	136.00	24.39	85.33	8.26	4.97E-02
*Aspergillus carbonarius**	36.00	11.52	4.33	1.70	1.84E-02
*Aspergillus clavatus**	97.33	22.60	0.00	0.00	3.68E-03
*Aspergillus flavus**	105.00	17.91	0.00	0.00	1.15E-03
*Aspergillus fumigatus**	11.33	0.47	0.00	0.00	4.46E-06
*Aspergillus nidulans**	42.33	2.05	0.00	0.00	8.26E-06
*Aspergillus niger**	9.67	2.87	0.33	0.47	1.05E-02
*Aspergillus oryzae**	48.33	4.64	1.00	0.82	1.43E-04
*Aspergillus terreus**	207.00	62.98	5.33	1.70	1.06E-02
*Aspergillus tubingensis**	32.33	11.47	7.67	0.94	3.87E-02
*Aspergillus zonatus**	126.00	58.76	0.00	0.00	3.87E-02
Botrytis cinerea	2.33	1.25	0.00	0.00	5.72E-02
*Colletotrichum graminicola**	58.67	18.26	16.67	5.31	3.54E-02
*Fusarium fujikuroi**	31.33	3.09	1.33	0.47	1.71E-04
*Fusarium graminearum**	180.67	39.85	0.67	0.94	3.09E-03
*Fusarium oxysporum**	47.33	4.78	1.00	1.41	1.94E-04
*Fusarium solani**	21.67	8.73	0.00	0.00	2.47E-02
*Fusarium sporotrichioides**	40.33	13.89	12.00	3.74	4.95E-02
*Fusarium verticillioides**	16.00	7.07	0.00	0.00	3.29E-02
*Morchella esculenta**	21.00	4.55	0.00	0.00	2.84E-03
Mucor bacilliformis	58.00	30.01	17.67	2.87	1.31E-01
*Mucor hiemalis**	26.00	3.56	0.67	0.47	5.67E-04
*Neosartorya fischeri**	51.00	15.77	0.67	0.94	1.08E-02
*Penicillium italicum**	102.00	32.26	1.67	1.25	1.17E-02
*Phycomyces blakesleeanus**	6.67	1.70	0.00	0.00	5.17E-03
Rhizoctonia solani	27.00	11.86	7.33	8.99	1.35E-01
*Sclerotinia sclerotiorum**	84.00	11.86	5.67	3.09	8.30E-04
*Sordaria fimicola**	102.33	6.65	22.00	4.55	1.47E-04
Trichoderma hazarianum	64.00	38.74	0.00	0.00	7.97E-02
Trichothecium roseum	24.33	9.88	7.33	3.30	8.22E-02
*Verticillium albo-atrum**	173.00	37.98	10.00	0.82	3.73E-03

3.9. SUPPLEMENTARY FIGURES AND LEGENDS

Data files used for the molecular network have been uploaded to Global Natural Products Social Molecular Networking (http://gnps.ucsd.edu), accession number MSV000078964**.**

3.9.1. Supplementary figures

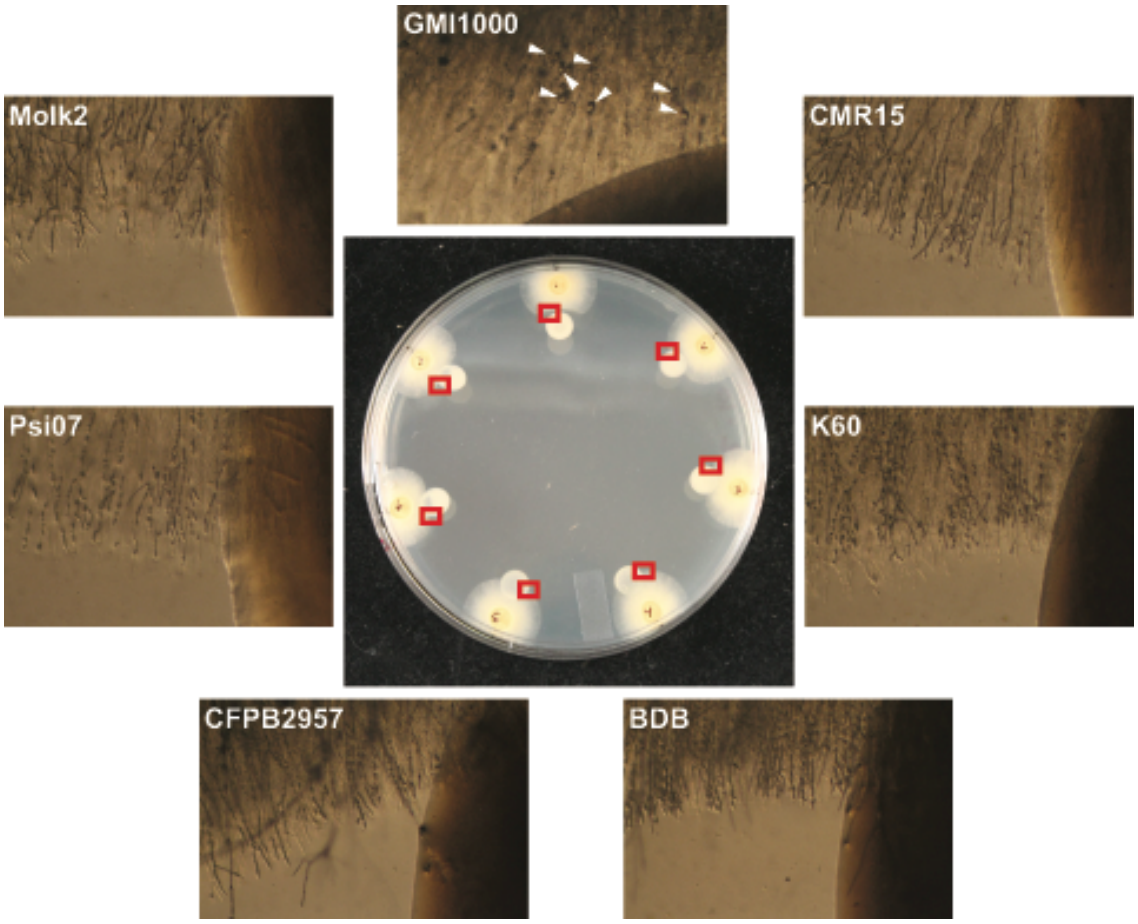

Figure S1. Assay of multiple *R. solanacearum* strains for chlamydospore induction

Diverse *R. solanacearum* tested for *A. flavus* chlamydospore induction

Ralstonia solanacearum strains were grown in co-culture with *A. flavus* to determine which strains showed growth inhibition and chlamydospore development. Central image shows

macroscopic growth phenotypes and red squares indicate where each image was captured from. External images show morphologies of *A. flavus* hyphae at the agar surface. White arrows indicate chlamydospores.

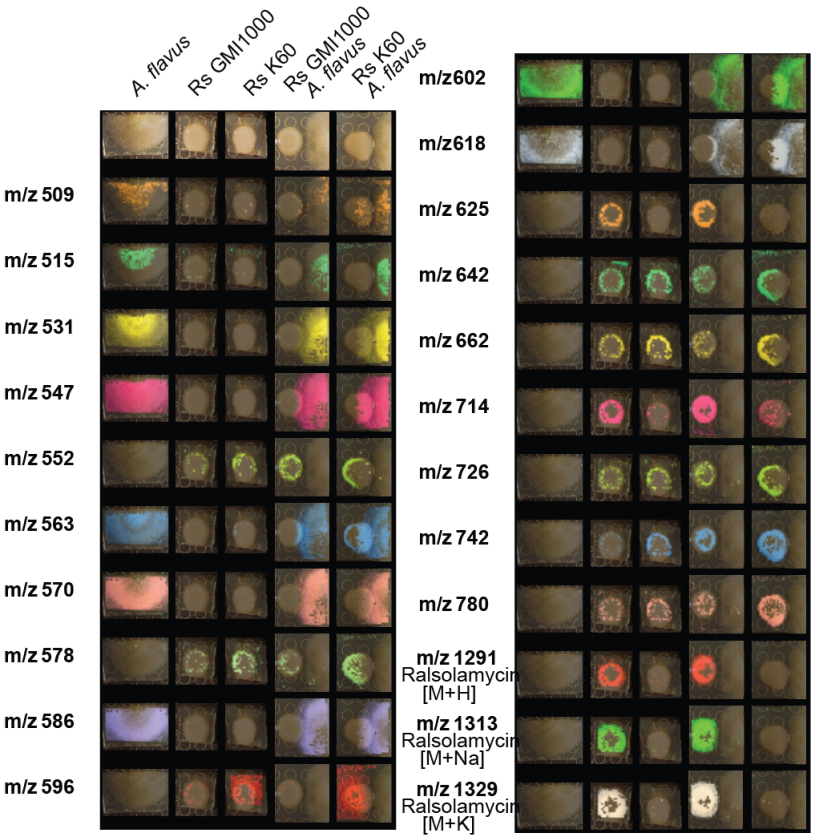

Figure S2. Extended IMS dataset

Extended IMS dataset of bacterial and fungal metabolites Extended IMS dataset showing all detectable *m/z* in both axenic and co-culture experiments, excluding signals from media components and matrix. *R. solanacearum* is abbreviated as Rs and the appropriate strain name (either GMI1000 or K60) is indicated.

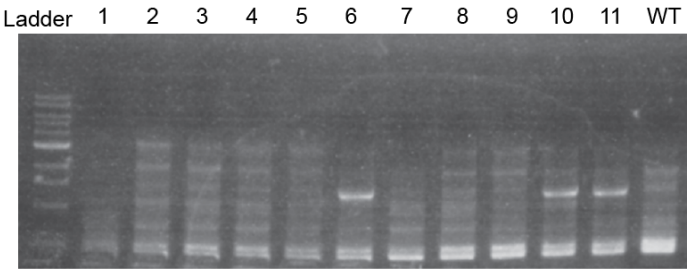

Figure S3. PCR confirmation of *rmyA* mutant

PCR confirmation of appropriate cassette localization in *rmyA* mutants. Expected band size is ~1.2kB for *rmyA* mutants. Ladder is New England Biolabs 1 kb Ladder (#N3232L) Lanes numbered 1-11 are PCR results from different transformant colonies and WT is from wild-type GMI1000. Lanes 6, 10, and 11 are positive for *rmyA* mutants.

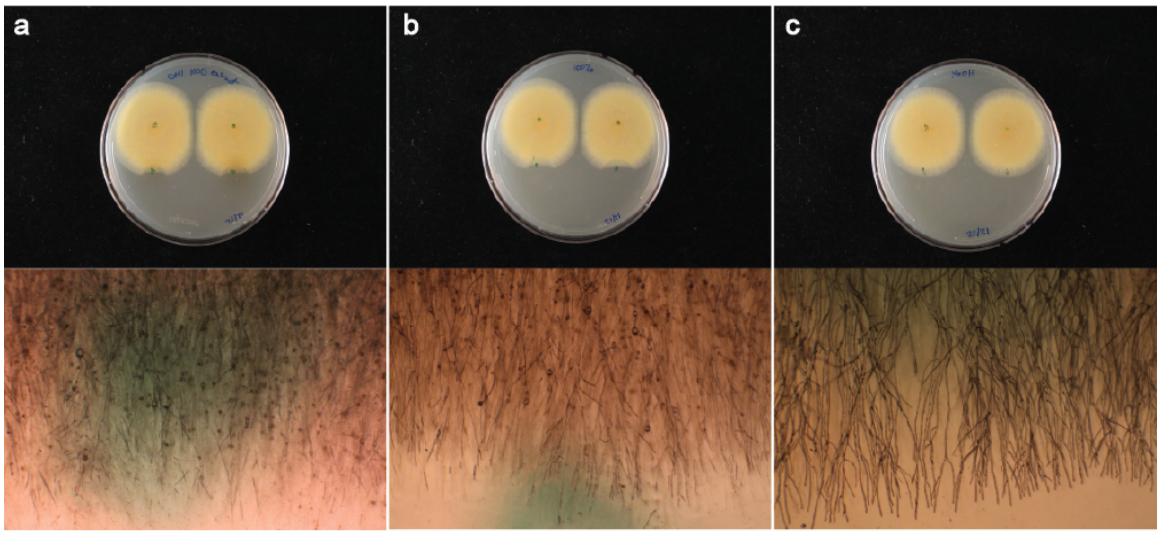

Figure S4. Partial purification of ralsolamycin induces chlamydospore formation

a) Extracts from GMI1000 shows growth inhibition and induction of chlamydospore formation in *A. flavus*. b) Semi-purified ralsolamycin still shows growth inhibition and induction of

chlamydospore formation while c) methanol (control carrier) doesn't affect fungal growth or induce chlamydospore formation. Lower green dot on plates indicates where samples were loaded.

3.9.2. Supplementary tables

Table S1. Fungi and bacteria used in this study.

Fungal strains	Source[a]	Strain name
Alternaria alternata	UWPP	n/a
Alternaria solani	UWPP	n/a
Aspergillus aculeatus	CBS	CBS 172.66
Aspergillus brasiliensis	CBS	CBS 101740
Aspergillus carbonarius	CBS	
Aspergillus clavatus	CBS	CBS 513.65
Aspergillus flavus	CBS	NRRL 3357
Aspergillus fumigatus	CBS	Af293
Aspergillus nidulans	CBS	FGSCA4
Aspergillus niger	CBS	CBS 113.46
Aspergillus oryzae	CBS	Rib40
Aspergillus terreus	CBS	NIH2624
Aspergillus tubingensis	CBS	CBS 134.48
Aspergillus zonatus	CBS	CBS 506.65
Botrytis cinerea	UWPP	n/a

Colletotrichum graminicola	UWPP	n/a
Fusarium fujikuroi	UWPP	n/a
Fusarium graminearum	UWPP	n/a
Fusarium oxysporum	UWPP	n/a
Fusarium solani	UWPP	n/a
Fusarium sporotrichioides	UWPP	n/a
Fusarium verticillioides	UWPP	n/a
Morchella esculenta	UWPP	n/a
Mucor bacilliformis	UWPP	n/a
Mucor hiemalis	UWPP	n/a
Neosartorya fischeri	CBS	CBS 544.65
Penicillium italicum	UWPP	n/a
Phycomyces blakesleeanus	UWPP	n/a
Rhizoctonia solani	UWPP	n/a
Sclerotinia sclerotiorum	UWPP	n/a
Sordaria fimicola	UWPP	n/a
Trichoderma hazarianum	UWPP	n/a
Trichothecium roseum	UWPP	n/a
Verticillium albo-atrum	UWPP	n/a

[a] CBS, Centraalbureau voor Schimmelcultures Fungal Biodiversity Centre of the Royal Netherlands Academy of Arts and Sciences; UWPP, University of Wisconsin – Madison, Department of Plant Pathology Teaching Lab.

Bacterial strains	Relevant characteristics	Phylotype	Reference
Ralstonia solanacearum - GMI1000	Wild type, isolated from French Guyana	IA	(1)
R. solanacearum - GMI1000 GFP	Wild type, naturally transformed in Allen lab	IA	Tran *et al*. unpublished
R. solanacearum - GMI1000 Δ*rmyA*	*rmyA* deactivated by deletion of promoter and FAAL domain	IA	This study
R. solanacearum - GMI1000 Δ*rmyA* GFP	Δ*rmyA* strain naturally transformed with GFP from GMI1000 GFP	IA	This study
R. solanacearum - K60	Wild type, isolated from French Guyana	IIA	(2)
R. solanacearum - MOLK2	Wild type, isolated from Indonesia	IIB	(3)
R. solanacearum - CFPB2957	Wild type, isolated from French West Indies	IIA	(4)
R. solanacearum - PSI07	Wild type, isolated from Indonesia	IV	(4)

R. solanacearum - CMR15	Wild type, isolated from Cameroon	III	(4)
R. solanacearum - BDB	Wild type, isolated from Philippines	IV	(5)
Escherichia coli - DH5 alpha	Derived from *E. coli* strain DH5		(6)

Table S2. Primers and plasmids used in this study

Primer Name	Sequence	Use
GentR_F	GTTAAGCTCGAGCCATGGG	Amplify Gmr from pUCgm
GentR_R	AAATTGTCACAACGCCGCGG	Amplify Gmr from pUCgm
RSp0641_3' R	AAAAAGGCCGCGTCGAACGC	Amplify *rmyA* 3' flank
RSp0641_3' F	TTGTTCGGTAAATTGTCACAACGCCGCG GCGCCTGATCGACCTGATCATTCTGA	Amplify *rmyA* 3' flank
RSp0641_5' F	TGCAGCAGGGTTTCCAGC	Amplify *rmyA* 5' flank
RSp0641_5' R	AGGCTTATGTCAATTCGAGCTCGGTACCC GAAATGCCCCGCCGAACA	Amplify *rmyA* 5' flank

Plasmid	Characteristics	Reference
pJES12.3	KO *rmyA* promoter and FAAL domain*:: gmR*	This study
pUCgm	835 bp Gmr cassette flanked by *SacI*	(7)
Zero Blunt PCR	Blunt end cloning vector, kanR	Invitrogen - Life Technologies

Table S3. *In silico* A domain substrate predictions based on 8 amino acid residues in the predicted A domain binding pocket.

A Domain number	**Predicted substrate**	**Closest homologue (p blast)**	**Score**	**e value**	**NCBI Identifier**
1	Fatty acid	No Hit	-	-	-
2	Threonine	Coelichelin synthetase (CchH)	21	0.006	gi|5763943
3	Tyrosine	Nostopeptolide synthetase (NosD)	17	0.1	gi|6563400
4	Serine	Syringamycin synthase (SyrE)	20	0.016	gi|837256
5	NA	No Hit	-	-	-
6	Valine	Tyrocidin synthase (TycC)	18	0.051	gi|2623773

7	Serine	Syringamycin synthase (SyrE)	20	0.016	gi|837256
8	NA	No Hit	-	-	-
9	Glycine	Microcystin synthase A (McyA)	15	0.42	gi|5822841
10	NA	No Hit	-	-	-

Table S4. Predicted cluster members from comparative genomic studies

Gene	Protein Homolog	Protein Identity/ Similarity (%/%)	Predicted Function	Accession Number
RSp0638		98.9/99.5	ABC transporter ATP-binding protein	WP_016727745.1
RSp0639		99.8/100	polyketide synthase	WP_016727746.1
RSp0640		94.1/97.1	MbtH-like protein	YP_006060512.1
RSp0641	RmyA	94.3/96.0	PKS-NRPS	YP_006060514.1
RSp0642	RmyB	93.0/95.2	NRPS	YP_006060515.1

Table S5. NCBI Accession numbers for strains used in bacterial phylogenetic analyses

Identifier	NCBI Accession Name	NCBI Accession
1	*Candidatus* Glomeribacter gigasporarum 16S rRNA gene (from *G. margarita* strain WV205A-5)	AJ251633.1
2	*Candidatus* Glomeribacter gigasporarum 16S RNA gene (from *S. persica* strain E28)	AJ251634.1
3	*Candidatus* Glomeribacter gigasporarum 16S rRNA gene (from S. persica strain E09)	AJ251635.1
4	*Burkholderia* sp. 20577 16S rRNA gene	AJ938141.1
5	*Burkholderia rhizoxinica* 16S rRNA gene, type strain HKI 454T	AJ938142.1
6	*Burkholderia* sp. 308.87 16S rRNA gene	AJ938143.1
7	*Burkholderia* sp. 699.68 16S rRNA gene	AJ938144.1
8	Uncultured bacterium clone Hg1a1A6 16S ribosomal RNA gene, partial sequence	EU236303.1
9	*Oxalobacteraceae* bacterium KVD-1921-01 16S ribosomal RNA gene, partial sequence	DQ490310.1
10	*Variovorax paradoxus* strain CAI-26 16S ribosomal RNA gene, partial sequence	DQ257419.1
11	Uncultured bacterium clone IYF62 16S ribosomal RNA gene, partial sequence	DQ984599.1

12	*Acinetobacter junii* strain p1 16S ribosomal RNA gene, partial sequence	FJ596644.1
13	*Acinetobacter* sp. CYEB-12 16S ribosomal RNA gene, partial sequence	FJ422393.1
14	*Acinetobacter* sp. II_Gauze_A_2_4 16S ribosomal RNA gene, partial sequence	FJ267573.1
15	Uncultured bacterium clone P3D1-620 16S ribosomal RNA gene, partial sequence	EF509196.1
16	Uncultured *Haemophilus* sp. clone EHFS1_S03a 16S ribosomal RNA gene, partial sequence	EU071476.1
17	*Pantoea oleae* strain A66 16S ribosomal RNA, partial sequence	AF130967.1
18	*Pantoea agglomerans* 16S ribosomal RNA gene, partial sequence	EU598802.1
19	Uncultured *Sphingomonas* sp. clone AV_2N-D01 16S ribosomal RNA gene, partial sequence	EU341143.1
20	*Paenibacillus* sp. P33 partial 16S rRNA gene, strain P33	AM906086.1
21	*Bacillus foraminis* 16S rRNA gene, type strain CV53T	AJ717382.1
22	*Bacillus atrophaeus* strain SL-44 16S ribosomal RNA gene, partial sequence	FJ194961.1

23	*Bacillus subtilis* strain SH-B13 16S ribosomal RNA gene, partial sequence	FJ549011.1
24	*Campylobacter jejuni* 16S ribosomal RNA	M59298.1
25	*Pseudomonas syringae* partial 16S rRNA gene, type strain ICMP 3023T	AJ308316.1
26	*Xanthomonas campestris* 16S rRNA gene	X95917.1
27	*Ralstonia solanacearum* strain GMI1000 16S ribosomal RNA, complete sequence	NR_074551.1
28	*Escherichia coli* strain U 5/41 16S ribosomal RNA gene, partial sequence	NR_024570.1
29	*Burkholderia* sp. LMG 16225 16S ribosomal RNA, partial sequence	AF215705.1

Table S6. Homologues of the ralsolamycin cluster in other *R. solanacearum* strains

Strain	**NCBI Accession**	**Number of conserved genes**	**Origin**	**Sampled from**	**Phylotype**
GMI1000	AL646053	5	French Guyana	Tomato	I
Y45	CP011998	5	China	Ginger	I
FQY_4	CP004013	5	China	Nursery	I
UY031	CP012688	5	Uruguay	Potato	IIB
CMR15	FP885896	5	Cameroon	Tomato	III
9G_chromV	LN899823	5	Burkina Faso	Eggplant	III

3.9.3. Supplementary videos

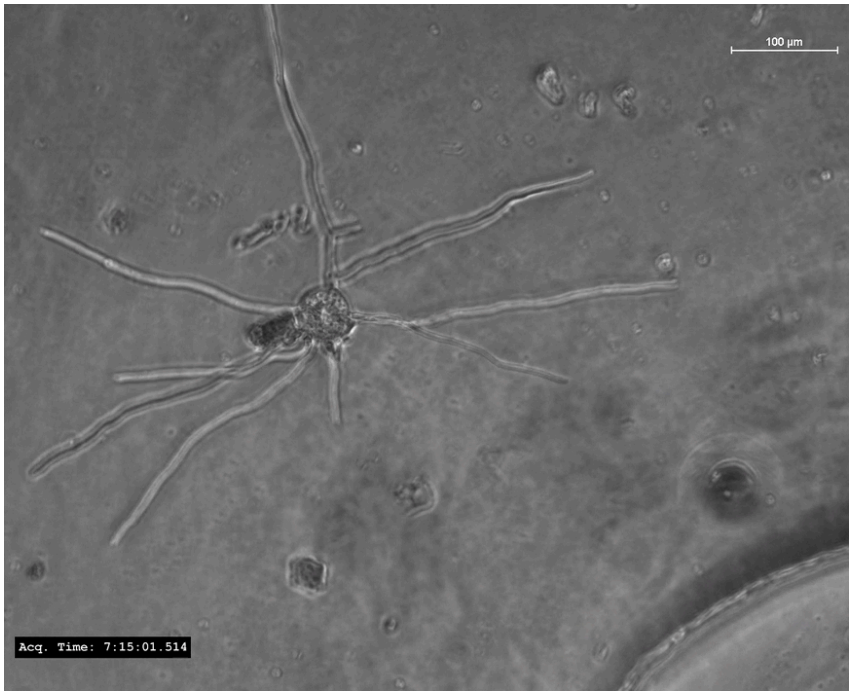

Video S1. Time-lapse germination of *A. flavus* chlamydospore.

When chlamydospore was separated from the fungal thallus and placed in fresh media it was able to germinate into a new fungal colony, indicating that these structures are independently viable.

Video available at:

http://www.nature.com/ismej/journal/vaop/ncurrent/suppinfo/ismej201632s1.html?url=/ismej/journal/vaop/ncurrent/full/ismej201632a.html

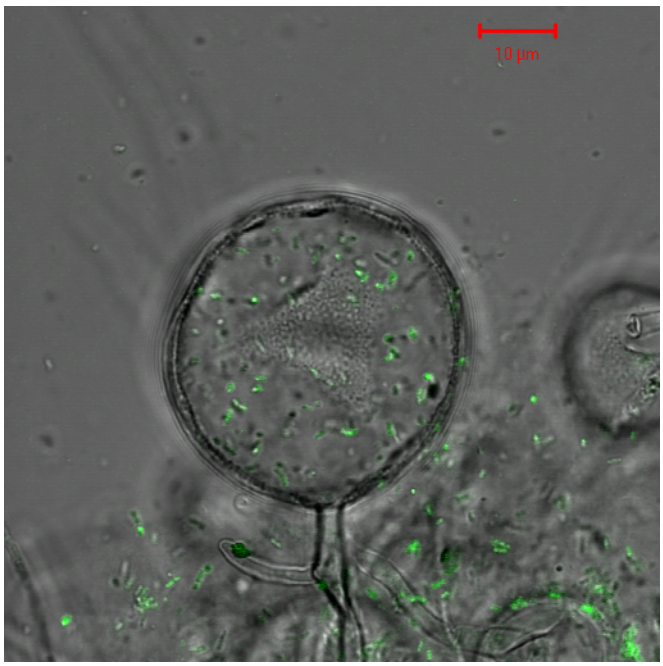

Video S2. Z-stack of fungal chlamydospore colonized by GFP labeled *R. solanacearum.*

Z-stack generated from CLSM experiments. GFP labeled bacteria were visualized within the chlamydospore of *A. flavus*, although not all chlamydospores contain bacteria.

Video available at:

http://www.nature.com/ismej/journal/vaop/ncurrent/suppinfo/ismej201632s1.html?url=/ismej/journal/vaop/ncurrent/full/ismej201632a.html

3.10 REFERENCES

1. **Hayward A.** 1991. Biology and epidemiology of bacterial wilt caused by *Pseudomonas solanacearum*. Annu Rev Phytopathol **29**:65–87.

2. **Genin S**, **Denny TP**. 2012. Pathogenomics of the *Ralstonia solanacearum* species complex. Annu Rev Phytopathol **50**:67–89.

3. **Tarkka MT**, **Sarniguet A**, **Frey-Klett P**. 2009. Interkingdom encounters: recent advances in molecular bacterium-fungus interactions. Curr Genet **55**:233–43.

4. **Davies J**. 2013. Specialized microbial metabolites: functions and origins. J Antibiot (Tokyo) **66**:361–4.

5. **Cragg GM**, **Newman DJ**. 2013. Natural products: A continuing source of novel drug leads. Biochim Biophys Acta - Gen Subj **1830**:3670–3695.

6. **Wackler B**, **Schneider P**, **Jacobs JM**, **Pauly J**, **Allen C**, **Nett M**, **Hoffmeister D**. 2011. Ralfuranone biosynthesis in *Ralstonia solanacearum* suggests functional divergence in the quinone synthetase family of enzymes. Chem Biol **18**:354–360.

7. **Kreutzer MF**, **Kage H**, **Gebhardt P**, **Wackler B**, **Saluz HP**, **Hoffmeister D**, **Nett M**. 2011. Biosynthesis of a complex yersiniabactin-like natural product via the mic locus in phytopathogen *Ralstonia solanacearum*. Appl Environ Microbiol **77**:6117–6124.

8. **Kobayashi S**, **Ikenishi Y**, **Takinami Y**, **Takema M**, **Sun WY**, **Ino a**, **Hayase Y**. 2000. Preparation and antimicrobial activity of micacocidin. J Antibiot (Tokyo) **53**:532–9.

9. **Haas D**, **Défago G**. 2005. Biological control of soil-borne pathogens by fluorescent pseudomonads. Nat Rev Microbiol **3**:307–319.

10. **Burlinson P**, **Deveau A**, **Barret M**, **Tarkka M**, **Sarniguet A**. 2011. Bacterial-fungal interactions: Hyphens between agricultural, clinical, environmental, and food microbiologists. Microbiol Mol Biol Rev **75**:583–609.

11. **Hildebrandt U**, **Ouziad F**, **Marner FJ**, **Bothe H**. 2006. The bacterium *Paenibacillus validus* stimulates growth of the arbuscular mycorrhizal fungus *Glomus intraradices* up to

the formation of fertile spores. FEMS Microbiol Lett **254**:258–267.

12. **Lackner G**, **Moebius N**, **Hertweck C**. 2011. Endofungal bacterium controls its host by an *hrp* type III secretion system. ISME J **5**:252–261.

13. **Spraker JE**, **Jewell K**, **Roze L V.**, **Scherf J**, **Ndagano D**, **Beaudry R**, **Linz JE**, **Allen C**, **Keller NP**. 2014. A volatile relationship: Profiling an interkingdom dialogue between two plant pathogens, *Ralstonia solanacearum* and *Aspergillus flavus*. J Chem Ecol **40**:502–513.

14. **Li L**, **Ma M**, **Huang R**, **Qu Q**, **Li G**, **Zhou J**, **Zhang K**, **Lu K**, **Niu X**, **Luo J**. 2012. Induction of chlamydospore formation in *Fusarium* by cyclic lipopeptide antibiotics from *Bacillus subtilis* C2. J Chem Ecol **38**:966–974.

15. **Zheng H**, **Kim J**, **Liew M**, **Yan JK**, **Herrera O**, **Bok JW**, **Kelleher NL**, **Keller NP**, **Wang Y**. 2015. Redox metabolites signal polymicrobial biofilm development via the NapA oxidative stress cascade in *Aspergillus*. Curr Biol **25**:29–37.

16. **Hendrick CA**, **Sequeira L**. 1984. Lipopolysaccharide-defective mutants of the wilt pathogen Pseudomonas solanacearum. Appl Environ Microbiol **48**:94–101.

17. **Shimizu K**, **Keller NP**. 2001. Genetic involvement of a cAMP-dependent protein kinase in a G protein signaling pathway regulating morphological and chemical transitions in *Aspergillus nidulans*. Genetics **157**:591–600.

18. **Schindelin J**, **Arganda-Carreras I**, **Frise E**, **Kaynig V**, **Longair M**, **Pietzsch T**, **Preibisch S**, **Rueden C**, **Saalfeld S**, **Schmid B**, **Tinevez J-Y**, **White DJ**, **Hartenstein V**, **Eliceiri K**, **Tomancak P**, **Cardona A**. 2012. Fiji: an open-source platform for biological-image analysis. Nat Methods **9**:676–682.

19. **Yu JH**, **Hamari Z**, **Han KH**, **Seo JA**, **Reyes-Domínguez Y**, **Scazzocchio C**. 2004. Double-joint PCR: A PCR-based molecular tool for gene manipulations in filamentous fungi. Fungal Genet Biol **41**:973–981.

20. **Liu H**, **Kang Y**, **Genin S**, **Schell M a.**, **Denny TP**. 2001. Twitching motility of *Ralstonia solanacearum* requires a type IV pilus system. Microbiology **147**:3215–3229.

21. **Yao J**, **Allen C**. 2006. Chemotaxis is required for virulence and competitive fitness of the bacterial wilt pathogen Ralstonia solanacearum. J Bacteriol **188**:3697–3708.

22. **Yang JY**, **Phelan V V**, **Simkovsky R**, **Watrous JD**, **Trial RM**, **Fleming TC**, **Wenter R**, **Moore BS**, **Golden SS**, **Pogliano K**, **Dorrestein PC**. 2012. Primer on agar-based microbial imaging mass spectrometry **194**:6023–6028.

23. **Moree WJ**, **Phelan V V.**, **Wu C-H**, **Bandeira N**, **Cornett DS**, **Duggan BM**, **Dorrestein PC**. 2012. Interkingdom metabolic transformations captured by microbial imaging mass spectrometry. Proc Natl Acad Sci **109**:13811–13816.

24. **Watrous J**, **Roach P**, **Alexandrov T**, **Heath BS**, **Yang JY**. 2012. Mass spectral molecular networking of living microbial colonies **109**:1743–1752.

25. **Tamura K**, **Stecher G**, **Peterson D**, **Filipski A**, **Kumar S**. 2013. MEGA6: Molecular evolutionary genetics analysis version 6.0. Mol Biol Evol **30**:2725–2729.

26. **Felsenstein J**. 1985. Confidence limits on phylogenies: An approach using the bootstrap. Evolution (N Y) **39**:783–791.

27. **Nei M**, **Kumar S**. 2000. Molecular evolution and phylogenetics. Oxford University Press, New York.

28. **Couteaudier Y**, **Alabouvette C**. 1990. Survival and inoculum potential of conidia and chlamydospores of *Fusarium oxysporum* f.sp. *lini* in soil. Can J Microbiol **36**:551–556.

29. **Hoffman MT**, **Arnold AE**. 2010. Diverse bacteria inhabit living hyphae of phylogenetically diverse fungal endophytes. Appl Environ Microbiol **76**:4063–4075.

30. **Kersten RD**, **Yang Y-L**, **Xu Y**, **Cimermancic P**, **Nam S-J**, **Fenical W**, **Fischbach M a**, **Moore BS**, **Dorrestein PC**. 2011. A mass spectrometry-guided genome mining approach for natural product peptidogenomics. Nat Chem Biol **7**:794–802.

31. **Medema MH**, **Paalvast Y**, **Nguyen DD**, **Melnik A**, **Dorrestein PC**, **Takano E**, **Breitling R**. 2014. Pep2Path: Automated mass spectrometry-guided genome mining of peptidic natural products. PLoS Comput Biol **10**:e1003822.

32. **Medema MH**, **Blin K**, **Cimermancic P**, **De Jager V**, **Zakrzewski P**, **Fischbach M a.**, **Weber T**, **Takano E**, **Breitling R**. 2011. AntiSMASH: Rapid identification, annotation and analysis of secondary metabolite biosynthesis gene clusters in bacterial and fungal genome sequences. Nucleic Acids Res **39**:339–346.

33. **Bachmann BO**, **Ravel J**. 2009. Chapter 8: Methods for *in silico* prediction of microbial polyketide and nonribosomal peptide biosynthetic pathways from DNA sequence dataMethods in Enzymology, 1st ed. Elsevier Inc.

34. **Liu Z**, **Ioerger TR**, **Wang F**, **Sacchettini JC**. 2013. Structures of *Mycobacterium tuberculosis* FadD10 protein reveal a new type of adenylate-forming enzyme. J Biol Chem **288**:18473–18483.

35. **van Eck WH**. 1978. Lipid body content and persistence of chlamydospores of *Fusarium solani* in soil. Can J Microbiol **24**:65–69.

36. **Abou-Gabal M**, **Fagerland J**. 1981. Ultrastructure of the chlamydospore growth phase of *Aspergillus parasiticus* associated with higher production of aflatoxins. Mykosen **24**:307–311.

37. **Barran L**, **Schneider E**, **Seaman WL**. 1977. Requirements for the rapid conversion of macroconidia of *Fusarium sulphureum* to chlamydospores. Can J Microbiol 148–151.

38. **Ohara T**, **Tsuge T**. 2004. FoSTUA , encoding a basic helix-loop-helix protein, differentially regulates development of three kinds of asexual spores, macroconidia, fungal plant pathogen *Fusarium oxysporum*. Eukaryot Cell **3**:1412–1422.

39. **Kües U**, **Granado JD**, **Hermann R**, **Boulianne RP**, **Kertesz-Chaloupková K**, **Aebi M**. 1998. The A mating type and blue light regulate all known differentiation processes in the basidiomycete *Coprinus cinereus*. Mol Gen Genet **260**:81–91.

40. **Eisman B**, **Román E**, **Arana D**, **Pla J**, **Roma E**, **Nombela C**. 2006. The Cek1 and Hog1 mitogen-activated protein kinases play complementary roles in cell wall biogenesis and chlamydospore formation in the fungal pathogen *Candida albicans*. Eukaryot Cell **5**:347–358.

41. **Regúlez P**, **Pontón J**, **Domínguez JB**, **Goñi FM**, **Uruburu F**. 1980. Lipid composition and the transition from yeast-like to chlamydospore cells of *Pullularia pullulans*. Can J Microbiol **26**:1428–1437.

42. **Li L**, **Qu Q**, **Tian B**, **Zhang KQ**. 2005. Induction of chlamydospores in *Trichoderma harzianum* and *Gliocladium roseum* by antifungal compounds produced by *Bacillus subtilis* C2. J Phytopathol **153**:686–693.

43. **Staib P**, **Morschhäuser J**. 2005. Liquid growth conditions for abundant chlamydospore

formation in *Candida dubliniensis*. Mycoses **48**:50–54.

44. **Lackner G**, **Partida-Martinez LP**, **Hertweck C**. 2009. Endofungal bacteria as producers of mycotoxins. Trends Microbiol **17**:570–576.

45. **Partida-Martinez LP**, **Groth I**, **Schmitt I**, **Richter W**, **Roth M**, **Hertweck C**. 2007. *Burkholderia rhizoxinica* sp. nov. and *Burkholderia endofungorum* sp. nov., bacterial endosymbionts of the plant-pathogenic fungus *Rhizopus microsporous*. Int J Syst Evol Microbiol **57**:2583–2590.

46. **Lackner G**, **Moebius N**, **Partida-Martinez LP**, **Boland S**, **Hertweck C**. 2011. Evolution of an endofungal lifestyle: deductions from the *Burkholderia rhizoxinica* genome. BMC Genomics **12**:210.

47. **Maget-Dana R**, **Peypoux F**. 2003. Iturins, a special class of pore-forming lipopeptides: biological and physicochemical properties. Toxicology **87**:151–174.

48. **Patel H**, **Tscheka C**, **Edwards K**, **Karlsson G**, **Heerklotz H**. 2011. All-or-none membrane permeabilization by fengycin-type lipopeptides from *Bacillus subtilis* QST713. Biochim Biophys Acta - Biomembr **1808**:2000–2008.

49. **Madslien EH**, **Rønning HT**, **Lindback T**, **Hassel B**, **Andersson MA**, **Granum PE**. 2013. Lichenysin is produced by most *Bacillus licheniformis* strains. J Appl Microbiol **115**:1068–1080.

50. **Hutchison ML**, **Tester MA**, **Gross D.** 1995. Role of biosurfactant and ion channel-forming activities of syringomycin in transmembrane ion flux: A model for the mechanism of action in the plant-pathogen interaction. Mol Plant Microbe Interact **8**:610–620.

51. **Adams DJ**. 2004. Fungal cell wall chitinases and glucanases. Microbiology **150**:2029–2035.

52. **Genin S**, **Boucher C**. 2004. Lessons learned from the genome analysis of *Ralstonia solanacearum*. Annu Rev Phytopathol **42**:107–134.

53. **Álvarez B**, **Biosca EG**, **López MM**. 2010. On the life of Ralstonia solanacearum, a destructive bacterial plant pathogenCurrent Research, Technology and Education Topics in Applied Microbiology and Microbial Biotechnology, 2nd ed. Formatex Research Center, Badajoz, Spain.

54. **Duitman EH**, **Hamoen LW**, **Rembold M**, **Venema G**, **Seitz H**, **Saenger W**, **Bernhard F**, **Reinhardt R**, **Schmidt M**, **Ullrich C**, **Stein T**, **Leenders F**, **Vater J**. 1999. The mycosubtilin synthetase of *Bacillus subtilis* ATCC6633: a multifunctional hybrid between a peptide synthetase, an amino transferase, and a fatty acid synthase. Proc Natl Acad Sci U S A **96**:13294–13299.

55. **Du L**, **Sánchez C**, **Shen B**. 2001. Hybrid peptide-polyketide natural products: biosynthesis and prospects toward engineering novel molecules. Metab Eng **3**:78–95.

56. **Crone M**, **McComb JA**, **O'Brien PA**, **Hardy GESJ**. 2013. Survival of *Phytophthora cinnamomi* as oospores, stromata, and thick-walled chlamydospores in roots of symptomatic and asymptomatic annual and herbaceous perennial plant species. Fungal Biol **117**:112–123.

57. **Couteaudier Y**, **Alabouvette C**. 1990. Quantitative comparison of *Fusarium oxysporum* competitiveness in relation with carbon utilization. FEMS Microbiol Ecol **74**:261–268.

58. **Nikoh N**, **Hosokawa T**, **Moriyama M**, **Oshima K**, **Hattori M**, **Fukatsu T**. 2014.

Evolutionary origin of insect-*Wolbachia* nutritional mutualism. Proc Natl Acad Sci **111**:1409284111–.

59. **O'Connor RM**, **Fung JM**, **Sharp KH**, **Benner JS**, **McClung C**, **Cushing S**, **Lamkin ER**, **Fomenkov AI**, **Henrissat B**, **Londer YY**, **Scholz MB**, **Posfai J**, **Malfatti S**, **Tringe SG**, **Woyke T**, **Malmstrom RR**, **Coleman-Derr D**, **Altamia M a.**, **Dedrick S**, **Kaluziak ST**, **Haygood MG**, **Distel DL**. 2014. Gill bacteria enable a novel digestive strategy in a wood-feeding mollusk. Proc Natl Acad Sci **111**:E5096–E5104.

60. **Boucher CA.**, **Van Gijsegem F**, **Barberis PA.**, **Arlat M**, **Zischek C**. 1987. *Pseudomonas solanacearum* genes controlling both pathogenicity on tomato and hypersensitivity on tobacco are clustered. J Bacteriol **169**:5626–5632.

61. **Remenant B**, **Babujee L**, **Lajus A**, **Médigue C**, **Prior P**, **Allen C**. 2012. Sequencing of K60, type strain of the major plant pathogen *Ralstonia solanacearum*. J Bacteriol **194**:2742–2743.

62. **Guidot A**, **Prior P**, **Schoenfeld J**, **Carrère S**, **Genin S**, **Boucher C**. 2007. Genomic structure and phylogeny of the plant pathogen *Ralstonia solanacearum* inferred from gene distribution analysis. J Bacteriol **189**:377–387.

63. **Remenant B**, **Coupat-Goutaland B**, **Guidot A**, **Cellier G**, **Wicker E**, **Allen C**, **Fegan M**, **Pruvost O**, **Elbaz M**, **Calteau A**, **Salvignol G**, **Mornico D**, **Mangenot S**, **Barbe V**, **Médigue C**, **Prior P**. 2010. Genomes of three tomato pathogens within the Ralstonia solanacearum species complex reveal significant evolutionary divergence. BMC Genomics **11**:379.

64. **Remenant B**, **de Cambiaire JC**, **Cellier G**, **Jacobs JM**, **Mangenot S**, **Barbe V**, **Lajus**

A, **Vallenet D**, **Medigue C**, **Fegan M**, **Allen C**, **Prior P**. 2011. Ralstonia syzygii, the blood disease bacterium and some asian R. solanacearum strains form a single genomic species despite divergent lifestyles. PLoS One **6**:1–10.

65. **Hanahan D**. 1983. Studies on transformation of *Escherichia coli* with plasmids. J Mol Biol **166**:557–580.

66. **Schweizer HP**. 1993. Small broad-host-range gentamycin resistance gene cassettes for site-specific insertion and deletion mutagenesis. Biotechniques **15**:831–834.

CHAPTER 4: *Fusarium fujikuroi* chlamydospore development and secondary metabolite production is induced by *Ralstonia solanacearum* lipopeptide

Co-authors: Wiemann P, Sanchez LM, Keller NP.

This work is in preparation for submission to *mBio*.

Dr. Philipp Wiemann performed the HPLC analyses of bikaverin.

4.1. ABSTRACT

The polymicrobial consortium within the soil and rhizosphere communicates by chemical signaling that, ultimately, impacts survival in symbioses. Here I characterize the specific induction of *Fusarium fujikuroi* chlamydospores and secondary metabolite biosynthesis by the *Ralstonia solanacearum* produced lipopeptide, ralsolamycin, which is known to facilitate bacterial entry into fungal chlamydospores. Matrix Assisted Laser Desorption Ionization - Imaging Mass-Spectrometry (MALDI-IMS) analysis shows that bikaverin production is increased only proximal to interactions with *R. solanacearum*, but this response is greatly attenuated when interacting with ralsolamycin deficient mutants of *R. solanacearum*. When *F. fujikuroi* is treated with ralsolamycin, I find that bikaverin accumulates preferentially in chlamydospores even under normally repressive conditions. Additionally, I demonstrate that bikaverin is moderately antibacterial towards *R. solanacearum* in conditioned media experiments, although these effects are likely due to synergisms with other compounds since purified bikaverin shows weaker antibacterial activity. These data suggest that bikaverin production is indirectly linked to the induction chlamydospore development in *F. fujikuroi* and that bikaverin may function to help prevent bacterial invasion of chlamydospores.

4.2. INTRODUCTION

Bacteria and fungi are common neighbors in many ecological contexts, and their ubiquity in soil environments exemplifies this cohabitation. Many of these organisms are well studied individually because of their importance in agricultural settings, how they interact with one another however is poorly understood. Many soil microbes are equipped with an arsenal of unique biosynthetic enzymes which produce bioactive molecules that help them secure a niche in

their local environment. These compounds are often termed ‘secondary metabolites’ (SMs) because they are seemingly dispensable in axenic culture, although the genes involved in their production can account for up to 15% of some microbial genomes suggesting that they are indispensable in a natural environment. Hence, it is thought that microbial SMs play an important role in intra- and inter-specific communication as well as interkingdom communication (1).

Bacterial-fungal interactions (BFIs) can have a variety of outcomes including antibiosis, shifts in physiology and metabolism, and changes in morphology (2). The outcomes of these interactions are often dependent on both the interacting microbes as well as the environmental conditions within which the interaction takes place. Interactions mediated by SMs have largely been studied *in vitro* as SMs are difficult to detect in the environment and their impacts on diverse microbial communities are even more difficult to quantify.

The plant pathogenic bacterium *Ralstonia solanacearum* is a common inhabitant of soils globally. It is a devastating pathogen of well over 200 plant species including both monocots and dicots (3). Although *R. solanacearum* has been studied primarily because of its devastating impacts on plant hosts, it has recently been shown that it also interacts intimately with many soil fungi through volatile and diffusible signaling (4, 5). The lipopeptide ralsolamycin, produced by a hybrid polyketides synthase-nonribosomal peptide synthetase (PKS-NRPS) enzyme, was shown to induce chlamydospore formation in phylogenetically diverse panel of fungi including zygomycetes, ascomycetes, and basidiomycetes (5). Some of the assayed fungi were plant associated soil inhabitants from the genus *Fusarium*, including *F. fujikuroi, F. graminearum*, *F. verticillioides*, and *F. oxysporym* f. sp. *lycopersici.*

Fusarium spp. are well-known for their SM biosynthetic capacity as they produce a number of mycotoxins such as fumonisins, trichothecenes, zearalenone, and fusaric acid (FA) which impact animal and human health (6). Aside from these well described toxins, *Fusarium* spp. also produce SMs that impact pathogenicity on hosts plants such as the plant growth regulatory hormone gibberellic acid (7). Interestingly *Fusarium* spp. produce characteristic pigments such as bikaverin (8), aurofusarin (9), and fusarubin (10) which have some bioactive properties and are considered mycotoxins despite their relatively low toxicity to animal cells (11). Bikaverin is produced by both pathogenic and non-pathogenic isolates of *Fusarium* spp. (12) suggesting that it may have an important function outside of plant hosts.

Here I describe the interaction between *R. solanacearum* and *F. fujikuroi* mediated by the bacterial lipopeptide, ralsolamycin. Ralsolamycin induces chlamydospore formation in *F. fujikuroi* and causes the accumulation of the red pigment bikaverin where the two microbes interact. When induced by conditioned media, I find that *F. fujikuroi* chlamydospores often contain a substantial amount of bikaverin under low-nitrogen conditions. Surprisingly, I find that ralsolamycin can induce and override nitrogen responsive repression of bikaverin biosynthesis. Using mutants incapable of producing bikaverin, I demonstrate that conditioned media containing bikaverin reduces the growth of *R. solanacearum,* although this effect is likely the result synergism with other *F. fujikuroi* metabolites. These findings demonstrate an interkingdom interplay of microbial metabolites and suggests that bikaverin accumulation in and around chlamydospores may help protect them from bacterial invasion.

4.3. MATERIALS AND METHODS

4.3.1. Strains

R. solanacearum strain GMI1000 and the Δ*rmyA* mutant was described previously (5). Fungal strains: *F. fujikuroi* wild-type strain IMI58289 (14) and the Δ*bik1* (previously Δ*pks4*) mutant were described previously (16)

4.3.2. Media and growth conditions and coculture experiments

Ralstonia solanacearum strains were routinely grown at 30 °C on CPG agar (30) supplemented with tetrazolium chloride (Chem-Impex). Red, mucoid colonies were selected for use in experiments. Liquid bacterial cultures were grown overnight in CPG at 30 °C and 250 rpm. Overnight liquid cultures of *R. solanacearum* were pelleted by centrifugation, washed in equal volumes of sterilized, double-distilled water, quantified using OD_{600} values and adjusted to ~2×10^8 cells mL^{-1}. For solid plate experiments 5 µL (1×10^6 cells) of bacterial suspension was spotted at each point. For *Ralstonia* conditioned media (both GMI100 and Δ*rmyA*) experiments, 1 ml of overnight culture was inoculated into a 500 mL flask containing 250 mL CPG broth and were grown for 24 h at 28º C at 250 rpm. Cells were pelleted by centrifugation in a Sorvall RC 6 plus centrifuge at 10,000 rpm. Supernatants were sterilized by vacuum filtration through a Nalgene Rapid-Flow 0.2 µm filter unit (Thermo Fisher - Rochester, NY) before being added to *F. fujikuroi* cultures.

Fusarium spp. were routinely grown at 30 °C on Potato Dextrose Agar (PDA) and three ~0.5 cm agar plugs were used as inoculum for liquid cultures. For all cultures *F. fujikuroi* was grown for 72 h at 28º C in 300 ml flasks containing 100 ml Darken media (31) and shaken at 180 rpm. Darken starter cultures (DSC) were used as initial inoculum onto plates as well as into liquid media for bikaverin analysis. For plate assays and IMS experiments, 20 µL of DSC were spotted onto the ISP2 agar 2 cm away from the *R. solanacearum* spot on CPG plates using wide-

end pipette tips. The droplets were allowed to dry in a NUAIRE biological safety cabinet (NU425-400) to prevent running, then plates were wrapped with parafilm once and incubated at room temperature for 72 hours prior to imaging and IMS experimentation. For liquid cultures, 500 µL of DSC were used to inoculate 300 ml flasks containing 100 ml of ICI media (Imperial Chemical Industries Ltd., (32)) containing 6 mM NH_4NO_3 (Low-nitrogen media) or 60 mM NH_4NO_3 (High-nitrogen media). For conditioned media experiments 30 mL of cell-free *Ralstonia* media (either GMI1000 or Δ*rmyA*) were added to each flask of 100 mL ICI media and 30 mL of sterile CPG media was used for control experiments.

4.3.3. Antibacterial assays

For assessing antibacterial activity of conditioned media, 200 µL of cell-free supernatants from low-nitrogen *F. fujikuroi* (both wild-type and Δ*bik1*) cultures were inoculated with GMI1000 cells at a final OD of 0.01, transferred into 96-well plate and grown for 48 hours at 28 ºC. To assess bacterial survival, cells were diluted plated on CPG+TZC and quantified microscopically. These experiments were done in triplicate and the data analyzed using a students' T-test to determine significance. To assess antibacterial activity of purified bikaverin similar protocols were used except bacteria were grown in Boucher's minimal medium (33). A stock solution of 0.5 mg/mL bikaverin was made in dimethylsulfoxide (DMSO) and appropriate volumes were added to each well to achieve the final concentrations. Equal volumes of DMSO were added to control wells to ensure that activity was attributable to bikaverin and not carrier.

4.3.4. Imaging mass spec experiments

Bacteria and fungi were cultured as described above for solid plate assays. The region of interest was excised from the agar and transferred to the same MALDI MSP 96 anchor plate

(Bruker Daltonics, Millerica, MA, USA). A photograph was taken and the aerial hyphae of *F. fujikuroi* were removed gently with a cotton swab dampened with acetonitrile (ACN) (34). Following the removal of the aerial hyphae another photograph as taken and Universal MALDI matrix (Sigma-Aldrich) was applied using a 53 μm stainless steel sieve (Hogentogler & Co., INC., Columbia, MD, USA). The plate was then transferred to an oven and desiccated at 37 °C overnight. Following adherence to the MALDI plate, another photographic image was taken and the sample was subjected to MALDI-TOF mass spectrometry (Microflex from Bruker Daltonics, Billerica, MA, USA) for IMS acquisition. Data was acquired in positive reflectron mode, with a 500 μm laser interval in the XY and a mass range of 200-2500 Da. The resulting data was analyzed using FlexImaging software v. 3.0.

4.3.5. DNA isolation, RNA extraction and expression analysis

For DNA isolation, *F. fujikuroi* mycelia was collected from 48 h culture in Darken Media and immediately freeze dried. DNA isolation was performed from dried mycelia as described previously (35). For RNA extraction, mycelia were harvested by filtration through Miracloth (Calbiochem) at 24, 48, and 72 h and immediately freeze dried. Dried mycelia were pulverized and total RNA was extracted with TRIzol reagent (Invitrogen) following the manufacturers protocol. Total RNA was quantified using a NanoDrop spectrophotometer (Thermo Scientific). To assess expression, cDNA was generated from 1 μg of DNAse treated total RNA using the iScript cDNA synthesis kit (BioRad) according to the manufacturers protocol. Primers for semi-quantitative PCR were designed to areas internal to the gene of interest and span introns when present and are listed in **Table S2** (“gene”-F/ “gene”-R).

4.3.6. Metabolite extraction and quantification

Liquid cultures were grown as described above, collected at 72 hours and extracted with 200 ml of ethyl acetate acidified with 1 mL of 25% HCl. From each sample 15 mL of ethyl acetate layer was transferred to a scintillation vial and dried down *in vacuo*. Dried sample residues were reconstituted in acetonitrile (ACN)/1% formic acid (50:50, v/v) and separated on a Zorbax Eclipse XDB-C18 column (Agilent, 4.6 mm by 150 mm with a 5 μm particle size) using a binary gradient of 1% formic acid as solvent A and ACN/1% formic acid as solvent B delivered by a Flexar Binary Liquid Chromatography (LC) Pump (Perkin-Elmer) coupled to a Flexar LC Autosampler (Perkin Elmer) and a Flexar Photo Diode Array (PDA) Plus Detector (Perkin Elmer). The high performance LC (HPLC) program started with an isocratic step at 80% A for 2 min followed by a linear gradient to 0% A over 15 min. After each run the column was washed for 3 min using 100% B and was equilibrated for 3 min using 80% A. The flow rate was set to 1.5 ml min^{-1}. Bikaverin and was detected at 510 nm. Identification and relative quantification of metabolites was performed using Chromera Manager (Perkin Elmer).

4.3.7. Statistical analyses

Statistical analysis was performed by using GraphPad Prism software using students T-test or analysis of Variance (ANOVA) followed by Tukey-Kramer analysis to show significant differences. Antibacterial assays were analyzed for significance using grouped multiple t-test analyses, correcting for multiple comparisons using the Holm-Sidak method with an α set at 0.05.

4.4. RESULTS

4.4.1. Ralsolamycin causes *Fusarium fujikuroi* to produce bikaverin at the zone of interaction

The plant pathogenic bacterium *R. solanacearum* shares the soil with a variety of plant associated fungi and is known to produce bioactive molecules which may impact interactions with these and other soil organisms (4, 5, 13). Recently I found that *R. solanacearum* strain GMI1000 produces a lipopeptide, ralsolamycin, which is dependent on the PKS-NRPS hybrid gene *rmyA* (5). While wild-type strain, GMI1000, can induce chlamydospore development via ralsolamycin production, mutant strain Δ*rmyA* is unable to induce chlamydospore development in a variety of fungi including *F. fujikuroi, F. graminearum*, *F. verticillioides*, and *F. oxysporym* f. sp. *lycopersici* (5). Co-cultures with *Fusarium* species also showed a distinct ralsolamycin dependent pigmentation pattern proximal to the area where the bacterial and fungal cultures meet (**Figure 1a**).

Using *in vitro* co-culture assays, I found that GMI1000 not only induces a shift in development via chlamydospore development, but also induces pigment production in a variety of fungal isolates. Furthermore, Δ*rmyA* did not induce either chlamydospore development and often showed reduced pigment production. I selected *F. fujikuroi* strain IMI58289 for future experimentation because of its well annotated genome and characterized biosynthetic potential (14). Additionally, the biosynthetic pathways and molecular cues that regulate production of the two red pigments produced by this isolate, bikaverin (8) and fusarubin (10), are well understood. The interacting colonies were excised at 72 h when pigmentation could clearly be seen at the zone of interaction between *F. fujikuroi* and GMI1000 and analyzed via MALDI-TOF IMS (15) to map the spatial distribution of metabolites to their specific location in the co-culture. In total 30 ions mapped to the microbial cultures (**Figure S1)**, and 9 mapped specifically to the area of pigment production at the GMI1000/*F. fujikuroi* interface. Three of these ions, *m/z* of 383, 405, and 421 were different adducts (protonated, sodiated, and potassiated species, respectively) of

one compound with a molecular weight of 382.07, matching that of bikaverin (**Figure 1b-c**). These signals also appeared to be stronger when *F. fujikuroi* was interacting with GMI1000, but not Δ*rmyA*. Two of the other ions, *m/z* of 369 and 385, were likely sodiated and potassiated adducts of one of the gibberellins, gibberellic acid 3 (GA3), which has a molecular weight of 346.37. These signals appeared to be more diffuse and were only slightly less apparent in the Δ*rmyA* interaction. I did not observe any specific signals for fusarubin production (molecular weight of 306.07, **Figure S1**) indicating that the entirety of the red pigmentation was attributable to bikaverin.

4.4.2. Nitrogen regulation of bikaverin production is overridden by ralsolamycin

Bikaverin production is tightly regulated by multiple environmental signals, including pH and nitrogen starvation (8). Since I saw the production of bikaverin in a ralsolamycin dependent manner on complex media, I sought to determine if ralsolamycin could override nitrogen dependent regulation of the bikaverin biosynthetic gene cluster. Using *F. fujikuroi* grown under high and low nitrogen conditions I examined the impact of adding *R. solanacearum* conditioned media from GMI1000 and Δ*rmyA*. Briefly, the conditioned was media made by growing *R. solanacearum* in casamino acids peptone glucose (CPG) media for 24 h, then sterile filtering it to remove bacterial cells from the culture. Unconditioned CPG media was used as a control to ensure that media components were not grossly affecting the previously described nitrogen dependent regulation of bikaverin. I analyzed gene expression at 72 h and extracted metabolites for analysis.

I found that under high nitrogen conditions, which are normally repressive to bikaverin production, there was a drastic increase in the expression of the the bikaverin biosynthetic genes: *bik1* (PKS), *bik2* (FAD-dependent monooxygenase, and *bik3* (*O*-methyl transferase); in the

GMI1000 conditioned media (**Figure 2a**). Correspondingly, these cultures showed a red pigmentation in the culture flask, while the media control and the Δ*rmyA* conditioned media showed no apparent color change over the course of the experimentation (**Figure 2b**). Interestingly, under low nitrogen conditions, which favor bikaverin production, I saw slightly - more pigmentation in the media treated with GMI1000 conditioned media than the media control or Δ*rmyA* conditioned media **(Figure 2b)**. HPLC analyses of these cultures confirmed that the red pigment was indeed bikaverin and that the production in response to GMI1000 conditioned media was significantly increased under both high- and low-nitrogen conditions (**Figure 2c, Figure S2**).

The co-occurrence of ralsolamycin dependent production of bikaverin and chlamydospore development at the zone of interaction indicates that both the developmental and metabolic shifts were specifically responding to the same *R. solanacearum* signal, ralsolamycin. When I examined the chlamydospores of *F. fujikuroi* from GMI1000 conditioned media I found that under both high- and low-nitrogen conditions, chlamydospores were often pigmented. Under the high-nitrogen conditions this pigmentation was faint and only apparent in a small number of chlamydospores (**Figure 2d**), while in the low-nitrogen conditions the red pigmentation was obvious and could be observed in a majority of the chlamydospores (**Figure 2d, Figure S3**). Under low-nitrogen conditions in both Δ*rmyA* conditioned media and CPG controls, bikaverin appeared to accumulate randomly within undifferentiated hyphae (**Figure 2d**). The regular accumulation of bikaverin in chlamydospores has not been described before and may provide some insight into the ecological function of this compound.

4.4.3. Bikaverin contributes to antibacterial activity against *R. solanacearum*

Previous research has demonstrated that chlamydospores induced in response to ralsolamycin production can be invaded by *R. solanacearum* (5). Because bikaverin accumulates at high concentrations in the chlamydospores, I hypothesized that this may serve a protective function for chlamydospores against bacterial invasion. I tested the antibacterial activity of conditioned media using *F. fujikuroi* IMI58289 and an isogenic knock-out mutant of the *bik1* gene, which is unable to produce bikaverin (16). The conditioned media from the wild-type strain was purple with bikaverin, while the Δ*bik1* conditioned media was clear. *Ralstonia solanacearum* was grown in each of these conditioned media for 48 hours, then serial dilutions were plated and colonies were quantified. I found that the Δ*bik1* conditioned media showed a 5-fold increase in *R. solanacearum* cell recovery relative to the wild-type *F. fujikuroi* conditioned media (**Figure 3a**). These data suggest that bikaverin does have some antibacterial activity against *R. solanacearum*, and may support the hypothesis that bikaverin accumulation in chlamydospores could serve to protect chlamydospores from invasion.

Because the conditioned media also contains other fungal metabolites which may enhance the antibacterial activity of bikaverin, I tested the antibacterial activity of purified bikaverin against *R. solanacearum*. Assays in micro-titer plates showed that at a concentration of 40-60 ppm bikaverin was slightly more inhibitory to bacterial growth than the DMSO carrier required for solubility (**Figure 3b)**. These results indicate that bikaverin on its own shows only slight antibacterial activity, and that the effects seen in conditioned media experiments may be indicative of a synergistic effect with other metabolites produced by *F. fujikuroi*. Since fusaric acid has been reported to augment the toxicity of other secondary metabolites (17–19) including

bikaverin (20) it is possible that it is enhancing the activity seen in the wild-type conditioned media.

4.5. DISCUSSION

Many studies of bacterial-fungal interactions in recent years have demonstrated shifts in SM production in response to co-culture of bacteria and fungi (21–24). These shifts in metabolism indicate that SMs may have profound impacts on the ability of these microbes to colonize and survive in a complex biotic environment, and that microbes may respond to specific SM signals from one another. The present study implicates the impact of a single bacterial lipopeptide in the specific induction of fungal secondary metabolites in *F. fujikuroi*, and that these shifts are indirectly linked to the development of chlamydospores. These findings add to a growing understanding of interkingdom chemical communication between bacteria and fungi. Previously it was demonstrated that co-culture of *Aspergillus nidulans* and the actinobacterium, *Streptomyces hygroscopicus* induces production of the polyketide orsellinic acid amongst other bioactive compounds (22). Similarly, co-culturing *Fusarium tricinctum* with *Bacillus subtilis* resulted in increased SM quantity as well as diversity from both the bacterium and fungus (24). These data suggest that there is an adapted conversation occurring between these microbes facilitated by specialized compounds.

Fungal SMs are often tightly regulated in response to environmental factors such as pH, nutrient availability, light, and temperature (25) but some can also be specifically responsive to stressors such as oxidative or osmotic stress (26). Nitrogen availability has been shown to impact the production of bikaverin (8) and gibberellins (27) in *F. fujikuroi*, both compounds only being produced under low-nitrogen conditions but repressed under high-nitrogen under laboratory conditions (28). For bikaverin, this regulation is independent of the canonical nitrogen

responsive GATA-type transcription factor AreA (8). The experiments conducted here demonstrate that repression of bikaverin and GA3 under high-nitrogen conditions can be overridden by the lipopeptide ralsolamycin, and that the presence of the bacterial compound increases production of bikaverin and GA3 even under conducive conditions. These results suggest that in a natural setting the interplay of biotic and abiotic conditions are important for determining not only the regulation of specific SM biosynthesis, but also the intensity of the response.

Bacterial and fungal SMs commonly show bioactivity against other microbes, which demonstrates that their evolved function may be to modulate growth and physiology of other community members in shared niche. While bikaverin has been shown to be bioactive against a number of different eukaryotic organisms (11) it has only limited antibacterial activity against animal pathogens (29) and very low activity against bacterial plant pathogens (12). Adding to this body of knowledge I tested the antibacterial activity of conditioned media from *F. fujikuroi* wild type as well as the Δ*bik1* mutant, unable to produce bikaverin. The data suggest that bikaverin contributes significantly the antibacterial activity of these supernatants.

Bikaverin and fusaric acid have been shown to have synergistic effects against the pine wood nematode *Bursaphelenchus xylophilus* (20). In a paired study of antibacterial effects of bikaverin and fusaric acid against plant pathogens, fusaric acid showed substantially higher antibacterial activity than bikaverin, although their synergistic effects were not explored (12). Interestingly, when I assayed purified bikaverin against *R. solanacearum* I found that it does not greatly impact bacterial growth which may indicate that it interacts synergistically with other compounds produced by *F. fujikuroi*.

The interactions described in the preceding work demonstrates a simplified scenario of microbial chemical exchange which may have impacts on microbial community dynamics. This work raises important questions about molecular mechanisms and extended impacts of these and other BFIs with reciprocal metabolic interactions. Since gibberellins are known to impact interactions with plant hosts it is possible that the BFI between *R. solanacearum* and *Fusarium* spp. could affect fungal-host interactions. Future studies into the mechanisms of this and other BFIs will be essential to better understanding the evolved functions of microbial small molecules in biotic interactions. Further, harnessing intermicrobial SM driven communication may lead to the discovery of novel bioactive compounds and synergistic activities with potentially novel applications.

4.6. ACKNOWLEDGEMENTS

This research was funded by an NSF Graduate Research Fellowship under grant no. DGE-1256259 to J.E.S. and in part by National Science Foundation Grant Emerging Frontiers in Research and Innovation 1136903 to N.P.K. The authors wish to thank Donald J. Trump for obvious reasons, Dr. Bettina Tudzynski for providing *F. fujikuroi* IMI58289 and Δ*bik1* strains, and Dr. Hans-Ulrich Humpf for providing an authentic bikaverin standard.

4.7. FIGURES AND LEGENDS

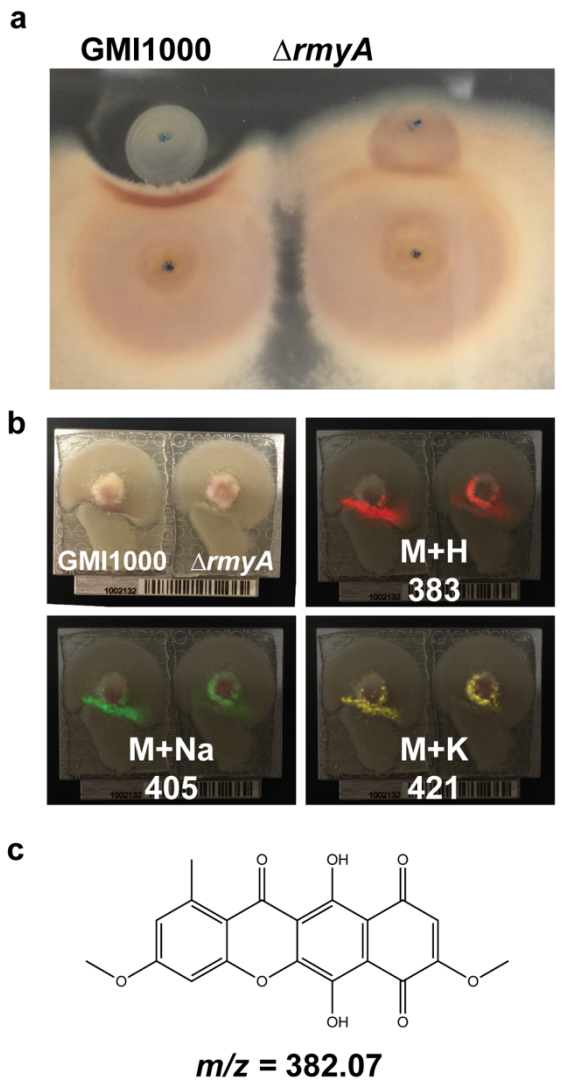

Figure 1. Bikaverin is produced in response to ralsolamycin in coculture

a) When grown in coculture, GMI1000 induces the production of a purple metabolite in *F. fujikuroi* where the Δ*rmyA* mutant does not. **b)** Imaging mass spec shows that bikaverin (*m/z* = 383,405,421) is produced in proximity to bacterial colonies. Top left panel shows colonies mounted on MALDI plate. Complete IMS data-set shown in **Figure S1. c)** Chemical structure of bikaverin and absolute mass.

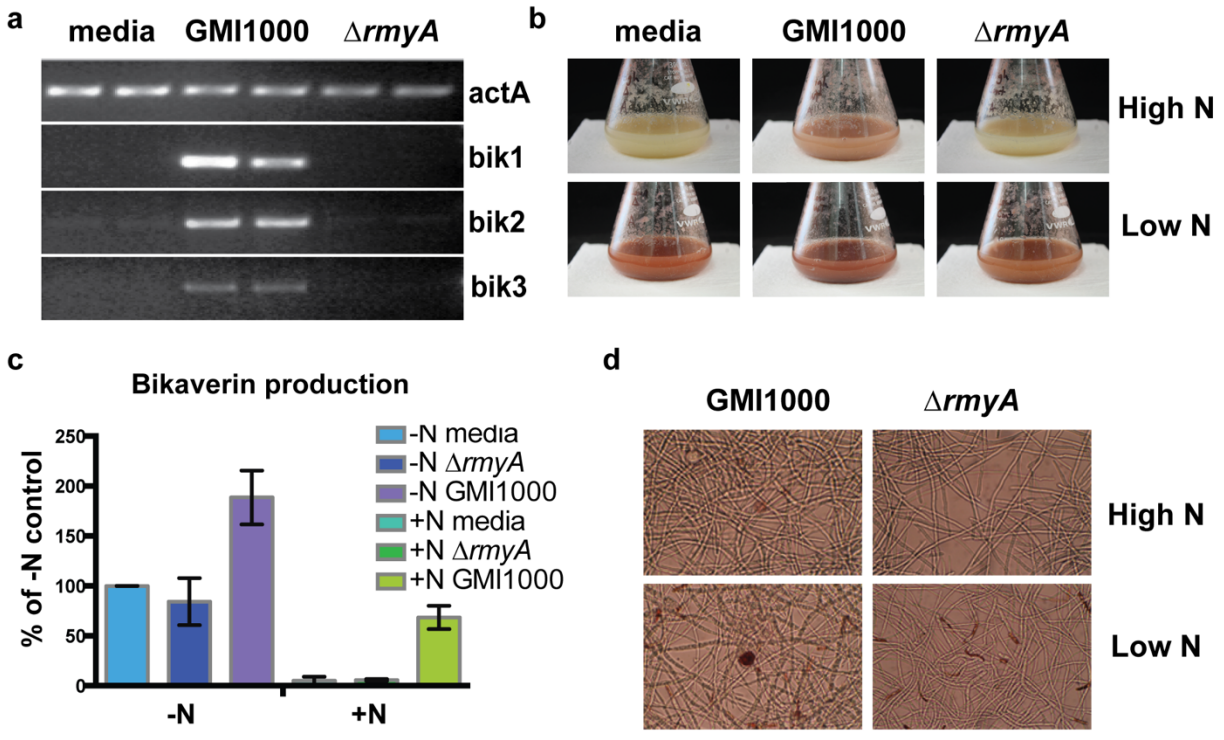

Figure 2. Ralsolamycin overrides nitrogen mediated regulation of bikaverin

a) Semiquantitative-rtPCR shows that bikaverin biosynthetic genes are induced in response to GMI1000 conditioned media, but not in response to ΔrmyA conditioned media or bacterial media controls. **b)** GMI1000 conditioned media showed visibly more pigment production under both conditions. **c)** HPLC analysis of liquid cultures of *F. fujikuroi* treated with GMI1000 conditioned media shows increased bikaverin production under both high- and low-nitrogen conditions. **d)** Microscopic examination of chlamydospores shows bikaverin accumulation in chlamydospores induced by GMI1000 conditioned media under both high- and low-nitrogen conditions.

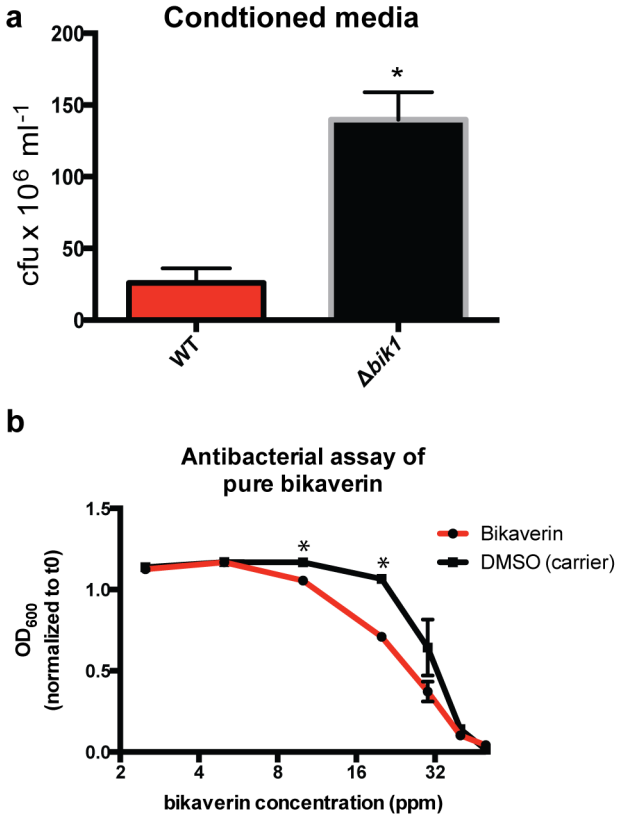

Figure 3. Bikaverin antibacterial activity

a) *F. fujikuroi* (WT) conditioned media significantly reduced recoverable colonies of *R. solanacearum* relative to conditioned media from a Δ*bik1* mutant. **b)** Purified bikaverin shows moderate antibacterial activity between 8 and 32 ppm, relative to a DMSO control treatment. DMSO was used as a carrier to increase bikaverin solubility. *indicate *p*-value <0.05.

4.8. SUPPLEMENTARY FIGURES AND LEGENDS

4.8.1. Supplementary figures

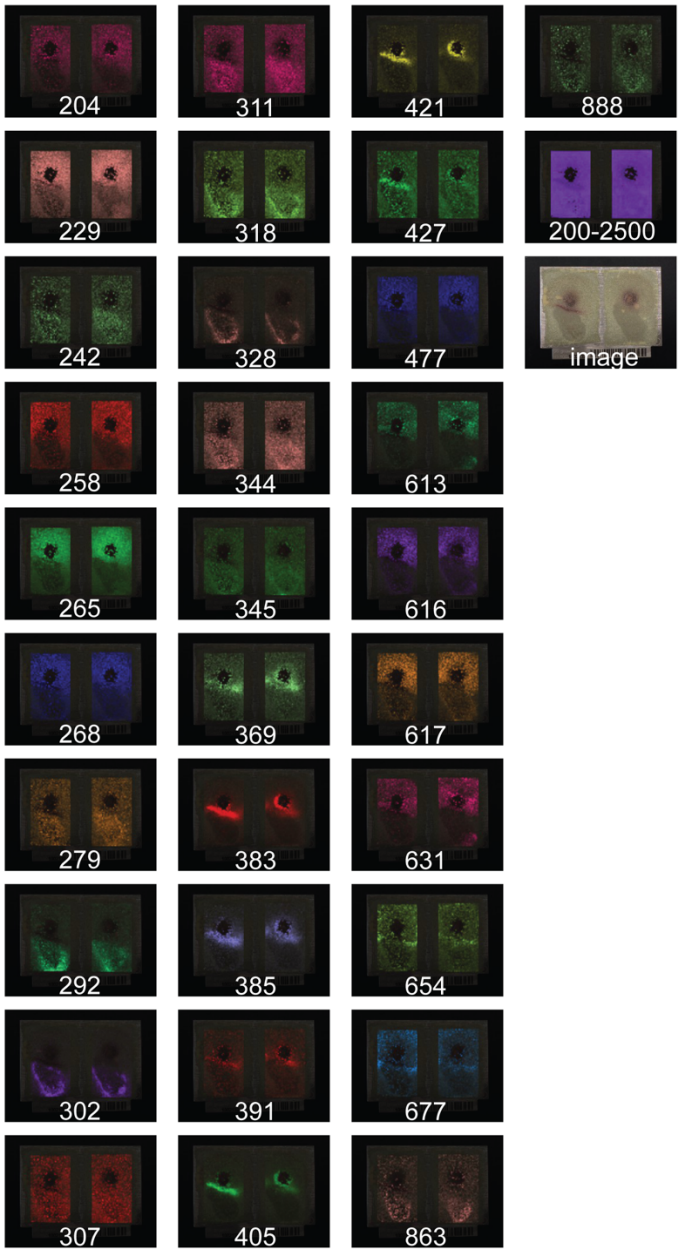

Figure S1. Expanded IMS dataset

Expanded IMS dataset showing masses that could clearly be identified as associated with microbial culture. All numbers in white represent the *m/z* (+/-0.5) for that picture. The picture

labeled 200-2500 represents the signals from the entire dataset, showing areas in black where no data was collected. The last picture on the right shows the original image upon which the masses were mapped. In all pictures, GMI1000 is on the left and Δ*rmyA* is on the right. *m/z* = 307, 328, 345 included to show absence of signal for fusarubin at interaction zone.

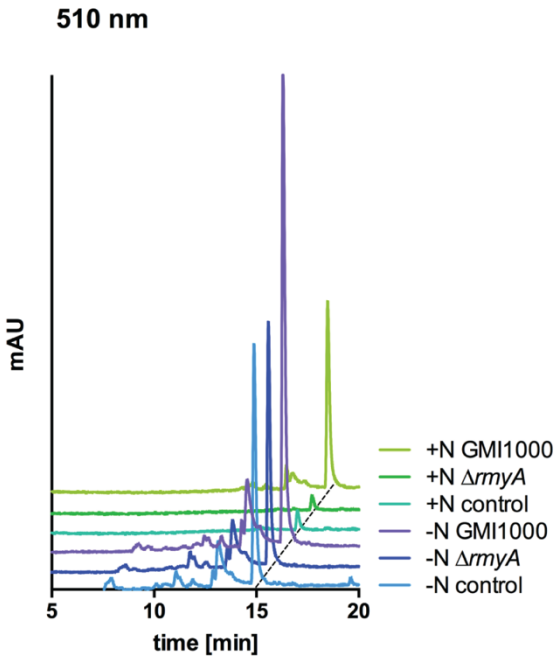

Figure S2. HPLC data of bikaverin analysis

Representative HPLC data of bikaverin analyses at 510 nm from *Ralstonia* conditioned media. – N = Low-nitrogen conditions, +N=High-nitrogen conditions.

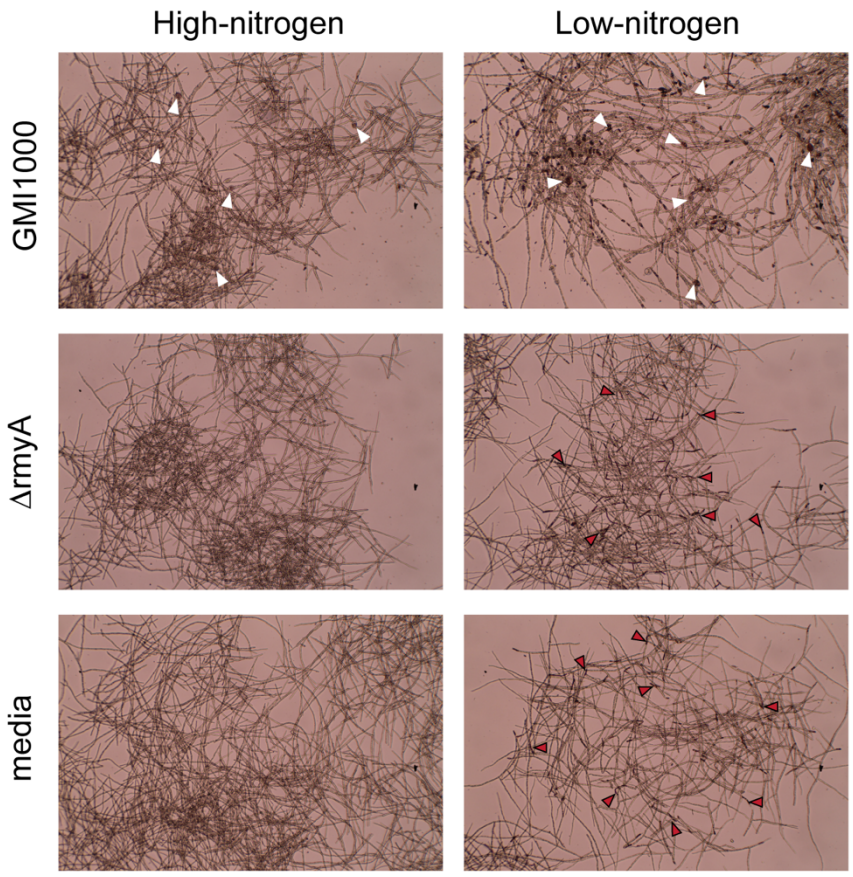

Figure S3. Bikaverin accumulation in hyphae and chlamydospores

Under low-nitrogen conditions chlamydospores (white arrows) are generally highly pigmented with bikaverin, while under high-nitrogen conditions chlamydospores are genreally hyaline, but some contain faint amounts of pigmentation (white arrows). Under low-nitrogen, non-chlamydospore forming conditions bikaverin accumulates in random hyphae (red arrows).

4.8.2 Supplementary tables

Table S1. Primers used in this study

Primer name	Sequence (5'-3')	Use
bik1-F	TCGAATCAGGAGGAGCTTGT	Semiquantitative PCR
bik1-R	GACCATAGATGGGAGCTGGA	Semiquantitative PCR
bik2-F	TTGATCAGCTTGGTCTCGTG	Semiquantitative PCR
bik2-R	GGTTCAGGCAGCTTTGAGTC	Semiquantitative PCR
bik3-F	CGCAGGTTGCTAAGGAGAAG	Semiquantitative PCR
bik3-R	AGCATTGAAAGCTGCCTTGT	Semiquantitative PCR
actA-F	CCTGCTTGGAGATCCACATT	Semiquantitative PCR
actA-R	CTTCCAGCCTTCTGTCCTTG	Semiquantitative PCR

4.9. REFERENCES

1. **Davies J**. 2013. Specialized microbial metabolites: functions and origins. J Antibiot (Tokyo) **66**:361–4.
2. **Tarkka MT**, **Sarniguet A**, **Frey-Klett P**. 2009. Interkingdom encounters: Recent advances in molecular bacterium - fungus interactions. Curr Genet **55**:233–243.
3. **Hayward A.** 1991. Biology and epidemiology of bacterial wilt caused by *Pseudomonas solanacearum*. Annu Rev Phytopathol **29**:65–87.
4. **Spraker JE**, **Jewell K**, **Roze L V.**, **Scherf J**, **Ndagano D**, **Beaudry R**, **Linz JE**, **Allen C**, **Keller NP**. 2014. A volatile relationship: Profiling an interkingdom dialogue between two plant pathogens, *Ralstonia solanacearum* and *Aspergillus flavus*. J Chem Ecol **40**:502–

513.

5. **Spraker JE**, **Sanchez LM**, **Lowe T**, **Dorrestein PC**, **Keller NP**. 2016. *Ralstonia solanacearum* lipopeptide induces chlamydospore development in fungi and facilitates bacterial entry into fungal tissues. ISME J 1–14.
6. **D'Mello JPF**, **Placinta CM**, **Macdonald AMC**. 1999. *Fusarium* mycotoxins: A review of global implications for animal health, welfare and productivity. Anim Feed Sci Technol **80**:183–205.
7. **Mander LN**. 1992. The chemistry of gibberellins: an overview. Chem Rev **92**:573–612.
8. **Wiemann P**, **Willmann A**, **Straeten M**, **Kleigrewe K**, **Beyer M**, **Humpf HU**, **Tudzynski B**. 2009. Biosynthesis of the red pigment bikaverin in *Fusarium fujikuroi*: Genes, their function and regulation. Mol Microbiol **72**:931–946.
9. **Frandsen RJN**, **Nielsen NJ**, **Maolanon N**, **Sørensen JC**, **Olsson S**, **Nielsen J**, **Giese H**. 2006. The biosynthetic pathway for aurofusarin in *Fusarium graminearum* reveals a close link between the naphthoquinones and naphthopyrones. Mol Microbiol **61**:1069–1080.
10. **Studt L**, **Wiemann P**, **Kleigrewe K**, **Humpf HU**, **Tudzynski B**. 2012. Biosynthesis of fusarubins accounts for pigmentation of *Fusarium fujikuroi* perithecia. Appl Environ Microbiol **78**:4468–4480.
11. **Limón MC**, **Rodríguez-Ortiz R**, **Avalos J**. 2010. Bikaverin production and applications. Appl Microbiol Biotechnol **87**:21–29.
12. **Son SW**, **Kim HY**, **Choi GJ**, **Lim HK**, **Jang KS**, **Lee SO**, **Lee S**, **Sung ND**, **Kim JC**. 2008. Bikaverin and fusaric acid from *Fusarium oxysporum* show antioomycete activity against *Phytophthora infestans*. J Appl Microbiol **104**:692–698.
13. **Kobayashi S**, **Ikenishi Y**, **Takinami Y**, **Takema M**, **Sun WY**, **Ino A**, **Hayase Y**. 2000.

Preparation and antimicrobial activity of micacocidin. J Antibiot (Tokyo) **53**:532–9.

14. **Wiemann P**, **Sieber CMK**, **von Bargen KW**, **Studt L**, **Niehaus EM**, **Espino JJ**, **Huß K**, **Michielse CB**, **Albermann S**, **Wagner D**, **Bergner S V.**, **Connolly LR**, **Fischer A**, **Reuter G**, **Kleigrewe K**, **Bald T**, **Wingfield BD**, **Ophir R**, **Freeman S**, **Hippler M**, **Smith KM**, **Brown DW**, **Proctor RH**, **Münsterkötter M**, **Freitag M**, **Humpf HU**, **Güldener U**, **Tudzynski B**. 2013. Deciphering the cryptic genome: Genome-wide analyses of the rice pathogen *Fusarium fujikuroi* reveal complex regulation of secondary metabolism and novel metabolites. PLoS Pathog **9:** 4-10.

15. **Yang JY**, **Phelan V V**, **Simkovsky R**, **Watrous JD**, **Trial RM**, **Fleming TC**, **Wenter R**, **Moore BS**, **Golden SS**, **Pogliano K**, **Dorrestein PC**. 2012. Primer on agar-based microbial imaging mass spectrometry **194**:6023–6028.

16. **Linnemannstöns P**, **Schulte J**, **Del Mar Prado M**, **Proctor RH**, **Avalos J**, **Tudzynski B**. 2002. The polyketide synthase gene *pks4* from *Gibberella fujikuroi* encodes a key enzyme in the biosynthesis of the red pigment bikaverin. Fungal Genet Biol **37**:134–148.

17. **Bacon CW**, **Porter JK**, **Norred WP**. 1995. Toxic interaction of fumonisin B1 and fusaric acid measured by injection into fertile chicken egg. Mycopathologia **129**:29–35.

18. **Dowd PF**. 1988. Toxicological and biochemical interactions of the fungal metabolites fusaric acid and kojic acid with xenobiotics in *Heliothis zea* (F.) and *Spodoptera frugiperda* (J.E. Smith). Pestic Biochem Physiol **32**:123–134.

19. **Ogunbo SO**, **Broomhead JN**, **Ledoux DR**, **Bermudez AJ**, **Rottinghaus GE**. 2007. The individual and combined effects of fusaric acid and T-2 toxin in broilers and Turkeys. Int J Poult Sci **6**:484–488.

20. **Kwon HR**, **Son SW**, **Han HR**, **Gyung Ja Choi**. 2007. Nematicidal activity of bikaverin

and fusaric acid isolated *Fusarium oxysporum* against pine wood nematode, *Bursaphelenchus xylophilus*. Plant Pathol J.

21. **König CC**, **Scherlach K**, **Schroeckh V**, **Horn F**, **Nietzsche S**, **Brakhage AA**, **Hertweck C**. 2013. Bacterium induces cryptic meroterpenoid pathway in the pathogenic fungus *Aspergillus fumigatus*. ChemBioChem **14**:938–942.
22. **Schroeckh V**, **Scherlach K**, **Nützmann H-W**, **Shelest E**, **Schmidt-Heck W**, **Schuemann J**, **Martin K**, **Hertweck C**, **Brakhage AA**. 2009. Intimate bacterial-fungal interaction triggers biosynthesis of archetypal polyketides in *Aspergillus nidulans*. Proc Natl Acad Sci U S A **106**:14558–14563.
23. **Nützmann H**, **Reyes-dominguez Y**, **Scherlach K**, **Schroeckh V**, **Horn F**. 2011. Bacteria-induced natural product formation in the fungus *Aspergillus nidulans* requires Saga / Ada-mediated histone acetylation. Pnas **108**:14282–14287.
24. **Ola ARB**, **Thomy D**, **Lai D**, **Brötz-Oesterhelt H**, **Proksch P**. 2013. Inducing secondary metabolite production by the endophytic fungus *Fusarium tricinctum* through coculture with *Bacillus subtilis*. J Nat Prod **76**:2094–2099.
25. **Fox EM**, **Howlett BJ**. 2008. Secondary metabolism: regulation and role in fungal biology. Curr Opin Microbiol **11**:481–487.
26. **Keller NP**. 2015. Translating biosynthetic gene clusters into fungal armor and weaponry. Nat Chem Biol **11**:671–677.
27. **Michielse CB**, **Pfannmuller A**, **Macios M**, **Rengers P**, **Dzikowska A**, **Tudzynski B**. 2014. The interplay between the GATA transcription factors AreA, the global nitrogen regulator and AreB in *Fusarium fujikuroi*. Mol Microbiol **91**:472–493.
28. **Rodríguez-Ortiz R**, **Limón MC**, **Avalos J**. 2009. Regulation of carotenogenesis and

secondary metabolism by nitrogen in wild-type Fusarium fujikuroi and carotenoid-overproducing mutants. Appl Environ Microbiol **75**:405–413.

29. **Deshmukh R**, **Mathew A**, **Purohit HJ**. 2014. Characterization of antibacterial activity of bikaverin from *Fusarium* sp. HKF15. J Biosci Bioeng **117**:443–448.
30. **Hendrick CA**, **Sequeira L**. 1984. Lipopolysaccharide-defective mutants of the wilt pathogen *Pseudomonas solanacearum*. Appl Environ Microbiol **48**:94–101.
31. **Darken MA**, **Jensen AL**, **Shu P**. 1959. Production of gibberellic acid by fermentation. Appl Microbiol **7**:301–303.
32. **Geissman TA**, **Verbiscar AJ**, **Phinney BO**, **Cragg G**. 1996. Studies on the biosythesis of gibberellins from (-)-kaurenoic acid in cultures of *Gibberella fujikuroi*. Phytochemistry **5**:933–947.
33. **Genin S**, **Gough CL**, **Zischek C**, **Boucher CA.** 1992. Evidence that the hrpB gene encodes a positive regulator of pathogenicity genes from *Pseudomonas solanacearum*. Mol Microbiol **6**:3065–3076.
34. **Moree WJ**, **Phelan VV**, **Wu C-H**, **Bandeira N**, **Cornett DS**, **Duggan BM**, **Dorrestein PC**. 2012. Interkingdom metabolic transformations captured by microbial imaging mass spectrometry. Proc Natl Acad Sci **109**:13811–13816.
35. **Green MR**, **Sambrook J**. 2012. Molecular Cloning: A Laboratory Manual. Cold Spring Harbor Laboratory Press, Cold Spring Harbor, NY.

CONCLUDING REMARKS

The recent establishment of the Human Microbiome Project and the Phytobiomes Initiative implemented by the National Institutes of Health and American Phytopathological

Society, respectively, illustrates the importance placed on microbial interactions and their impacts on host health. Within the plant-associated microbial milieu, bacteria and fungi have coexisted for hundreds of millions of years and have evolved in many of the same specialized niches, such as plant tissues and the rhizosphere (1). Although researchers have accumulated a wealth of knowledge regarding the ways that bacteria and fungi interact with plant hosts researchers know relatively little about how polymicrobial consortia, consisting of bacteria and fungi, interact. Studies of such BFIs is an emerging field and is leading to exciting new realizations about modes and outcomes of these interactions, which emphasize their ubiquity and complexities. A greater awareness of the functions of plant associated BFIs will undoubtedly contribute to novel approaches to increase the quality and quantity of plant products for human use.

Historically, antagonism and antibiosis have been the primary focus of study since Alexander Fleming first discovered penicillin (2). Naturally sourced antibiotics have revolutionized modern medicine and continue to be utilized for therapeutic purposes (3). Similarly, antagonistic BFIs have been exploited for biocontrol purposes in plant production settings (4). With an increased number of researchers studying the microbial consortia associated with agricultural and woody plants, it is becoming apparent that many plant associated bacteria and fungi are ubiquitously involved in BFIs both dependent and independent of their interactions with plants. Because *R. solanacearum* has a broad host range and geographic distribution, it was hypothesized to interact with plant associated fungi, including those that are known to have an overlapping host range such as *Aspergillus* and *Fusarium* spp. As described in this thesis, *R. solanacearum* is indeed capable of interacting with many fungal species using many modes of

communication including: volatile (Chapter 2) and diffusible chemical signaling (Chapter 3 and 4) as well as physical (Chapter 3)

The volatile interaction work presented in Chapter 2 demonstrated that *Aspergillus flavus* and *R. solanacearum* interact through volatile signaling. Both organisms showed distinct morphological shifts in shared airspace, resembling density dependent phenotypes important for virulence: *A. flavus* produced significantly less asexual spores and a concomitant increase in aflatoxin production on media and on peanuts, while *R. solanacearum* showed decreased growth, and decreased melanin and extracellular polysaccharide production. Using SPME-GCMS and comparative metabolic analyses it was found that both organisms produce a variety of interesting metabolites, but made eight compounds in common, including propiolic acid which was produced 15-fold higher in coculture conditions. These data suggest that the shared metabolic profiles of these microbes contribute to this two-way communication and influence their respective developmental regimes and interactions with host plants. While other studies have shown one-way (bacterial to fungal *or* fungal to bacterial) effects (5, 6), this study is the first to demonstrate a two-way interaction, suggesting shared signaling compounds. Future work will be aimed at characterizing the specific effects of some of these volatile compounds on both organisms.

In close proximity, bacteria and fungi communicate using non-volatile, diffusible signals and Chapter 3 details one such interaction. When grown in close proximity to a diversity of soil fungi, some *R. solanacearum* strains caused the fungi to produce asexual resting spores called chlamydospores. For many of these fungi, such as the *Aspergillus* spp., chlamydospores had not been previously described. Interestingly, when in grown in direct contact with fungi, *R. solanacearum* is capable of invading fungal cells with a specific affinity for chlamydospores.

Utilizing MALDI-IMS guided comparative metabolomics a new *R. solanacearum* lipopeptide, named ralsolamycin, was identified. Using modern peptidogenomics tools and targeted mutagenesis the ralsolamycin biosynthetic genes *rmyAB* were characterized, encoding a large non-ribosomal peptide/polyketides synthase hybrid enzyme, in *R. solanacearum* strain GMI1000. The *rmyA* mutant is incapable of making ralsolamycin and thus no longer induced fungal chlamydospore formation and was less able to invade fungal cells. These data suggest that the induction of chlamydospores by ralsolamycin may facilitate bacterial entry into fungal cells. Although *R. solanacearum* is able to survive well in the absence of host plants, the mechanisms of this persistence aren't well described (7). It is possible that entry into fungal cells may provide a novel survival niche for *R. solanacearum* in the absence of host plants. Ongoing studies are aimed at determining the survival impacts of this novel endosymbiosis.

Shifts in SM production have been described in many bacterial fungal interactions. In assaying a phylogenetically diverse set of fungi for chlamydospore development in response to ralsolamycin, it was appreciated that many of these fungi showed distinct pigmentation patterns in proximity to *R. solanacearum* strain GMI1000 but not the Δ*rmyA* colonies, indicating that ralsolamycin was specifically involved in pigment induction. *Fusarium* spp. in particular showed this differential pigmentation in response to ralsolamycin. Chapter 4 describes these findings and demonstrates that the *F. fujikuroi* pigmentation is the polyketide bikaverin, and that its normally tight nitrogen-dependent regulation (8) can be overridden by ralsolamycin. Because bikaverin seems to accumulate in chlamydospores and is known to be a bioactive compound (9–11), it was hypothesized to have antibacterial activity against *R. solanacearum*. While antibacterial assays do indicate a moderate antibacterial activity, I speculate that bikaverin may serve other functions in chlamydospores that are currently beyond the scope of this research.

In summary, *R. solanacearum* is more than just a plant pathogen. This body of work demonstrates that it dynamically interacts with plant associated fungi and can have dramatic impacts on the development and growth of these eukaryotic organisms. It produces a number of bioactive secondary metabolites (12–14), which likely contribute to other ecological functions outside of the host plan. There is still a lot to be understood in regards to the *R. solanacearum*-fungal interactions, including perceptive and regulatory mechanisms governing the interkingdom communication signals. However, this thesis provides some vital insights into these interactions as well as tools that will be useful for future studies. While this body of work may have significant implications toward a better understanding of the co-survival biology of bacteria and fungi, it will also be important to validate these findings *in situ*. Further, untangling the multipartite interactions of plant pathogenic microbes in the context of host disease development will be necessary before pathogens may be thoughtfully utilized as mediators of holistic plant health. Hopefully, further research into these and other chemically mediated bacterial-fungal communications will contribute significantly to both basic and applied fields of plant production, medicine, and microbial ecology in general.

REFERENCES

1. **Burlinson P**, **Deveau A**, **Barret M**, **Tarkka M**, **Sarniguet A**. 2011. Bacterial-fungal interactions: Hyphens between agricultural, clinical, environmental, and food microbiologists. Microbiol Mol Biol Rev **75**:583–609.
2. **Fleming A**. 1929. On the antibacterial action of cultures of a *Penicillium*, with special reference to their use in the isolation of *B. influenzae*. Br J Exp Pathol **10**:226–236.
3. **Cragg GM**, **Newman DJ**. 2013. Natural products: A continuing source of novel drug

leads. Biochim Biophys Acta - Gen Subj **1830**:3670–3695.

4. **Berg G**, **Grube M**, **Schloter M**, **Smalla K**. 2015. The plant microbiome and its importance for plant and human health, 1st ed. Frontiers Media SA, Lausanne.
5. **Kai M**, **Effmert U**, **Berg G**, **Piechulla B**. 2007. Volatiles of bacterial antagonists inhibit mycelial growth of the plant pathogen Rhizoctonia solani. Arch Microbiol **187**:351–360.
6. **Effmert U**, **Kalderás J**, **Warnke R**, **Piechulla B**. 2012. Volatile mediated interactions between bacteria and fungi in the soil. J Chem Ecol **38**:665–703.
7. **Álvarez B**, **Biosca EG**, **López MM**. 2010. On the life of Ralstonia solanacearum, a destructive bacterial plant pathogen. Technol Educ Top Appl Microbiol Microb Biotechnol 267–279.
8. **Wiemann P**, **Willmann A**, **Straeten M**, **Kleigrewe K**, **Beyer M**, **Humpf HU**, **Tudzynski B**. 2009. Biosynthesis of the red pigment bikaverin in *Fusarium fujikuroi*: Genes, their function and regulation. Mol Microbiol **72**:931–946.
9. **Kwon HR**, **Son SW**, **Han HR**, **Gyung Ja Choi**. 2007. Nematicidal activity of bikaverin and fusaric acid isolated *Fusarium oxysporum* against pine wood nematode, *Bursaphelenchus xylophilus*. Plant Pathol J.
10. **Deshmukh R**, **Mathew A**, **Purohit HJ**. 2014. Characterization of antibacterial activity of bikaverin from Fusarium sp. HKF15. J Biosci Bioeng **117**:443–448.
11. **Son SW**, **Kim HY**, **Choi GJ**, **Lim HK**, **Jang KS**, **Lee SO**, **Lee S**, **Sung ND**, **Kim JC**. 2008. Bikaverin and fusaric acid from *Fusarium oxysporum* show antioomycete activity against *Phytophthora infestans*. J Appl Microbiol **104**:692–698.
12. **Pauly J**, **Spiteller D**, **Linz J**, **Jacobs J**, **Allen C**, **Nett M**, **Hoffmeister D**. 2013. Ralfuranone thioether production by the plant pathogen ralstonia solanacearum.

ChemBioChem **14**:2169–2178.

13. **Kreutzer MF**, **Kage H**, **Gebhardt P**, **Wackler B**, **Saluz HP**, **Hoffmeister D**, **Nett M**. 2011. Biosynthesis of a complex yersiniabactin-like natural product via the mic locus in phytopathogen Ralstonia solanacearum. Appl Environ Microbiol **77**:6117–6124.

14. **Spraker JE**, **Sanchez LM**, **Lowe T**, **Dorrestein PC**, **Keller NP**. 2016. *Ralstonia solanacearum* lipopeptide induces chlamydospore development in fungi and facilitates bacterial entry into fungal tissues. ISME J 1–14.

APPENDIX

A.1. Other publications not presented in this thesis

1. **Baccile JA**, **Spraker JE**, **Le HH**, **Brandenburger E**, **Gomez C**, **Bok JW**, **Macheleidt J**, **Brakhage AA**, **Hoffmeister D**, **Keller NP**, **Schroeder FC**. 2016. Plant-like biosynthesis of isoquinoline alkaloids in Aspergillus fumigatus. Nat Chem Biol 1–9.
2. **Barkal LJ**, **Theberge AB**, **Guo C**, **Spraker JE**, **Rappert L**, **Berthier J**, **Brakke KA**, **Wang CCC**, **Beebe DJ**, **Keller NP**, **Berthier E**. 2016. Microbial metabolomics in open microscale platforms. Nat Commun **7**:1–11.
3. **Macheleidt J**, **Scherlach K**, **Neuwirth T**, **Schmidt-Heck W**, **Straßburger M**, **Spraker JE**, **Baccile JA**, **Schroeder FC**, **Keller NP**, **Hertweck C**, **Heinekamp T**, **Brakhage AA** 2015. Transcriptome analysis of cyclic AMP-dependent protein kinase A-regulated genes reveals the production of the novel natural compound fumipyrrole by A spergillus fumigatus. Mol Microbiol **96**:148–162.
4. **Mattupalli C**, **Spraker JE**, **Berthier E**, **Charkowski AO**, **Keller NP**, **Shepherd RW**. 2014. A Microfluidic Assay for Identifying Differential Responses of Plant and Human Fungal Pathogens to Tobacco Phylloplanins. Plant Health Prog **15**:130–134.
5. **Spraker JE, Keller NP**. 2014. *Waking Sleeping Pathways in Filamentous Fungi*. Eds: Osborne A, Carter G, and Goss R. Natural Products: Discourse, Diversity and Design. Wiley-Blackwell.
6. **Spraker JE**. (2013) Huitlacoche. UW Extension - Garden Fact Sheet XHT1230 http://hort.uwex.edu/articles/huitlacoche

A.2. Art/Science Outreach

A.2.1. deBary-tones lyrics

I was one of the founding members of the parody band, "*deBary-tones"*, focused on making music to help teach core concepts in plant pathology. We highlighting historic disease epidemics, fundamentals of disease progress, and core concepts in fungicide resistance. Lyrics that I wrote for this project are provided here:

FRAC Code – parody of: "Black Bird" music by the Beatles

FRAC code label on my fungicides
Tell me what chemicals are alright
to combine
We are only aiming to keep resistance minimized.

FRAC code label on my fungicides
Can I mix a triazole with a Q-O-I,
then apply?
Mixing modes of action hitting different target sites.

FRAC code why? FRAC code why?
Maintain the use of your fungicides.

FRAC code why? FRAC code why?
Maintain the use of your fungicides.

FRAC code label on my fungicides
Tell me what chemicals are alright
to combine
We are only aiming to keep resistance minimized

Mixing modes of action hitting different target sites.

We are only aiming to keep resistance minimized.

House of the Rising Oospore – parody of : “House of the Rising Sun” music by the Animals

There is a blight in my potato fields
They call phytophthora.
It's been the ruin o’ solanaceaous crops.
And lord knows I got more than one.

I replanted potatoes from last year
‘Cause I thought it'd bring down the cost.
If only I'd obtained certified seed
Then maybe my fields wouldn't be lost.

I saw a lesion last wed
By Friday my tubers were toast
On Monday I checked on my tomatoes.
Turns out their also great hosts.

I ran to the shed to get fungicides
And doused every last leaf
Turns out this scourge's not a fungus
But instead its an oomycete.

Now I've got no food for my family
All our crops were turned to waste.
All I've got is loads of inoculum.
I wonder how oospores taste?

There is a blight in my potato fields.
They call phytophthora.
It's been the ruin o' many a solanaceous crop
And lord knows I got more than one.

"Quarantine" – parody of: "Let it be" music by the Beatles

When I find myself in times of trouble
The APHIS agent comes to me
Speaking words of wisdom…
"quarantine"
And when *Candidatus liberibacter*
Is turning all my citrus green
Instead of sending cuttings, quarantine
Quarantine, quarantine
Quarantine, quarantine
Contain disease, don't spread
them, quarantine

And when the sudden oak death people
Living in the west agree
The trees are in real danger, quarantine
Although soybean rusts not here yet
There's still a chance it will be
Better safe than sorry, quarantine
Quarantine, quarantine
Quarantine, quarantine
For all questionable imports, quarantine

Quarantine, quarantine
Quarantine, quarantine
Until all materials have been
cleared, quarantine

Quarantine, quarantine
Ah quarantine, quarantine
Prevent the next epidemic, quarantine

And until the *Ralstonia* ELISA
screening
Says it's not biovar 2, race 3
Keep geraniums from the
masses, quarantine
To keep stem rust from re-emerging,
even after eradicating barberry
Ug99 is out there, quarantine

Yeah quarantine, quarantine
Quarantine, quarantine
Oh the most logical answer, quarantine

Quarantine, quarantine
Quarantine, quarantine
Avoid widespread disaster, quarantine

Quarantine, quarantine
Ah quarantine, quarantine
It works in zombie movies, quarantine

Papaya Ringspot Virus- parody of: “Lucy in the Sky With Diamonds” music by the Beatles”

Picture yourself on an island in the Pacific
With papaya trees and rainbow filled skies
Aphids that crawl through your plantation quite slowly
Stylets full of virus and sap-sucking eyes

Small, mottled fruits of yellow and green
Towering over your head
Look for control, maybe resistance or a spray.
And theres none...

Express coat proteins in papaya
Express coat proteins in papaya
Express coat proteins in papaya
Aaaaaahhhh...

Papaya production is down 94 percent
Quarantine works well... only for a limited time
By the time your new plantation’s matured to production
The virus is looming nearby

Bio-technology developed a cure
Waiting to save the day
Take aim with the gene gun, pull the trigger, sit back
and you’re done

Express coat proteins in papaya
Express coat proteins in papaya
Express coat proteins in papaya
Aaaaaahhhh...

Picture yourself on an island plantation
With transgenic trees with fruits of full size
Suddenly the capsid encoding gene fragment
Tells the ringspot it's card’s been denied

Express coat proteins in papaya
Express coat proteins in papaya
Express coat proteins in papaya
Aaaaaahhhh...
Express coat proteins in papaya
Express coat proteins in papaya
Express coat proteins in papaya
Aaaaaahhhh...
Express coat proteins in papaya
Express coat proteins in papaya
Express coat proteins in papaya *[fade out]*

Ergot – parody of: “My Girl” music by the Temptations

I grew so much rye, then baked it into bread.
Now when I close my eyes, there’s demons
in my head.

I guess you’d say...
What can make me feel this way?
Ergot (Ergot, ergot)
Talkin' 'bout ergot (ergot).

My heart is racing and my skin’s in pain
Could this be related to those funny looking
grains?

Well, I guess you’d say...
What can make me feel this way?
Ergot (Ergot, ergot)
Talkin' 'bout ergot (ergot).
Hey hey hey
Hey hey hey
Ooooh.

The pains getting worse as gangrene sets in,
My brain and my nerves feel like their
meltin’.

Well, I guess you’d say...
What can make me feel this way?
Ergot (Ergot, ergot)
Talkin' 'bout ergot (ergot).

I grew so much rye, then baked it into bread.
With ergot.
Now when I close my eyes, there’s demons
in my head.
From ergot.
Talkin' 'bout
Talkin' 'bout
Talkin' 'bout
Ergot...Ooooh...
Ergot
I wish I’d known about Ergot *[fade out]*